INVESTIGATION OF HAND POSTURE DURING REACH AND GRASP FOR ERGONOMIC APPLICATIONS

by

Sung Chan Bae

A dissertation submitted in partial fulfillment
of the requirements for the degree of
Doctor of Philosophy
(Mechanical Engineering and Industrial and Operations Engineering)
in the University of Michigan
2011

Doctoral Committee:

 Professor Thomas J. Armstrong, Co-Chair
 Associate Professor Brent Gillespie, Co-Chair
 Associate Professor Bernard J. Martin
 Research Professor James A. Ashton-Miller

To My Family

ACKNOWLEDGEMENTS

TABLE OF CONTENTS

LIST OF TABLES

LIST OF FIGURES

xiii

ABSTRACT

INVESTIGATION OF HAND POSTURE DURING REACH AND GRASP FOR ERGONOMIC APPLICATIONS

by

Sung Chan Bae

Co-Chairs: Thomas J. Armstrong and Brent Gillespie

New methods were developed to study the effect of object and task attributes on prediction of hand posture and finger motion during reach and grasp. The results of three studies in young adults showed: (1) Finger motion during reach and grasp for pinching cylindrical objects was described using selected spatial (initial, maximum open, final postures) and temporal parameters (delay and total times) as a function of object properties (e.g., object size and orientation, reach distance). Those parameters were used to predict finger motion using a constrained fourth order polynomial function (R^2 ranging from 0.54 to 1). (2) Two new metrics, openness and flatness, which represent fingertip positioning and finger shape, respectively, were used to describe the effect of object shape on hand posture during reach and grasp. Object aspect ratio and cross-sectional

shape caused changes in hand posture. Pinching long objects (e.g., cylinders) resulted in up to 25% greater hand opening than pinching symmetric objects (e.g., spheres). Pinching objects with edges (e.g., cubes) resulted in up to 12% greater hand opening than objects with curved surfaces (e.g., spheres). (3) Different hand postures were observed for reach and pinch than for reach and power-grip. Use of power grasp involved greater hand opening than pinch (the mean difference of finger joint angles ranges from 1.8 to 11.9°), and the effect of grasp type occurred from earlier in the reach for the MCP joints than for the PIP and DIP joints. In summary, we conclude that these methods can be used to reliably predict finger motion for selected jobs and to estimate tendon excursion for studying musculoskeletal disorders in the hand.

CHAPTER 1

INTRODUCTION

1.1. THESIS STATEMENT

Hand posture during reach and grasp can be predicted by capturing the effect of object condition on finger motion characteristics. Knowledge of prehensile behavior can provide necessary information to describe the way people reach and grasp and further to assess specific tasks for tackling ergonomic issues, such as tendon excursion.

1.2. RESEARCH OBJECTIVES

To address the above thesis the following objectives are established:

(1)   Development of a finger motion model that can predict finger motion during reaching for and grasping cylindrical objects of varying sizes, in varying orientations, and at varying reach distances, using pinch grasp (Chapter 2).

(2)   Investigation of the effect of object shape on finger motion during reaching for and grasping objects that vary by aspect ratio and cross-sectional shape, using pinch grasp (Chapter 3).

(3)   Investigation of the effect of grasp type (grip vs. pinch) on finger motion during reaching for and grasping cylindrical objects of varying sizes and at varying orientations (Chapter 4).

(4) Demonstration of finger motion prediction during reach and grasp by using the proposed model for ergonomic applications, such as tendon excursion (Chapter 2 and Chapter 5).

1.3. RATIONALE

Human hands are involved in nearly all activities of daily living, work and recreation. For example, hands are used not only in everyday activities, such as picking up a coffee cup, but also in specialized industrial tasks, such as manipulating a flexible hose. Understanding behavior of the hand during reach and grasp is important because it provides useful information about hand posture for applications strongly related to the industrial field.

First, hand posture determines the space required to perform a manual task such as joining parts in industrial plants, by which the workspace design can be improved by reducing mechanical interference between the hand and work environment [1-3]. Lack of knowledge of the required space can lead to improper workspace design, in which workers are potentially exposed to acute hand injury, such as laceration and crush, due to collision with undesirable objects or obstacles [4-6]. Therefore, prediction of hand posture during reach and grasp is needed to define required space for the design of safe workplace.

Second, final hand posture determines the hand strength required to complete a given task [7-11]. It was also shown that final hand posture depends on how hand posture is shaped prior to the contact with an object [12]. Previous hand models [13] assumed unrealistic finger segmental motions that preclude accurate predictions of the spatiotemporal sequencing of how the fingers actually close around an object to grip it. Accordingly, prediction of hand posture during reach and grasp is needed for refined prediction of grip posture to evaluate hand strength for work objects.

Last, hand posture affects tendon loads and excursions and stresses on adjacent tissues, such as synovial membranes and nerves [14-17]. Previous studies have shown that tendon excursion is associated with the risk of work-related musculoskeletal

disorders (WMSDs) of the upper extremities [3, 18-22]. The WMSDs account for 29 percent of all workplace injuries causing worker disability and economic loss to the employer and society, and the upper extremities is the second leading body part affected by WMSDs [23-26]. Hence, prediction of hand posture is needed for estimating relevant tendon movement during reach and grasp for assessing the risk of WMSDs.

Addressing those needs first requires fundamental understanding of prehensile behavior that has been studied in behavioral and motor control disciplines. Jeannerod [27] reported that two phased movements occur during reach and grasp: (1) an initial fast high velocity phase (from initial movement to peak deceleration of the wrist), where the hand opens as the fingers extend, and (2) a second slow phase, beginning after maximum aperture (aperture is the distance between the tips of an index finger and a thumb), where much corrective finger movement occurs as the hand approaches the object to be grasped. The transport (hand transportation) and the grasp (finger grip formation) were shown to be performed based on information processed by two visuomotor channels from extrinsic (e.g., reach distance) and intrinsic (e.g., object size) object properties, respectively.

Subsequent studies showed how object and task attributes affect reach and grasp in a specific way. Physical properties of the object to be grasped influence how we grasp it. For example, the effect of object size and reach distance on the transport and the grasp was established [28-32], and object shape was shown to cause different planning and execution of reach and grasp [33-36]. These studies were able to identify the effect of object properties on hand posture, but not able to describe hand posture for predicting finger motion during reach and grasp. It has also been shown that what we intends to do with the object affects reach and grasp behavior. A representative example is 'the end-state comfort effect,' which suggests that initially awkward postures are selected for the sake of more comfortable final postures [37, 38]. Forceful manipulation required after grasp was shown to affect grasp selection, pinch or grip [2], and accuracy requirement after grasp influenced mainly hand transportation rather than finger grip formation [39, 40]. These studies imply that intention for manipulating the object needs to be considered for examining reach and grasp motion, but it is first to know how finger motion, in

3

general, can be described when prehensile behavior is selected on the basis of an object to be grasped with a specific goal.

Kinematic models of the hand have been developed for predicting grip posture, based on experimental studies or computational algorithms [3, 13, 41-43]. These models mostly examined mechanical fit between the hand and the work object but depended on hypothetical finger motion algorithms; for example, finger joints were assumed to rotate one at a time from the proximal to the distal joints [13], or to rotate simultaneously at the same rate [3]. Since those assumed joint rotations are far from what actually occurs, an effort has been made to describe finger motion during reach and grasp by using mathematical models [44, 45]. However, those studies did not consider the whole period of reach and grasp with sufficient details to be used for its prediction by means of the kinematic hand models. Further studies are needed to develop finger rotation models that can simulate finger motion on the basis of human prehension behavior.

In summary, this work contributes to modeling finger motion for opening and closing of the fist during reach and grasp capable of adjusting prediction based on object and task attributes. Accurate and natural hand posture prediction can address ergonomic issues, such as the design of tools and workspaces [46, 47] and the evaluation of workers' capability and disability in regard to typical reach and grasp task [7-11, 48, 49].

1.4. DISSERTATION OUTLINE

In this dissertation, the effect of object and task conditions on finger motion during reach and grasp is investigated for prediction of hand posture and its consideration of ergonomic applications.

In Chapter 2, a finger motion model is developed to describe finger motion during reach and grasp by characterizing finger movement. This model provides the basis, on which further studies depend for extending limited condition to another.

In Chapter 3, the effect of object shape (aspect ratio and cross-sectional shape) on finger motion during reach and grasp is investigated. New metrics that capture the detailed hand posture are proposed for a quantitative comparison of hand posture between

cylindrical and non-cylindrical objects. The finger motion model is used to predict finger motion for non-cylindrical objects.

In Chapter 4, the effect of grasp type (pinch vs. grip) on finger motion during reach and grasp is investigated. The relationship between grasp type and hand shaping is characterized for a set of object size and orientation, which can provide clues of how hand shaping is developed for given grasp type. The finger motion model is used to predict finger motion for power grip.

Chapter 5 summarizes the major findings of this dissertation, demonstrates the use of those findings, and suggests potential future work.

Appendix A includes a detailed description of computing tendon excursion for industrial jobs, presented in Chapter 5.

CHAPTER 2

A FINGER MOTION MODEL FOR REACH AND GRASP

ABSTRACT

This study aimed to develop a model that describes human finger motion for simulation of reach and grasp for selected objects and tasks. Finger joint angles and timing of their changes were measured for six subjects as they reached 20-40cm and grasped cylindrical handles (1.3-10.2cm D) of varying orientation (vertical/axial). The empirical results from multiple regression analyses served as inputs to allow a fourth order polynomial to predict motion of each finger joint. The proposed model showed good fit with observations, with high coefficients of determination from 0.54 to 1 and reasonable errors from 0.04° to 5.44° for all conditions considered. The proposed finger motion model was implemented in an existing kinematic hand model to employ a contact algorithm for refined prediction of grip posture and to illustrate its predictive power by graphically displaying the opening and closing of the hand.

2.1. INTRODUCTION

The aim of this work was to develop a model that can describe finger motion during reach and grasp. Finger motion models can be used with kinematic hand models to predict hand postures. Information of hand postures is needed for designing tools, controls, handles, and other objects that are grasped, held or used by the hand.

2.1.1. Importance of hand study

First, hand posture determines the space required to perform manual tasks. Baker [1] measured the required space for using hand tools by two dimensional photographic images. These results are useful for the specific tools examined under static conditions, but cannot be easily generalized to other sizes of tools or different tools, or to dynamic tasks. Using a three dimensional motion capture system, Grieshaber et al. [50] measured hand space envelopes of hose insertion jobs of different insertion methods. Although this method is useful for dynamic tasks, the findings are also not easily applied to other object sizes and shapes. Choi [3] demonstrated the use of a three dimensional kinematic model to predict space required for holding cylindrical handles. The study can be applied for various object conditions, but cannot predict the required space during reach. Finger motion models are needed to describe how the fingers move during reach and grasp.

Second, final hand posture is an important factor determining hand strength [7, 8, 10]. Those studies examined the effect of grip span on grip strength by measuring subjects' maximal force with different handle separations. Since the relationship between grip posture and grip strength has been investigated, further information about grip posture will permit evaluation of grip strength. Finger motion models can contribute to predicting accurate terminal grip postures by providing a finger rotation algorithm during reach and grasp.

Last, hand posture affects tendon loads and excursions and stresses on adjacent tissues, such as synovial membranes and nerves [14-17, 51]. Previous studies have shown that tendon excursion is associated with repetitiveness in industrial jobs and the risk of

work-related musculoskeletal disorders (WMSDs) of the upper extremities [3, 18-22]. However, since most studies only examined tendon excursion at the wrist, finger motion models are needed to consider tendon excursion at fingers for more detailed evaluation of jobs.

2.1.2. Prehension behavior and kinematic models

In developing a hand model, an empirical study of human prehension can provide data for inputs into the model. Prehension has been postulated to consist of the transport and the grasp components that work independently [27]. The transport and the grasp components are thought to be performed based on information processed by two visuomotor channels from extrinsic (e.g., distance) and intrinsic (e.g., size) object properties, respectively. Many studies have examined how those object attributes affect reach and grasp using aperture (the distance between the thumb tip and the index fingertip). Maximum aperture during reach was known to be related linearly to object size; farther reach distance induced longer movement time, and both object distance and size had an effect on time to maximum aperture during reaching [29-31]. Instead of using aperture, Smeets and Brenner [45] used the independent trajectories of the thumb and finger tips to describe reach and grasp. Both aperture and fingertip trajectories are limited to describe hand posture in that they cannot exclusively define hand shape in finger-joint-level-detail. Further studies are needed to describe how finger joint angle and rotation are affected by object properties during reach and grasp.

Kinematic models of the hand have been developed for predicting grip posture, based on experimental studies or computational algorithms [41-43]. These models mostly examined fit between the hand and the work object. Buchholz and Armstrong [13] developed a kinematic model of the human hand using ellipsoids to predict the hand posture for grasping of ellipsoidal objects based on a contact algorithm. Choi [3] developed a three dimensional kinematic model of the hand for predicting the hand posture of grasping a range of objects with varying shapes and sizes, also with an aid of a contact algorithm. Lee and Zhang [43] explored a different approach for the posture

prediction, where an optimization-based model was developed that minimized the sum of distances from the finger joints to the object surface. Those predictions can assess workers' capability and disability [7, 8, 10, 48, 49] and provide design guidelines for work environments [46, 47].

Despite their ability to predict accurate mechanical fit between the hand and the object, the previous kinematic models depended on hypothetical finger motion algorithms. For example, Buchholz and Armstrong [13] assumed that joints rotate one at a time, starting from the proximal joint and continuing until it reaches its limit or there is contact between the finger and the object. Choi [3], instead, supposed that all joints rotate simultaneously at the same rate until they reach their motion limits or the contact is achieved between the finger and the object. However, those assumed joint rotations are far from what actually occurs during finger movement. As an effort to explain the finger motion during grasping, Braido and Zhang [44] employed a mathematical model using a hyperbolic tangent function for quantitative analysis of finger motion for cylinder grasping. Nevertheless, it considered only finger flexion that initiates from the fully extended posture, excluding the opening (extension) of the hand. Smeets and Brenner [45] used fingertip trajectories of the thumb and fingers to describe finger motion during reach and grasp, but the results could not provide sufficient information to explain finger joint rotation. Therefore, further studies are needed for development of finger rotation models simulating finger motion during reach and grasp on the basis of human prehension behavior.

2.1.3. Proposed hand model

Toward those needs for finger motion models, this study aimed to develop a model that can be used to predict finger motion for selected reach and grasp tasks. This study began with an empirical study in which finger joint angles and timing of changes in finger joint angles were measured during reach to grasp of objects of known size, orientation and distance from the subjects. Finger joint angles at the beginning, the maximum open, and the end were then taken from the empirical study and entered into a

predictive finger motion model. This model used a fourth order polynomial to predict finger joint motion during reach and grasp. The model prediction was incorporated into an existing kinematic hand model that had a contact algorithm but lacked realistic finger rotation algorithm for improved prediction of hand postures at contact as well as preceding contact.

2.2. METHODS

2.2.1. Experimental protocol

Six subjects (3 males, 3 females) with no history of musculoskeletal disorders in the upper extremities participated in the experiment. We chose the study population by their hand lengths; their demographic and anthropometric information are shown in Table 2.1. The subjects were seated, and started from a relaxed hand posture with their elbows flexed at about 90° and no abduction in the shoulder (Figure 2.1A). They were then directed to reach for and grasp the cylindrical handles fixed in space using a pulp pinch grip between the tips of their fingers and the tip of their thumb, as observed by Grieshaber and Armstrong [52] and Seo et al. [53]. Participants were told not to exert more force than necessary to stabilize the hand onto the surface of cylinders, and the resulting posture was similar in form to those reported by Napier [54]. The experiment design included three independent variables: (1) three object sizes (1.27, 3.81, 10.16 cm in diameter), (2) three reach distances (20, 30, 40 cm from the subject), and (3) two object orientations (vertical and axial). These three independent variables were chosen because they have been shown to be significant factors affecting hand movement [27, 29-31], and were presented in a random order with three repetitions for each condition. The experimental protocol was approved by the Institutional Review Board of the University of Michigan at Ann Arbor and all subjects gave the written consent to participate in the study.

Table 2.1. Summary of study participants.

Gender	Age	Hand Length	Hand Length Range (cm)[a]
	18	18.3	
Male (n=3)	28	19.4	18.3(5%) – 20.1(70%)
	28	20.1	
	20	19.1	
Female (n=3)	20	17.6	17.1(16%) – 19.1(90%)
	28	17.1	
Pooled	23.7	18.6 ± 1.1	17.1(16%F) – 20.1(70%M)

[a] Percentiles in parentheses are based on Garrett [55].
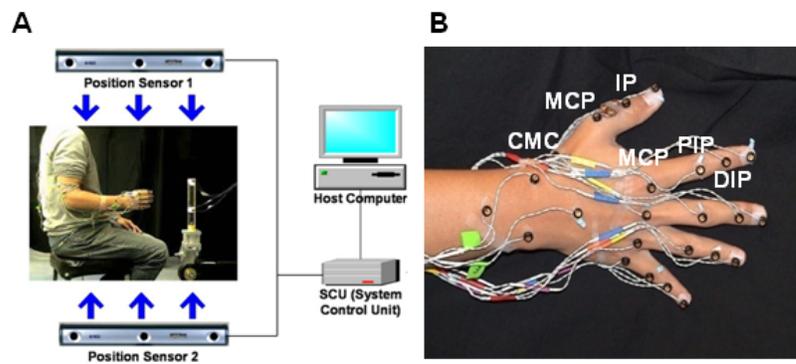
Figure 2.1. (A) Laboratory setup: two position sensors are horizontally mounted on each side of a subject seated in front of a vertically oriented object. (B) Markers attached on the dorsal side of the hand with zero degree joint angles.

2.2.2. Data acquisition and processing

To record finger motion during reach and grasp, an OptoTrak® Certus™ motion tracking system (Northern Digital Inc.) was utilized with thirty-one markers attached on the upper extremity of the subject and on the object; 27 markers were secured at every tip and joint of the fingers and the wrist on the dorsal side, including Distal Interphalangeal (DIP), Proximal Interphalangeal (PIP), and Metacarpophalangeal (MCP) joints with Interphalangeal (IP) and Carpometacarpal (CMC) joints of the thumb (Figure 2.1B). Using 3D video motion analysis to measure finger joint angles using dorsal markers has

been found to be within 5° errors from those measured by kinematic linkages [56]. Two position sensors were properly located to simultaneously track the positions of markers during the task at a sampling frequency of 50 Hz with resolution of 0.01mm. If the sensors failed to capture some markers at the final posture for certain conditions, a digitizer was used to reconstruct the missing markers. The data obtained were processed with MATLAB® software. The inter-digit joint angles were calculated from the three dimensional marker position data, using dot products of the adjacent vectors, each of which represents each finger segment. Joint angles were defined as zero when the adjacent vectors are aligned (fully extended posture), as shown in Figure 2.1B, with positive values meaning flexion of the joints. To make the joint angle data more tractable, the joint angle profiles were passed through a second-order Butterworth low-pass filter with a cutoff frequency of 3Hz. Butterworth filter was chosen for its good all-around performance, and the selection of the cutoff frequency as well as the sampling frequency (50Hz) was justified by the power spectral density examination of the raw data that the power below 3Hz was predominant (99.3% on average). Other investigators reported using a similar cutoff frequency of 5Hz [44, 57]. When there was small fraction of missing points in finger joint angle profiles, they were interpolated by piecewise-cubic-Hermite interpolation.

2.2.3. Characterization of hand movement and finger motion

Spatial and temporal characteristics can be used to describe hand movement and finger motion during reach and grasp. Finger motion is represented by finger joint angles as a function of time, while hand movement is described by distance between the hand and the object. Finger flexion/extensions – CMC, MCP, and IP joints for the thumb and MCP, PIP, and DIP for the index to little fingers (a total of 15 degree of freedoms) – were analyzed in the current study. Figure 2.2 shows a sample plot of an MCP joint angle profile of the index finger and a hand-object distance profile for reaching 40cm and pulp-pinching a vertically oriented 3.8cm diameter cylinder. In general, starting from a relaxed initial hand posture (θ_i), the finger joint angles decrease to the maximum open hand

posture (θ_o) with the hand opening as the hand approaches the object. Depending on the reach distance, there exists a delay before the hand opens. The finger joint angles then increase to the final hand posture (θ_f) as the hand closes around the object. Hence, the finger motion can be represented in terms of θ_i, θ_o, and θ_f and their corresponding timings, such as delay (t_{delay}), open (t_{open}), and close (t_{close}) times (Figure 2.2). The initial posture and reach time (t_{reach}) are detected using the threshold movement velocity of 25 mm/sec at the beginning and the end of the distance profile, whereas the delay time and the final posture are identified when the joint angular velocity stays within 5°/sec at the beginning and the end, respectively. The total time (t_{total}) is the summation of the delay, open, and close time.
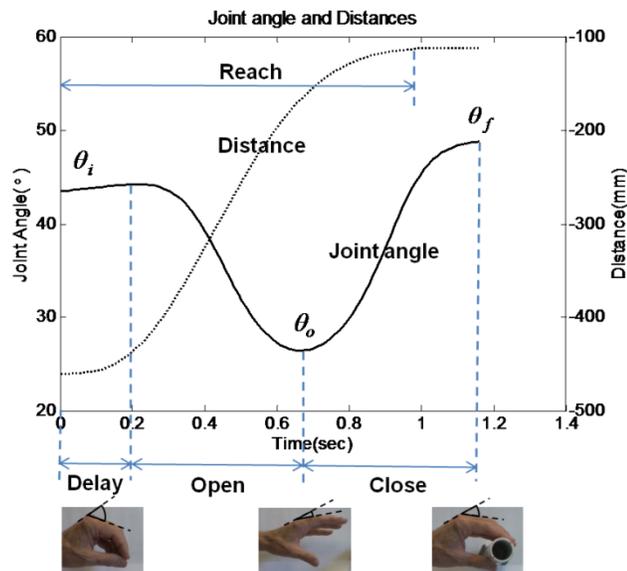
Figure 2.2. A sample index MCP joint angle (solid) and distance between the object and the hand (dotted), for reaching 40cm and pulp-pinching a vertically oriented 3.8cm diameter cylinder with selected spatial and temporal parameters.

2.2.4. Empirical study

A least squared multiple regression analysis was used to determine significant experimental factors affecting dependent variables, the spatial and temporal parameters:

$$Y = \beta_c + \beta_o \,(\text{orientation}) + \beta_s \,(\text{object size}) +$$
$$\beta_d \,(\text{distance}) + \beta_l \,(\text{hand length}) \pm \varepsilon \qquad (2.1)$$

where Y's are dependent variables including θ_i, θ_o, θ_f, t_{delay}, t_{open}, t_{reach}, and t_{total} of 15 finger joints; *orientation* is 0 for axial and 1 for vertical orientation; *object size* is a cylinder diameter in centimeters; *distance* is the reach distance in centimeters; *hand length* is the length of a person's hand in centimeters; β's are corresponding coefficients to the experimental factors, including the constant term (β_c), and ε is the errors of prediction. Hand length was chosen as a representative of hand anthropometry because the length of each finger segment can be modeled by its linear relationship with hand length [58].

Based on equation (2.1), factors that are statistically significant need to be selected for each dependent variable to form linear regression equations with significant terms; since there are 15 equations for each dependent variable, the factor is considered statistically significant if more than 10 finger joint are significantly affected ($p<0.05$) or the same joints (e.g., MCP) for all fingers are significant ($p<0.05$). Consequently, object size is included for all dependent variables, hand length for spatial parameters, orientation only for the final posture, and distance for temporal parameters:

$$\theta_i, \theta_o = \beta_c + \beta_s \,(\text{object size}) + \beta_l \,(\text{hand length}) \pm \varepsilon \qquad (2.2)$$

$$\theta_f = \beta_c + \beta_o \,(\text{orientation}) + \beta_s \,(\text{object size}) + \beta_l \,(\text{hand length}) \pm \varepsilon \qquad (2.3)$$

$$t_{delay}, t_{open}, t_{reach}, t_{total} = \beta_c + \beta_s \text{(object size)} + \beta_d \text{(distance)} \pm \varepsilon \qquad (2.4)$$

2.2.5. Finger motion model

Finger joint motion during reach and grasp can be described by a fourth order polynomial that is constrained by five observed constraints: three extreme points (θ_i, θ_o, θ_f) of the joint angle profile determined in the empirical study and zero angular velocity at the beginning and the end of the joint angle profile. A polynomial function model has a simple form and moderate flexibility of shapes. Although polynomials behave poorly at the extremes, the fact that the constraints are imposed at the extremes in this model reduces the disadvantage. Three extreme points at the beginning, the maximum open, and the end of the joint angle profile require the polynomial function to be the fourth order at least. The fourth order polynomial was selected so that the model can be analytically computed, rather than 'fitted', based on five observed constraints. Since the joint angle is almost constant during delay time, only open and close period are modeled as a function of normalized time:

$$\tau = \frac{t - t_{delay}}{t_{open} + t_{close}} \qquad (2.5)$$

where t is real time, t_{delay} the delay period, t_{open} the open period, and t_{close} the close period. Hence, the finger motion model is formulated with constraint conditions as follows:

$$f(\tau) = a_0 + a_1\tau + a_2\tau^2 + a_3\tau^3 + a_4\tau^4, \quad 0 \leq \tau \leq 1 \qquad (2.6)$$
$$\text{subject to: } f(0) = \theta_i, \ f(1) = \theta_f, \ f'(0) = f'(1) = 0, \ f(a_2/2a_4) = \theta_o$$

where θ_i is an initial angle, θ_f a final angle, and θ_o a maximum open angle. The last constraint, $f(a_2/2a_4) = \theta_o$, results from algebraic derivation that the function has its local minimum at $\tau = a_2/2a_4$, given the other constraints. These constraint conditions produce the following five equations for five unknowns:

15

$$a_0 = \theta_i \tag{2.7}$$

$$a_1 = 0 \tag{2.8}$$

$$a_2 + a_3 + a_4 = \theta_f - \theta_i \tag{2.9}$$

$$2a_2 + 3a_3 + 4a_4 = 0 \tag{2.10}$$

$$a_4{}^4 + 8(\theta_i - 2\theta_o + \theta_f)a_4{}^3 + 18(\theta_i - \theta_o)^2 a_4{}^2 = 27(\theta_i - \theta_f)^4 \tag{2.11}$$

Although equation (2.11) is the fourth order equation of a_4 so possibly containing four solutions, the shape of the joint angle profile restricts the solution of a_4 to be a negative real root. The other coefficients, from a_0 to a_3, can be easily calculated by the remaining linear equations (2.7) - (2.10). The computation was performed by MATLAB$^{®}$ software.

2.2.6. Implementation of the finger motion model

The proposed finger motion model can be combined with an existing three dimensional kinematic model, such as Choi's model [3], to exploit advantages of the two models: finger motion prediction for the former, and grip posture prediction for the latter. The kinematic hand model created the hand as open chains of rigid body segments constructed by truncated cones and worked in a Visual C++ environment with OpenGL graphic functions displaying a hand and an object in varying conditions. With proper inputs provided, the kinematic model can reasonably predict terminal grip postures that reflect mechanical fit between the hand and the object by using contact algorithms. However, it lacked detailed information of how finger joints open and close during the period prior to the contact. Figure 2.3 shows a flowchart that describes the relationship between the empirical study, the finger motion model, and the kinematic model. For given inputs (e.g., object size and hand length), the empirical study generated data for the

finger motion model to use in predicting finger motion for reach and grasp. These data included particular points of finger joint angles (θ_i, θ_o, θ_f) and of timing of changes in finger joint angles (t_{delay}, t_{total}), on which the effect of the inputs were examined by statistical analyses. Consequently, the finger motion model generated arrays of finger joint angles as a function of time; with their implementation in the kinematic hand model, these data were used to guide the finger joint until the contact was detected by contact algorithms (See section 2.3.3. for detail).

Inputs
- Object: size, orientation, distance
- Grip mode: power grasp, pulp pinch
- Hand size

Empirical Study
- Spatial parameters: finger joint angles $(\theta_i, \theta_o, \theta_f)$
- Temporal parameters: timing of changes in finger joint angles (t_{delay}, t_{total})

Finger Motion Model
Finger joint angles as a function of time $[\theta(t)]$

3D Kinematic Model
Equipped with a contact algorithm

Improved Prediction of Hand Posture and Motion During Reach and Grasp

Figure 2.3. A flowchart showing the relationship between the empirical study, the finger motion model and the 3D kinematic model.

2.3. RESULTS

2.3.1. The empirical study of reach and grasp

The effect of object attributes on hand movement and finger motion was examined using multiple linear regressions. Table 2.2 shows the coefficients of the linear regression equations (equations (2.2) - (2.4)) of all finger joints. The effect of object size and hand length on the spatial parameters was significant for nearly all joints ($p < 0.05$), while that of reach distance was not statistically significant. For the digits 2-5, in general, the results accounted for the variance of the spatial parameters of the MCP joint even better than that of the other joints; the coefficients of determination (R^2) of the open and the final postures were 0.55 and 0.73 on average for the MCP joints, compared to 0.14 and 0.15 for the PIP and the DIP joints, respectively. Since the pulp pinch grip has limited contact with an object primarily concentrated at the very distal segments of the fingers, it might be restricted to explain the variance of the finger joints in the middle of the finger segments (PIPs and DIPs). In addition, for example, as the cylinder diameter increased, the MCP joints of the middle finger at the maximum open and the final posture extended at the average rate of 2.5 and 3.6°/cm, respectively. As to the effect of the hand length, the maximum open and the final posture of the middle MCP joint flexed at the average rate of 1.4 and 1.6°/cm, respectively, as the subject's hand length increased. The object orientation was a significant factor only for the final posture ($p < 0.05$). Similar to other fingers, the linear regression better explained the proximal joint (CMC) of the thumb.

In case of the temporal parameters, reach distance was the most influential factor on the total, delay, open, and reach times at almost all joints ($p < 0.001$). Those temporal parameters increased when the object was positioned farther, as the positive coefficients (β_d) implied. In addition, the temporal parameters decreased for gripping a larger size cylinder. This decrease could be due to the effect of the object size on the final posture, which is that a larger object needs less finger flexion. Note that the reach time is independent of finger joint movements since it is defined by the hand transportation – distance between the hand and the object. The results of the total, open, and reach times

Table 2.2. The coefficients (β_c, β_o, β_s, β_l, β_d) of linear regression (equations (2.2) - (2.4)), for temporal (t_{delay}, t_{open}, t_{reach}, t_{total}) and spatial parameters (θ_i, θ_o, θ_f) of all finger joints. The coefficients of effects that are considered significant for each parameter are listed.

Spatial Parameters	Finger joints	constant β_c (°)	orientation β_o (°)	size β_s (°/cm)	hand length β_l (°/cm)	R²	Temporal Parameters	constant β_c (sec)	distance β_d (sec/cm)	size β_s (sec/cm)	R²
θ_i (°)	CMC	-129.08	-	-0.27	8.98	**0.55**		0.056	0.003	-0.006	0.21
	MCP1	-9.79	-	0.33	0.91	0.06		0.009	0.003	-0.003	0.20
	IP	34.98	-	0.39	-1.11	0.17		0.038	0.003	-0.002	0.15
	MCP2	48.08	-	-0.63	0.02	0.08		0.007	0.003	-0.004	0.16
	PIP2	78.65	-	-0.09	-2.65	0.28		0.024	0.003	-0.001	0.10
	DIP2	-1.92	-	0.09	0.69	0.02		0.070	0.002	-0.004	0.11
	MCP3	74.68	-	-1.22	-1.37	0.13		0.017	0.003	-0.005	0.17
	PIP3	113.95	-	0.11	-4.41	0.32	t_{delay} (sec)	0.039	0.003	-0.003	0.15
	DIP3	4.98	-	0.04	0.38	0.01		0.074	0.002	-0.002	0.11
	MCP4	147.68	-	-0.87	-5.84	0.33		0.003	0.003	-0.003	0.16
	PIP4	110.65	-	0.25	-4.01	0.23		0.028	0.003	-0.004	0.22
	DIP4	-24.88	-	0.22	2.06	0.12		0.029	0.003	-0.002	0.17
	MCP5	145.88	-	-1.01	-5.48	0.37		0.046	0.003	-0.006	0.19
	PIP5	85.31	-	0.24	-3.09	0.16		0.025	0.003	-0.005	0.22
	DIP5	-14.75	-	0.57	1.42	0.09		0.014	0.004	-0.003	0.22
θ_o (°)	CMC	-102.28	-	-1.07	7.45	**0.53**		0.752	0.013	-0.022	0.37
	MCP1	-128.53	-	0.34	6.66	**0.55**		0.842	0.007	-0.014	0.15
	IP	-37.86	-	0.09	2.59	0.23		0.692	0.012	-0.010	0.25
	MCP2	53.74	-	-1.27	-0.60	0.38		0.872	0.010	-0.008	0.19
	PIP2	-4.67	-	-0.17	1.17	0.05		0.900	0.008	-0.020	0.20
	DIP2	-3.02	-	-0.04	0.57	0.02		0.764	0.013	-0.015	0.24
	MCP3	15.97	-	-2.53	1.44	**0.63**		0.914	0.009	-0.001	0.12
	PIP3	63.22	-	-0.26	-2.10	0.07	t_{total} (sec)	0.867	0.008	-0.021	0.23
	DIP3	-3.62	-	0.11	0.61	0.09		0.809	0.012	-0.013	0.17
	MCP4	55.55	-	-1.94	-1.28	**0.61**		0.987	0.009	-0.013	0.14
	PIP4	66.08	-	-0.82	-1.94	0.23		0.746	0.012	-0.020	0.30
	DIP4	-60.49	-	0.27	3.64	0.32		0.775	0.011	-0.004	0.14
	MCP5	93.24	-	-1.82	-2.90	**0.57**		0.962	0.012	-0.017	0.18
	PIP5	-6.05	-	-0.53	1.25	0.10		0.675	0.013	-0.009	0.21
	DIP5	-34.64	-	0.22	2.26	0.25		0.700	0.015	-0.002	0.17
θ_f (°)	CMC	-59.33	1.97	-2.58	6.24	**0.66**		0.122	0.007	0.016	0.30
	MCP1	-94.18	0.88	0.61	5.17	0.32		0.379	0.003	-0.007	0.07
	IP	-22.88	2.92	-0.01	2.14	0.18		0.217	0.007	0.003	0.15
	MCP2	29.45	-5.63	-2.17	1.93	**0.66**		0.310	0.003	-0.001	0.02
	PIP2	36.96	6.12	-0.27	-0.72	0.10		0.376	0.006	-0.006	0.20
	DIP2	23.46	1.40	-0.01	-0.45	0.01		0.289	0.006	0.000	0.09
	MCP3	39.00	-5.09	-3.58	1.63	**0.75**		0.258	0.004	0.008	0.13
	PIP3	75.80	1.19	-0.65	-2.20	0.08	t_{open} (sec)	0.274	0.008	-0.005	0.25
	DIP3	-7.17	-0.97	0.03	1.32	0.05		0.242	0.007	-0.003	0.15
	MCP4	73.28	-5.23	-3.29	-0.55	**0.78**		0.302	0.003	0.004	0.05
	PIP4	92.13	-0.36	-0.84	-2.80	0.16		0.295	0.007	-0.001	0.23
	DIP4	-79.26	-4.54	0.53	5.12	0.30		0.343	0.008	-0.014	0.25
	MCP5	93.46	-6.47	-3.24	-1.30	**0.76**		0.219	0.005	0.009	0.19
	PIP5	-7.63	-9.19	-0.78	1.97	0.39		0.316	0.008	0.003	0.17
	DIP5	-2.75	-5.86	0.20	1.11	0.11		0.237	0.006	0.004	0.08
							t_{reach}	0.564	0.011	-0.012	0.32

were comparable to those observations reported by Chieffi and Gentilucci [29], as further considered in Discussion.

2.3.2. The finger motion model of reach and grasp

The finger motion of each finger joint was constructed fitting a fourth order polynomial function to the mean observed finger joint angle trajectories for a given condition. Each trial for the given condition was first normalized during the open and close periods, sampled for 100 points, and then averaged for all subjects. Some trials were removed because of an extended period of data loss or abnormal behavior.

Figure 2.4 shows finger joint angles from all subjects and their mean trajectory and standard deviation over normalized time for reaching 40cm and pinching a vertically oriented 3.8cm diameter cylinder. Although some trials are apart from others, especially for the MCP joint, they also followed a similar pattern of opening and closing the fist. The inputs to the model were three spatial parameters – the initial (θ_i), the final (θ_f) and the maximum open angle (θ_o) – of the mean joint angle profile and two mean temporal parameters – the delay (t_{delay}) and the total time (t_{total}). Since the resultant model equations were a function of normalized time, it was necessary to reconstruct them in real time using the relation between real time and normalized time defined by equation (2.5). In addition, a constant delay period, which was removed in the model, also had to be restored by adding the initial angle (θ_i) during the delay period.
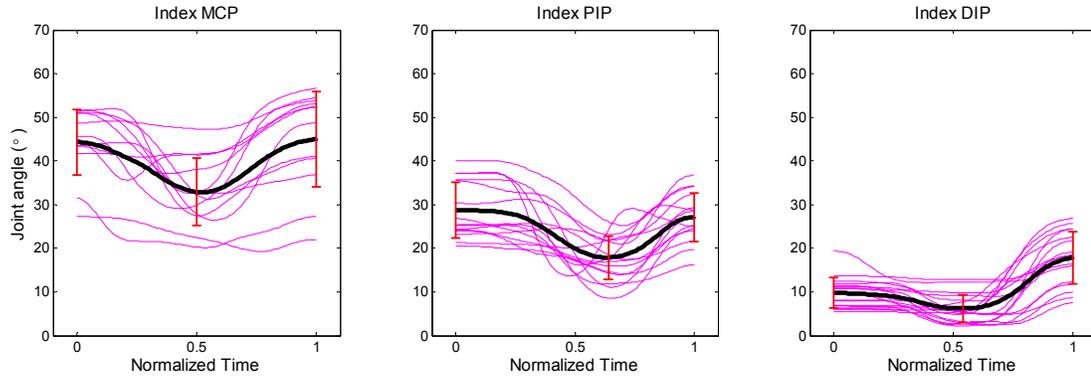
Figure 2.4. Index finger joint angles from all subjects and their mean trajectory (thick line) and standard deviation (errorbars) across all subjects for reaching 40cm and pinching a vertically oriented 3.8cm diameter cylinder.

Figure 2.5 shows the mean observed joint angle profiles and model predictions of the index finger for the aforementioned condition (reaching 40cm and pinching a vertically oriented 3.8cm diameter cylinder). The model's predicted finger motion looked very close to the observed mean profile for each joint. To quantitatively clarify how well the model predicted finger motion, Table 2.3 lists the model equations for each finger joint along with corresponding coefficients of determination (R^2) and root-mean-squared-errors (RMSEs). The R^2 provides information about the goodness of fit of the model by measuring the residual errors between the observed data and the modeled values. The RMSE is a good measure of accuracy in that it represents how much the difference between the observed data and the modeled values is in the same unit as the data. For all conditions, the finger motion model resulted in the R^2 ranging from 0.54 to 1.00 and the RMSE from 0.04° to 5.83°. Excluding the proximal joints (CMC joint for a thumb and MCP joints for digits 2-5), the model prediction improved with mean R^2 and RMSE of 0.94 (±0.07) and 0.76 (±0.68)°, respectively, when compared to 0.93 (±0.07) and 1.17 (±1.01)° for all joints. This might largely result from imprecise prediction of maximum open timing in the proximal joints; in experimental results, CMC and MCP joints often ended their opening earlier than the other joints, whereas the model prediction gives consistent maximum open timing for all joints. In addition, the temporal parameters, the delay and the total time, are also presented in Table 2.3. The delay time forms 13 percent of the total time on average for this given condition, and the knowledge of the delay and

21
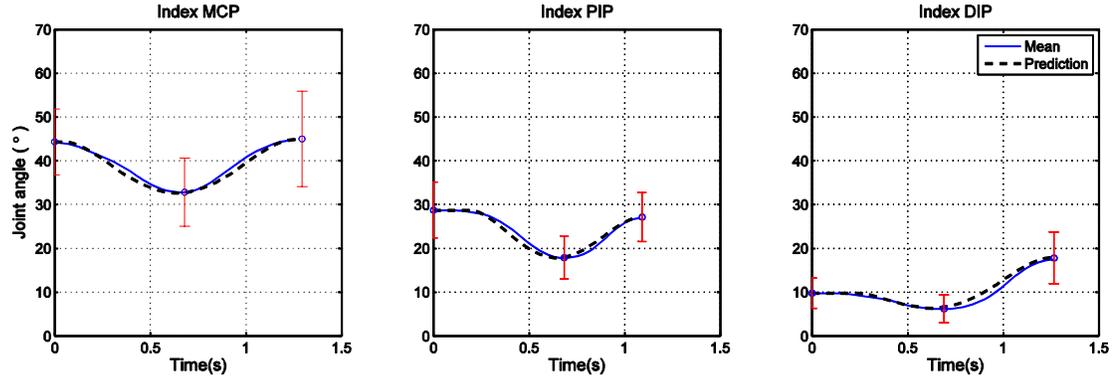
Figure 2.5. Mean observations (solid) and model predictions (dash) of the index finger joint angles for reaching 40cm and pinching a vertically oriented 3.8cm diameter cylinder (See Table 2.3). Error bars show standard deviation of spatial parameters (θ_i, θ_o, θ_f).

Table 2.3. Model equations (equation (2.6)) and their comparison (R^2, RMSE) with mean observations of all finger joints for one condition (reach 40cm and pulp-pinch a vertically oriented 3.8 cm diameter cylinder). Temporal inputs (t_{delay}, t_{total}) to the model are also shown.

	Model Equation (°)	R^2	RMSE(°)	t_{delay} (sec)	t_{total} (sec)
CMC	$-137\tau^4 + 251\tau^3 - 102^2 + 39$	0.99	0.62	0.20	1.17
MCP1	$-91\tau^4 + 184\tau^3 - 95^2 + 7$	0.95	0.70	0.12	1.05
IP	$-108\tau^4 + 211\tau^3 - 102^2 + 17$	0.99	0.26	0.20	1.25
MCP2	$-189\tau^4 + 377\tau^3 - 187^2 + 44$	0.99	0.72	0.04	1.29
PIP2	$-161\tau^4 + 325\tau^3 - 165\tau^2 + 29$	0.97	0.74	0.19	1.09
DIP2	$-111\tau^4 + 205\tau^3 - 87\tau^2 + 10$	0.98	0.63	0.22	1.27
MCP3	$-245\tau^4 + 479\tau^3 - 228\tau^2 + 41$	0.95	1.78	0.11	1.36
PIP3	$-121\tau^4 + 258\tau^3 - 144\tau^2 + 30$	0.95	1.07	0.12	1.02
DIP3	$-152\tau^4 + 287\tau^3 - 127\tau^2 + 13$	0.96	0.97	0.14	1.35
MCP4	$-243\tau^4 + 470\tau^3 - 220\tau^2 + 37$	0.85	2.90	0.14	1.43
PIP4	$-91\tau^4 + 196\tau^3 - 112\tau^2 + 29$	0.99	0.44	0.19	1.09
DIP4	$-134\tau^4 + 269\tau^3 - 134\tau^2 + 14$	0.94	0.78	0.14	1.30
MCP5	$-195\tau^4 + 377\tau^3 - 174\tau^2 + 39$	0.95	1.25	0.23	1.37
PIP5	$-160\tau^4 + 358\tau^3 - 216\tau^2 + 29$	0.98	1.39	0.19	1.55
DIP5	$-103\tau^4 + 217\tau^3 - 119\tau^2 + 16$	0.99	0.36	0.22	1.46

the total time enables reconstruction of the model prediction in real time. Since the three spatial parameters (θ_i, θ_f, θ_o) are independent of reach distance ($p>0.05$), the model equations in Table 2.3 might be applicable to the other reach distance conditions by using the corresponding temporal parameters determined from the empirical study.

The finger motion model prediction could assess the possible relationship between adjacent joint angles for a given finger during reach and grasp. For each finger in a given condition, a line was fitted to relate PIP to MCP joint angle and also to relate DIP to PIP joint angle. Table 2.4 shows mean regression assessment of the relationship between PIP (θ_2) and MCP (θ_1) as well as DIP (θ_3) and PIP for all eighteen object conditions on the open and close phases. For each comparison, a longer piece of data was properly cropped to match the shorter one. During both open and close phases, highly linear relationships between adjacent joint angles were found in each period ($R^2 > 0.95$). During the open phase, θ_2/θ_1 slope was significantly larger than θ_3/θ_2, while the close phase resulted in larger θ_3/θ_2 ($p<0.05$). In a comparison between the open and close phases, θ_2/θ_1 slope was significantly larger for the open than for the close period ($p<0.05$).

Table 2.4. Mean linear regression assessment (slope, R^2) of the relationship between pairs of joints from model predictions for all conditions and all fingers.

| | θ_2 / θ_1 (PIP/MCP) | | | | θ_3 / θ_2 (DIP/PIP) | | | |
| | Open | | Close | | Open | | Close | |
Finger	Slope	R^2	Slope	R^2	Slope	R^2	Slope	R^2
Thumb[a]	1.93	0.97	0.73	0.98	0.92	0.98	1.14	0.97
Index	1.57	0.96	0.88	0.98	0.33	0.98	0.83	0.98
Middle	0.72	0.98	0.78	0.95	0.44	0.99	0.76	0.97
Ring	0.85	0.98	0.74	0.97	0.66	0.99	0.73	0.97
Little	1.81	0.98	0.60	0.96	0.43	0.98	1.02	0.96

[a] For the thumb, θ_1 is a CMC, θ_2 is an MCP, and θ_3 is an IP joint angle.

2.3.3. Implementation of the finger motion model in a kinematic model

The empirical study results provide the inputs that are necessary for the finger motion model to predict finger motion over time. The fourth order polynomial function successfully predicted the finger motion close to the experimental results. Since these empirical-oriented models do not consider the physical contact between the hand and the work object, we need to implement them into a kinematic model for employing contact algorithms. To demonstrate the implementation, a simulation was performed, where we need to predict the finger motion for reaching and pulp-pinching a cylindrical handle of 5cm diameter located at 30cm reach distance by a male with 50% hand length.

Figure 2.6 illustrates a joint angle profile predicted by the finger motion model along with contact algorithms: (A) the MCP joint of the index finger, and (B) the MCP joint of the ring finger. The finger motion model prediction guides finger joints until the contact is detected by contact algorithms. Since it is not known whether real contact would be detected within the model prediction trajectory, we define a threshold time, after which linear extrapolation is needed. Although there are several feasible ways to select the threshold time, the preferred candidate is reach time, which indicates the period where the hand is in reach motion. Employing the reach time can be physically meaningful: (1) finger joints are in deceleration after finishing the hand transportation, and (2) the reach time can be determined from the empirical study. By this implementation, the accuracy of the final posture prediction can be considerably improved; however, this comes at the cost of change in temporal aspects of movement, i.e., the total time (t_{total}). Additionally, Figure 2.6C shows simulation of hand postures shown on the kinematic hand model.
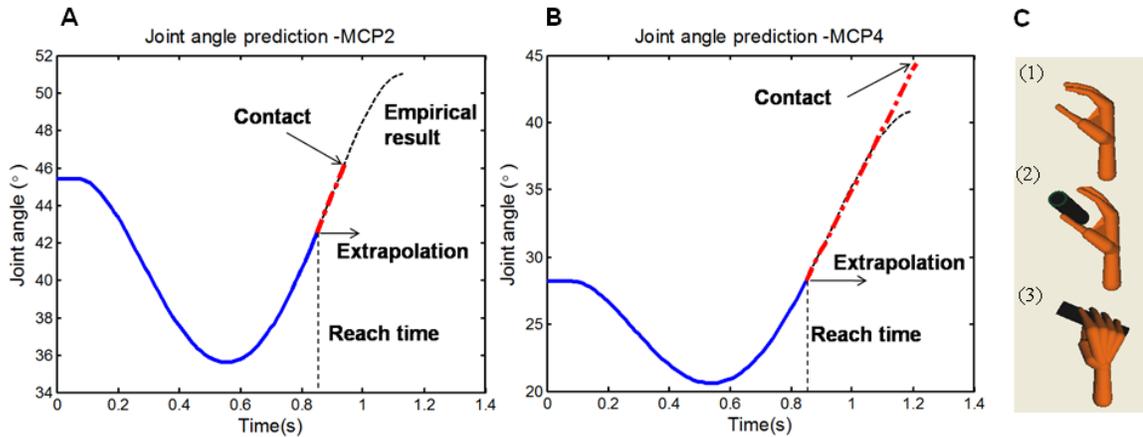
Figure 2.6. Joint angle profiles predicted by the finger motion model and contact algorithms when the contact occurs after the threshold time ($t_{TS} = t_{reach}$), (A) of the index MCP joint, (B) of the ring MCP joint. (C) Graphical representations of the hand on a kinematic hand model, (1) initial, (2) maximum open, (3) final posture.

2.3.4. Application to an industrial job: tendon excursion

To illustrate potential application of the proposed finger motion model, an industrial job was selected for further analysis on tendon excursion. A corn-packing job contains repetitive movement of both hands (Figure 2.7), but we consider one hand movement only in this analysis. The job cycle starts from reaching and gripping a corn (reach/grasp, Figure 2.7A-B), followed by moving and releasing it (movement/release, Figure 2.7C). Video observations of the job led to the following assumptions that can simplify the problem:

(1)   Worker: 50% male by hand length

(2)   Object condition: A corn (D=5cm) is axially located at 30cm reach distance.

(3)   Total cycle time: 1.7 sec/cycle

(4) $t_{movement} = t_{reach/grasp}$, where $t_{movement}$ is duration of movement and $t_{reach/grasp}$ is duration of reach and grasp.

(5) $t_{release} = 0.3 \times t_{reach/grasp}$, where $t_{release}$ is duration of release.

Figure 2.7. A corn-packing job cycle: (A) Initial posture, (B) reach/grasp, (C) move/release.

Based on those assumptions, finger joint angles during reach and grasp can be predicted by the finger motion model combined with contact algorithms, as described previously in 3.3. During movement period after reach and grasp, no change in finger joint angles was assumed, followed by release period, where the final posture returns to the initial posture. The release period was approximated using piecewise cubic hermite interpolation polynomial. The resultant prediction of index finger movement for one cycle of the job is shown in Figure 2.8A.
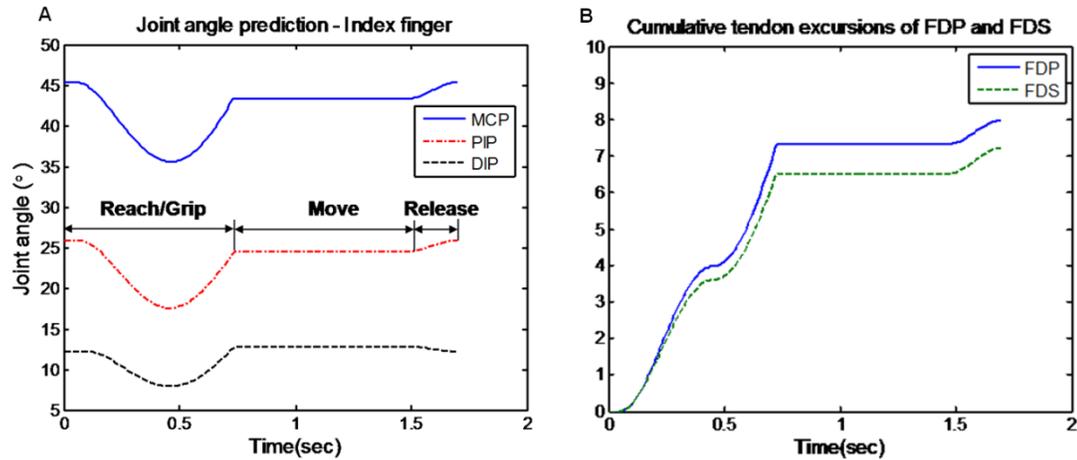
Figure 2.8. (A) Index finger joint angle prediction during one cycle (reach/grip, movement, release). (B) Cumulative tendon excursions of the FDP and FDS tendon of the index finger.

From finger posture predictions, tendon excursions of the flexor digitorum profundus (FDP) and flexor digitorum superficialis (FDS) at the finger joints (MCP, PIP, DIP) could be calculated using the predictive model developed by Armstrong and Chaffin [14]. Subsequently, cumulative tendon excursions (CTE), indicating the distance that the tendons travel, were computed for one cycle of hand movement (Figure 2.8B). For the purpose of comparison between different jobs, a normalized CTE is used to specify the distance for a given amount of time (i.e., one hour). Normalized CTEs of the index finger were 16.9m/hr and 15.3m/hr for FDP and FDS, respectively. These were comparable to CTEs observed at hand and wrist of low repetition tasks from Moore et al. [20] and to CTEs observed at wrist of medium-risk jobs from Choi [3].

2.4. DISCUSSION

This study aimed to develop a model that describes human finger motion for simulation of reach and grasp for selected objects and tasks. As a grip type, we chose a pulp pinch grip, in which the contact is supposed to occur at the tips of the fingers and the tip of the thumb. The selection of this grip type could be justified by comparing our observations to previous studies. For smaller objects, all contact was between the tip of

the thumb and the tips of the fingers; however, as the object size was increased, there was increasing contact between the object and proximal portions of the fingers and the thumb and the palm. Although these postures are similar in form to precision and power grip as described by Napier [54], they are different functionally in that our subjects did not apply significant force or manipulate the object. Rather, they were similar to postures observed in both field and laboratory studies. Grieshaber and Armstrong [52] observed that workers in assembly line often use both pinch and grip postures to grasp and manipulate work objects, such as flexible hoses. Additionally, Seo et al. [53] have examined pressure distributions between the hand and various size cylinders, and found that the pressure distribution is concentrated mainly on the tips of the fingers and the thumb. Depending on the diameter of the object, the fingers and the thumb may oppose each other or they may work together against the palm. In either case, the tips of the fingers and the thumb are the primary source of coupling force.

We performed an empirical study that describes the finger joint angles and timing of joint angle changes across reach and grasp as a function of the object attributes, such as object size and orientation and reach distance, and hand length. This investigation of finger joint motion could enhance a way to describe prehension with more detail than previous studies that had described prehension by simple parameters, such as aperture or fingertip trajectories [27, 45]. The statistical analyses showed significant effects of those object attributes on finger joint angles and timing of their changes, indicating that the transport component and the grasp component were affected by extrinsic (distance and orientation) and intrinsic (size) object properties, respectively, as found by Jeannerod [27]. For spatial parameters, object size was the most influential factor, which accounts for 40-76% of the variance not accounted for by the other factors, followed by hand length (1-19%), object orientation (1-18%), and reach distance (0-8%). For example, the maximum hand opening (θ_o) was shown to be a function of the object size and hand length, as other studies found that maximum grip aperture was positively related to the object size [27, 29-31]. The object orientation was added to explain the final grip posture (θ_f); in particular, change of the object orientation produced considerable difference of the proximal joint postures, which suggested that the proximal joint of each finger plays a

primary role in adjusting the grip posture to a given object orientation. It was also noticeable that the initial angles (θ_i) of the MCP joints decreased as the size of the objects increased ($p<0.05$). For instance, the middle MCP joint extended more by about 11° for 10.3cm handle than for the 1.3cm handle, while there was little difference in the PIP and DIP joints. In other words, subjects tended to shape their hands in anticipation of reach for a given object condition. Further studies are required for actual work tasks because θ_i's would be more determined by the interaction between successive tasks. Conversely, reach distance was not a significant factor on the spatial parameters, including the maximum hand opening, in contradiction to earlier results showing that hand opening tended to decrease or increase with object distance [29-31]. This discrepancy might be attributable to the difference in representing the hand posture, in that earlier studies used the aperture whereas we employed finger joint angles.

In case of temporal characteristics, reach distance was proved to be the most dominant factor accounting for 10-24% of the variance not accounted for by the other factors, followed by object size (0-14%), orientation (0-9%), and hand length (0-2%), in accordance with other studies [29-31]. However, those previous studies showed inconsistency in the effect of object size on temporal aspects, although our study showed that the total time would decrease when a larger object is presented. This is reasonable given that a larger object would tend to produce earlier contact. Figure 2.9 compares our model prediction of the temporal parameters – total and reach time – with Chieffi and Gentilucci [29] and the MTM technique [59], one of traditional predetermined motion time systems. The assumed task was selected to match Chieffi's experiment condition (reaching 17.5 cm and grasping a 3.5 cm diameter cylinder), and the MCP joint of the index finger was chosen to represent our empirical study. Work elements for MTM analysis were R7A (reaching 7 in for an object at a fixed location) and G1A (pick up any size object by itself or easily grasped). Note that total time of our model and Chieffi's experiment is decomposed into reach and grasp time for comparison to MTM work elements. Our model results showed that grasp is finished 0.3 second after reach is completed, as Figure 2.2 indicates. Although our model predicted greater reach and grasp time than Chieffi's experiment, the two methods produced closer results than MTM

results. A possible main cause was that MTM gave an estimation of the normal work time, i.e., the time expected for most well trained workers, whereas the other results came from self-paced non-workers.
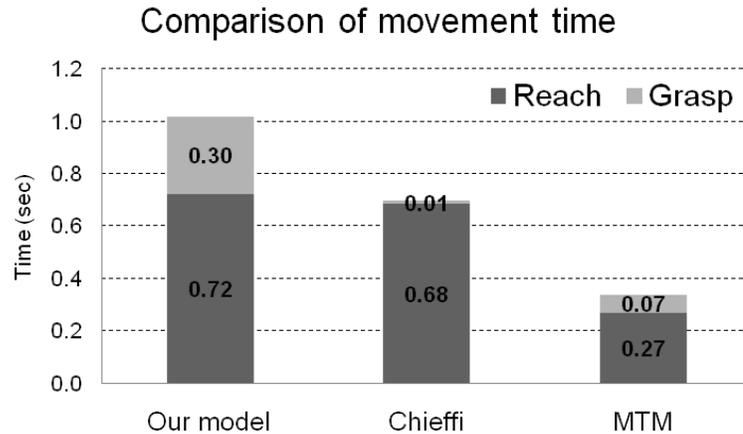
Figure 2.9. Comparison of temporal parameters prediction (total and reach times) with Chieffi and Gentilucci [29] and the MTM technique [59] for the case reaching 17.5 cm and grasping a cylinder of 3.5 cm diameter. MTM elements correspond to R7A and G1A.

To predict finger motion using its spatial and temporal characteristics under a given object condition, we proposed a constrained fourth order polynomial. Although the model prediction of the open time did not exactly agree with observations because of no temporal constraints imposed on the model formulation, it matched well with the observed motion as a whole. For validation of the finger motion model, the model predictions were compared with previous studies by considering relationships between pairs of joints in a finger and between adjacent fingers for a given type of joint. The linear relationship well explained the PIP-MCP and the DIP-PIP correspondence with the mean slope of 0.99 and 0.65 for combined open and close periods across fingers from the index to little fingers (Table 2.4), respectively, where the slopes were between those described by others [60, 61]. It was also noticeable that the pattern of the relative finger

joint movement depended on the movement phase, open or close. The proximal finger joints have greater change in displacement when the hand opens, whereas the distal finger joints are relatively more activated during the close phase. In addition, movement in one finger was closely correlated with the other fingers for a given joint. The coefficients of determination (R^2) for the MCP and PIP, ranging from 0.77 to 0.98, were even larger than those within a finger, as other studies showed [60, 62]. The highly correlated finger movement between finger joints suggests that although there exists variability between subjects (Figure 2.4), finger motion can be characterized in a consistent way for all subjects.

The proposed model is a statistical description of observed hand movement and finger motion. An important feature of the proposed model is the prediction of finger rotations during opening and closing the fist. However, it does not consider physical contact between the hand and the object. By using a kinematic model equipped with contact algorithms [3], we can predict the contact location on the object surface and the final grip posture. The feasibility of combining those two models was demonstrated and it was shown that the combination can result in more realistic and accurate prediction of the whole hand posture from reaching to grasping.

There are a few limitations that merit discussion. First, this study was performed for a small set of object conditions with cylindrical handles of three sizes, two orientations, and three reach distances and the selected grip type (pulp pinch grip). Those limited object conditions confine application of our empirical study, which was based on linear regression, to conditions within considered ranges of objects (interpolation), rather than to those beyond (extrapolation). Also, further study is needed to examine how finger motion is affected by the selection of different final postures (e.g., pinch vs. grip) for subsequent force applications. Second, a sample size of six right-handed university students provided limited statistical power and represented only a limited subset of the whole population. Although it can determine the relative importance of factors in the empirical study and demonstrate the proposed polynomial for describing the opening and closing of the fist, a larger sample size is needed to capture additional variability between subjects caused by age, anthropometry, and work experience. Third, this study used

surface-marker defined joint angles, which might have resulted in differences from kinematic joint angles, although reliability of using 3D video motion analysis has been evaluated [56]. Fourth, since only flexion and extension of finger joints were examined, prediction of the thumb CMC and the MCP joints cannot be entirely accurate because of the palm arch, especially for grasping non-cylindrical work objects such as spherical shapes [63]. Lastly, for predicting the final posture in the kinematic model where the finger motion model was implemented, an empirical model developed by Choi [3] was used to provide the relative position of the object with respect to the hand at grasping. The spatial relationship between the hand and the object at grasping, along with the degrees of freedom in the CMC and the MCP joints, would affect the prediction of the final posture and the location of fingers on the object.

However, applications of the proposed model can be extended to a wider range of conditions – different shapes, sizes, and orientations of the grip object as well as hand length – in that this requires only some characteristic parameters. Not only can the finger motion model guide digital human models similar to the way to human movement, but its prediction of finger motion can also be used to estimate tendon excursions and required space during reaching and grasping. Since biomechanical models that predict muscular forces of the hand, or hand strength, are derived using the relationship between tendon displacements and finger joint postures, kinematic models capable of predicting tendon excursions can play an important role in developing biomechanical models [64-67]. On the other hand, few studies have investigated the space necessary to perform reach and grasp task, which can contribute to improving a work space design [3, 50]. Since industrial tasks, in particular, often involve repeated hand motion, including reach and grasp as well as manipulation, we will be able to evaluate jobs by required spaces and tendon excursions using the proposed model and to offer necessary information for ways of preventing WMSDs.

2.5. CONCLUSIONS

This study proposed a finger motion model that can predict hand posture during reach and grasp. Based on statistical analyses of human behavior, the finger motion

model could predict how the hand opens and closes in finger-joint-level detail. By combining this model with contact algorithms, prediction of the final hand posture was improved to be accurate and realistic through simulation of finger motion. The proposed model could be applied to solving ergonomic issues in industries, such as predicting tendon excursions for repetitive manual work.

CHAPTER 3

THE EFFECT OF OBJECT SHAPE ON HAND POSTURE DURING REACH AND GRASP

ABSTRACT

This study examined how hand shaping occurs while reaching for and grasping objects of various sizes and shapes, and how hand shaping might most efficiently be described during such prehensile motions. Hand shaping has been investigated using aperture and finger joint angles, but these metrics are either limited or inefficient for describing finger shape. For enhanced description of hand shape, this study proposes two new metrics, called openness and flatness. These metrics characterize hand shape by describing the shape and position of each finger relative to the palm. Openness indicates the positions of finger-tips based on MCP joint angles. Flatness indicates the extent to which each finger is flat or curved, based on the PIP joint angles. The two metrics were employed to test the hypothesis that hand shaping during reach and grasp is affected by object size and shape. Objects were divided into two groups according to their aspect ratios (cylinders and rectangular or square prisms in one group, and spheres and cubes in the other). Grasping objects with a long axis resulted in greater maximum opening, especially for the index (up to 25%) and little finger (up to 9%), than symmetric objects. This tendency persisted to the final posture, which implies that finger movement is prepared carefully from the middle to the end of movement. Flatness identified the effect of object shape on the final posture, eliciting that grasping symmetric objects resulted in less flatness for smaller objects (up to 41%) but greater flatness (up to 17%) for large objects. Within a group with the same aspect ratio, objects whose surfaces contain edges

generally induced greater hand opening than objects without edges (up to 12% greater openness for cubes than spheres), possibly due to ensuring sufficient clearance. The present results suggest that object shape determine the coordination pattern for finger movement, and that this pattern can be quantified in an efficient form for prediction of hand posture.

3.1. INTRODUCTION

Planning and execution of prehensile movements depend on properties of the target object, such as its size and shape. The relationship between hand shaping and object attributes is required for predicting finger motion and is an integral part of kinematic hand models [12, 13, 68]. Hand posture during reach and grasp affects the required space for the hand [50], the fit of tools for the hand [10], and the risk of work-related musculoskeletal disorders in the upper extremities [3, 20].

Jeannerod [27] proposed that prehension can be understood using two independent components: the transport (hand transportation or reach) and the grasp (finger grip formation). The two components were shown to be planned before hand movement begins [69, 70], and some investigators developed models for hand movement prediction based on the assumption that final hand posture is predetermined [45, 71]. Support for this claim has been provided by observing different characteristics between postures prior to the contact and at the contact in the upper extremities [37, 40, 72, 73]. Although those studies showed that final hand posture is predictable for given object attributes, they did not consider intermediate postures between the beginning and end of reach and grasp. Quantitative description of finger motion from reach to grasp is needed to construct kinematic models capable of predicting hand posture [3, 13].

It has been established that hand posture is executed in a manner that reflects given object attributes to accordingly achieve reach and grasp. The transport and the grasp are believed to be based on information processed by two visuomotor channels, the first involving extrinsic object properties (having to do with the object's relationship with the environment, e.g., distance) and the second involving intrinsic object properties (having to do with the object itself, e.g., size, shape), respectively [27]. Aperture (the distance between the thumb tip and the index fingertip) has been used almost universally to describe the effect of object properties on the grasp. For example, maximum aperture during reach increases for grasping larger objects [29, 30, 74], where the slope of the maximum aperture versus object size (e.g., cylinder diameter, rectangular block width) is about 0.77 [28, 32], and time to maximum aperture occurs earlier for grasping smaller

objects [74]. Cuijpers et al. [33] showed that the maximum grip aperture during reach is scaled to both an object's depth (the dimension along an axis from the subject to the object) and width (the dimension perpendicular to depth). Some studies instead employed finger joint angles to examine the effect of object properties on hand posture. By measuring the metacarpo-phalangeal (MCP) and the proximal inter-phalangeal (PIP) joint angles, Santello and Soechting [34] showed that the effect of object shape (flat, concave, convex) on hand shaping is weak throughout much of reaching but becomes stronger as the hand approaches the object. Bae and Armstrong [68] showed that object size, orientation, and reach distance affect spatial and temporal characteristics of finger joint angle profiles during reach and grasp. However, the relationship between hand posture and object shape (e.g., cylinder, sphere) has not been systematically explored.

While simple metrics used to describe hand posture may be efficient, they are of limited use for capturing detail, especially hand shape during reaching motion that may be tied to the shape of the target object. Aperture by itself does not define hand shape in terms of finger joints nor in terms of individual fingers. On the other hand, an array of finger joint angles is overly complicated for illustrating hand shaping. To address some of these limitations, Supuk et al. [75] proposed the use of a planar pentagon, formed by interconnecting the tips of adjacent fingers, as a model for quantitative estimation of hand shape. The pentagon model describes overall hand shape, but does not contain information about individual finger postures.

In this study, we propose two descriptive metrics, 'openness' and 'flatness', to describe hand shaping during reach and grasp. The two metrics are formulated in vectors to indicate both the opening of the fingers to encompass an object (openness) and the general shape of an individual finger (flatness). To evaluate the utility of these metrics, we test the hypothesis that the effect of object size and shape on hand posture can be captured neatly and efficiently using openness and flatness. Specifically, the present study is concerned with how hand shaping for reach and grasp is affected by knowledge of object size and shape (aspect ratio and cross-sectional shape) and with how the effect of object shape can be quantified to predict hand postures for grasping various shapes of objects.

37

3.2. METHODS

To achieve the stated aims, hand postures were measured while subjects reached for and grasped objects of various sizes and shapes. A motion capture system recorded the three-dimensional locations of markers secured to the hand and fingers, from which the inter-digit joint angles in each finger were ascertained during reach and grasp. Using this joint angle information, new metrics were proposed to obtain a concise and functional description of hand posture.

3.2.1. Experimental protocol

Eight right-handed subjects (4 males, 4 females) from the University of Michigan student population, who had no history of upper extremity disorders, participated in the experiment. Male and female subjects were selected to obtain a wide range of hand size, from 20 percentile female to 80 percentile male [55]. Subjects were seated before the table, on which objects were presented individually at elbow height on the sagittal plane at a horizontal reach distance (from the wrist center to the object) of 35cm. The experiment design included two independent variables: (1) object size (small: 2.5cm, medium: 5cm, large: 10cm), and (2) object shape (cylinder, square-prism, rectangular-prism, cube, sphere (Figure 3.1)). Five shapes of objects were divided into two groups based on their aspect ratios (AR): Spheres and cubes belong to a group of AR 1, whereas cylinder, square prism, and rectangle prism correspond to a group of AR larger than 1. One geometric dimension represents each object shape; for example, a diameter for cylinders and spheres, an edge length of cross-section for square-prisms and cubes, and a frontal edge length (width) of cross-section for rectangular-prisms (width×depth: 2.5×10cm, 5×10cm, 10×2.5cm). Independent variables were presented in a random order with three repetitions for each condition. Objects with a long axis (cylinder and square/rectangular-prisms) were presented in a vertical orientation.
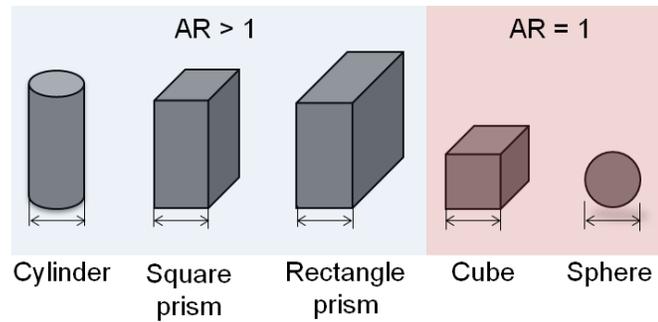
Figure 3.1. Object shapes of the same representative size (arrow): one group contains objects with a long axis (aspect ratio (AR)>1), and the other group includes symmetric objects (AR=1).

Before recording the data, subjects were asked to practice reaching for and grasping a given object with a pulp pinch grip at a comfortable speed, then lifting and placing the object to the side. They were also asked to maintain torso posture during the task. Once subjects felt familiar with a given task, only the reach-to-grasp period was recorded. Subjects were instructed to start from the same posture, i.e., a thumb in contact with the index finger, to keep the initial posture consistent. Also, subjects were told to grasp a side surface of cylinders and prisms, and to grasp cubes and spheres from above to avoid constraint on the hand by contact with the ground. The experimental protocol was approved by the Institutional Review Board of the University of Michigan at Ann Arbor and all subjects gave written consent in advance of participating in the study.

3.2.2. Data acquisition and processing

Finger motion during reach and grasp was recorded using an OptoTrak® Certus™ motion tracking system (Northern Digital Inc.) with 32 markers attached to the right upper extremity of the subject and on the object; 30 markers were secured on the dorsal side of every tip and joint of the fingers and the wrist, including Distal Interphalangeal (DIP), Proximal Interphalangeal (PIP), and Metacarpophalangeal (MCP) joints along with Interphalangeal (IP) and Carpometacarpal (CMC) joints of the thumb. This 3D motion capture system with dorsal markers was chosen because its accuracy of

measurement compares favorably (within 5° errors) with that measured by kinematic linkages [56]. Two position sensors were properly located so as to simultaneously track the positions of markers during the task at a sampling frequency of 30 Hz with resolution of 0.01mm. If the sensors failed to capture some markers, that trial was removed and repeated.

The inter-digit joint angles of digits 2-5 were calculated from three dimensional marker position data using MATLAB® routines. For the DIP and PIP joints, dot products of the adjacent vectors, each of which represents each finger segment, were used for representing joint flexion from 0 to 180°. For the MCP joint angle calculation, it was necessary to consider hyperextension of the joint, which often occurred for grasping a large object. To do this, a normal vector of the plane (plane A) created by two adjacent MCP joints and a wrist marker position was selected as a reference vector, and a dot product between this normal vector and the MCP-to-PIP joint vector of a finger of interest was used for representing joint angles theoretically from 90° hyperextension to 90° flexion. To expand the range to greater than 90° flexion, the MCP-to-PIP joint vector was projected into the plane A, and a dot product between this projection vector and the MCP-to-wrist joint vector was used.

Joint angles were defined as zero when the adjacent vectors were aligned (fully extended posture) with positive values indicating flexion of the joints. The joint angle profiles were passed through a second-order Butterworth low-pass filter with a cutoff frequency of 3Hz to make the joint angle data more tractable. The Butterworth filter was chosen for its good all-around performance, and the selection of the cutoff frequency as well as the sampling frequency (30Hz) was justified on the basis of an examination of power spectral density, showing that the power below 3Hz was predominant (99.0% on average) in the raw data. Other investigators reported using a cutoff frequency of 5Hz [44, 57]. When there was only a small fraction of missing points in finger joint angle profiles, they were interpolated by piecewise-cubic-Hermite interpolation.

3.2.3. Metrics to describe hand shape

Hand movement during reach and grasp can be described by finger joint angles (Figure 3.2). Generally, finger joint angles start from an initial hand posture (θ_i), extend to the maximum open posture (θ_o), and then flex to the final posture (θ_f) when the hand contacts to grasp an object. The opening and closing of the hand is referred to as 'hand shaping'. An array of finger joint angles (MCP, PIP, DIP) provides more detail than necessary and does not embody hand shape in compact way. At the opposite extreme, finger aperture, which has been widely used to describe hand shaping, does not capture sufficient detail regarding hand shape; not only can multiple hand shapes generate the same aperture (Figure 3.3A-B), but also aperture alone cannot capture relative finger positioning (Figure 3.3C-D).
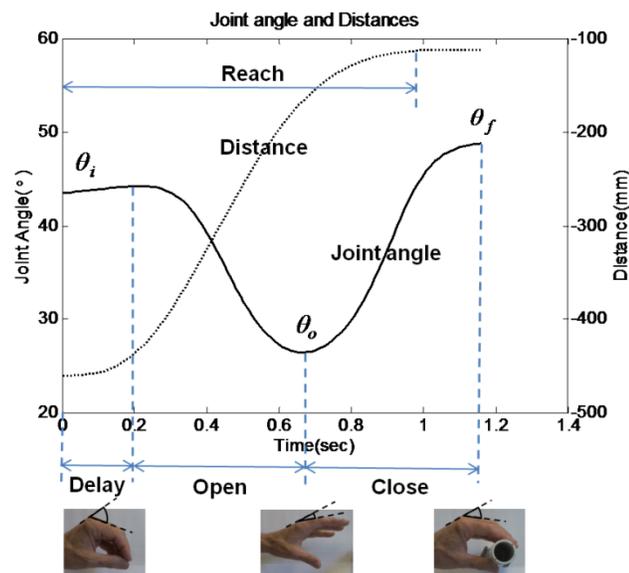
Figure 3.2. Profiles of a typical finger joint angle (solid) and distance (dotted) over time for reach and grasp with selected spatial and temporal parameters: Index MCP joint for reaching 40cm and pulp-pinching a vertically positioned 3.8cm diameter cylinder [68].
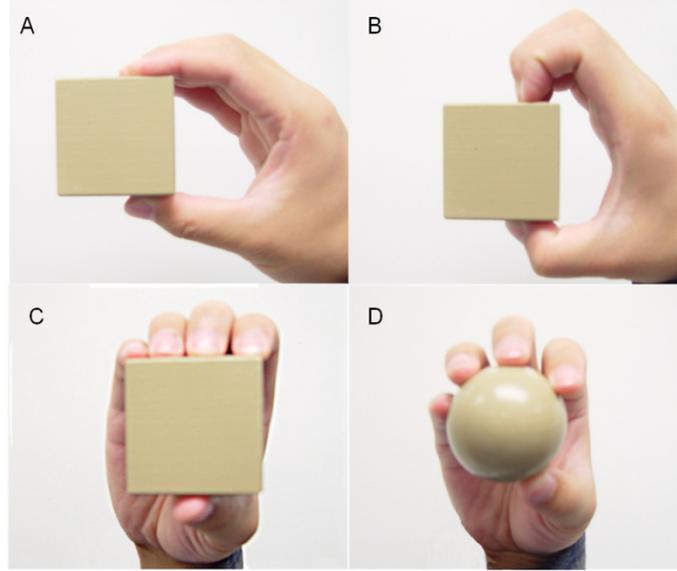
Figure 3.3. (A-B) Two different hand postures are possible for given aperture. (C-D) Relative finger positioning depends on object shapes.

To address this problem, we propose two metrics, 'openness' and 'flatness', to characterize the location and curvature of the fingers. Openness represents how far each fingertip is located from the palm, and flatness depicts whether each finger is close to flat or curved in shape. The openness level vector (**OL**) and the flatness level vector (**FL**) are composed of openness and flatness from each finger, respectively. A simple kinematic description of the finger segments can be used to define **OL**. Figure 3.4 illustrates a schematic diagram of the index finger with relevant joint angles and segment lengths. Based on a coordinate system anchored at the MCP joint, the position of the fingertip is represented:

$$x_{tip} = l_1 \cos\theta_{MCP} + l_2 \cos(\theta_{MCP} + \theta_{PIP}) + l_3 \cos(\theta_{MCP} + \theta_{PIP} + \theta_{DIP}) \tag{3.1}$$

$$y_{tip} = l_1 \sin\theta_{MCP} + l_2 \sin(\theta_{MCP} + \theta_{PIP}) + l_3 \sin(\theta_{MCP} + \theta_{PIP} + \theta_{DIP}) \tag{3.2}$$

from which the differential displacements are computed:

$$\Delta x_{tip} = -\left[l_1 \sin\theta_{MCP} + l_2 \sin(\theta_{MCP} + \theta_{PIP}) + l_3 \sin(\theta_{MCP} + \theta_{PIP} + \theta_{DIP})\right]\Delta\theta_{MCP}$$
$$-\left[l_2 \sin(\theta_{MCP} + \theta_{PIP}) + l_3 \sin(\theta_{MCP} + \theta_{PIP} + \theta_{DIP})\right]\Delta\theta_{PIP} \qquad (3.3)$$
$$-\left[l_3 \sin(\theta_{MCP} + \theta_{PIP} + \theta_{DIP})\right]\Delta\theta_{DIP}$$

$$\Delta y_{tip} = \left[l_1 \cos\theta_{MCP} + l_2 \cos(\theta_{MCP} + \theta_{PIP}) + l_3 \cos(\theta_{MCP} + \theta_{PIP} + \theta_{DIP})\right]\Delta\theta_{MCP}$$
$$+\left[l_2 \cos(\theta_{MCP} + \theta_{PIP}) + l_3 \cos(\theta_{MCP} + \theta_{PIP} + \theta_{DIP})\right]\Delta\theta_{PIP} \qquad (3.4)$$
$$+\left[l_3 \cos(\theta_{MCP} + \theta_{PIP} + \theta_{DIP})\right]\Delta\theta_{DIP}$$

Differentials of x and y positions (equations 3.3 and 3.4) can determine components that contribute to change in the finger tip position, which shows that the coefficient associated with the MCP joint angle is the greatest due to an additional term including l_1. Hence, the MCP joint is the most dominant one affecting the finger tip position, whereas the PIP and the DIP joints play relatively insignificant roles.
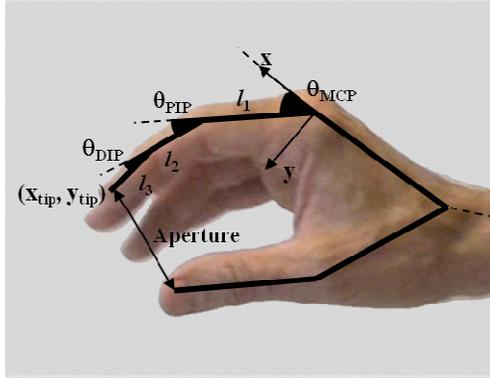
Figure 3.4. Schematic description of the segments of the index finger: finger joint angles of MCP (θ_{MCP}), PIP (θ_{PIP}), and DIP (θ_{DIP}) joints, the segment lengths of proximal (l_1), intermediate (l_2), and distal phalanges (l_3), the coordinate system (x-y), and the position of the fingertip (x_{tip}, y_{tip}).

Using this kinematic property, **OL**, which consists of openness elements from each finger, can be defined to describe the degree of hand opening:

$$OL_i = 1 - \frac{\theta_{MCP}}{90} \quad (i = 2, 3, 4, 5) \qquad (3.5)$$

43

where OL_i is openness of the i-th digit, and θ_{MCP} is the MCP joint angle in degrees. As equation (3.5) indicates, each element of **OL** is determined only by the MCP joint angle to reflect its dominance on the fingertip location (MCP > PIP > DIP). Each **OL** element is normalized to have a range between 0 and 1; OL_i is close to 1 as the MCP joint extends and close to 0 as it flexes. In case of hyperextension of the MCP joint, OL_i becomes greater than 1. The **OL** can represent the relative positioning of fingers since each element of the **OL** measures each finger's opening.

On the other hand, the flatness level (**FL**) depicts the extent to which each finger is close to a flat posture. It has been shown that the PIP and DIP joints move together due to the oblique retinacular ligament [76], and a linear relationship between the two joints has been assumed in hand models for computer animation and virtual reality research [77, 78]. Hence, the **FL** can be defined only by the PIP joints to represent the curvature of each finger:

$$FL_i = 1 - \frac{\theta_{PIP}}{90} \text{ (i = 2, 3, 4, 5)} \tag{3.6}$$

where FL_i is flatness of the i-th digit, and θ_{PIP} is the PIP joint angle in degrees. Each element of the **FL** is also normalized to a range between 0 and 1; 1 for fully extended posture ($\theta_{PIP} = 0°$), and 0 for fully flexed posture ($\theta_{PIP} = 90°$). Although the two parameters are not completely independent of each another, their combination can span a wide range of hand postures. Figure 3.5 shows the example hand postures characterized by aperture, openness and flatness of the index finger. In this study, repeated measures analysis of variance with subjects as a random factor was performed for statistical analyses of these metrics. P-values less than 0.05 were regarded as significant.
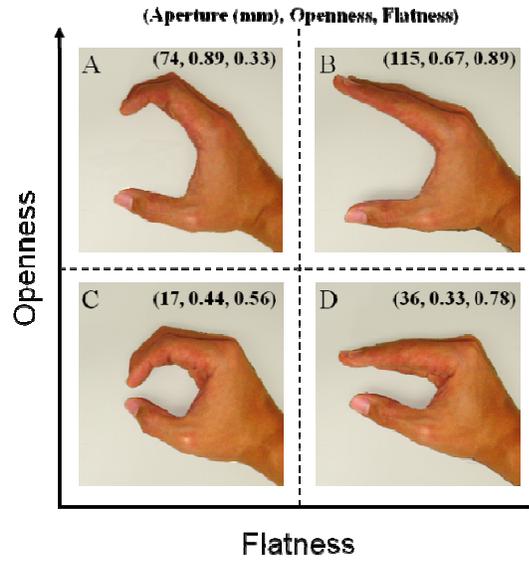
Figure 3.5. Description of various hand postures by openness and flatness of the index finger.

3.3. RESULTS

3.3.1. OL and FL vs. aperture and finger joint angles

Our results indicate that openness and flatness are the efficient and complete metrics for describing hand shape, compared to aperture and an array of finger joint angles. Figure 3.6A shows a sample plot of the relationship between aperture and finger joint angles (MCP, PIP, DIP) of the index finger for one subject grasping medium size (5cm) objects with a long axis. The correlation coefficients showed that most of the variance in aperture is due to the MCP joint (0.95), rather than the PIP (0.67) and DIP (<0.01) joints, which supports our kinematic analysis on the contribution of finger joints to the finger tip position. This trend was also observed for the other subjects and object conditions; the mean correlation coefficients were 0.84±0.11, 0.35±0.27, and 0.10±0.13 for the MCP, PIP, and DIP joints, respectively. Figure 3.6B shows a relationship between OL_2 and aperture for the same condition as in Figure 3.6A, and it was observed that openness is closely related, as expected, to aperture ($R^2 = 0.96$), which implies that one element of the **OL** contains information similar to aperture in representing hand shape.
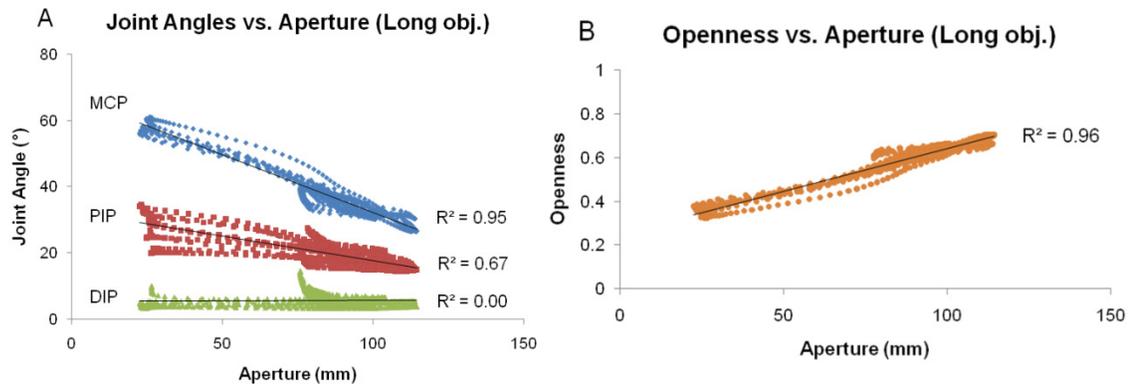
Figure 3.6. (A) The relationship between the index finger joint angles and aperture, (B) the relationship between the openness of the index finger and aperture (One subject reaching for and grasping 5cm objects of cylinders and square/rectangle prisms).

Figure 3.7 shows mean joint angle profiles for reaching and grasping medium size (5cm) objects of each shape. Although every joint has a common pattern of extension followed by flexion, the range of motion (ROM) during reach and grasp is even larger for the MCP joints (30.0°) than for the PIP (8.7°) and DIP (4.5°) joints, in which ROM was averaged over fingers and object shapes. In other words, the MCP joints are the most sensitive to identify the effect of object shape with the DIP joints the least. Hence, the combination of *OL* and *FL*, represented by the MCP and PIP joints, respectively, are employed in the present study to examine the effect of object size and shape on finger motion.
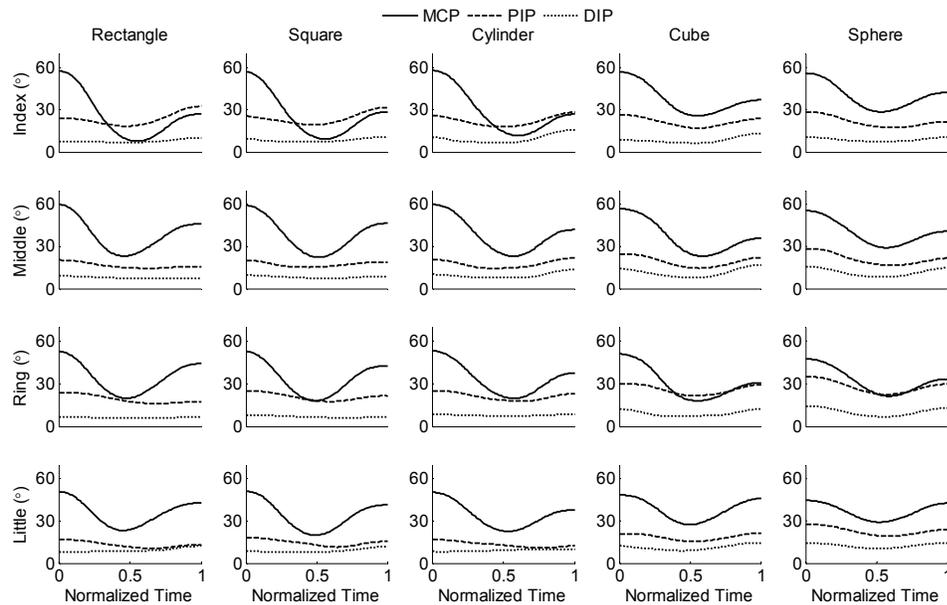
Figure 3.7. Mean joint angle profiles for reaching and grasping medium size objects of various shapes.

3.3.2. The effect of object size

Object size affects hand posture at both the maximum open and final postures; in particular, the effect on openness (defined by MCP) was consistent, while that on flatness (defined by PIP) depended on object shape. Figure 3.8 shows the effect of object size on *OL* at the maximum open (A) and at the final posture (B) for cylindrical objects. The larger the object to be grasped is, the wider the hand opens at both postures ($p<0.001$); the difference in *OL* was greater between large (7.5cm) and medium size (5cm) – 0.22 and 0.37 at the maximum open and final postures, respectively, averaged over fingers – than between medium and small sizes (2.5cm) – 0.12 and 0.15 at the maximum open and final postures, respectively, averaged over fingers. This effect of object size was consistent for other object shapes. On the other hand, the effect of object size on *FL* varied across object shapes. In general, finger shapes were flatter at the maximum open posture for grasping larger objects, with greater discrepancy at the ring and little fingers for spheres and cubes ($p<0.05$) (Figure 3.9A). A similar pattern of *FL* persisted until the final posture for spheres and cubes (Figure 3.9B), but as Figure 3.9C shows, grasping square prisms and rectangular prisms of large sizes required greater finger flexion, particularly for the middle and ring fingers ($p<0.05$).
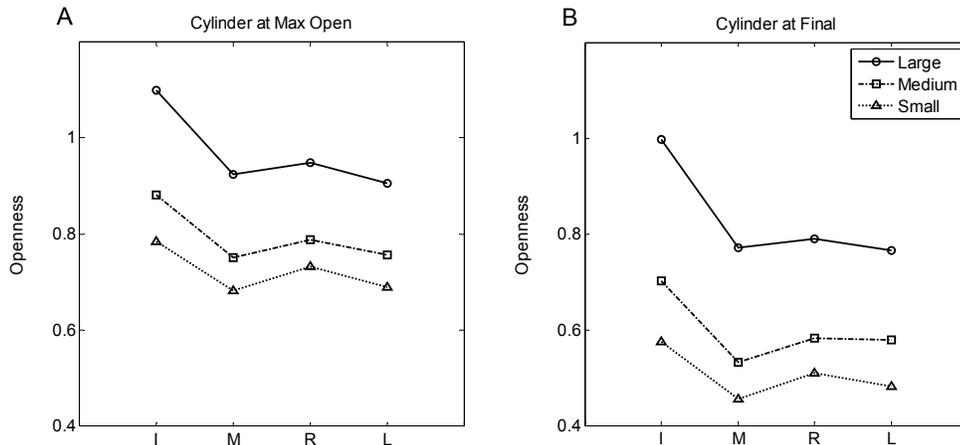
Figure 3.8. The openness for reaching and grasping cylindrical objects of different sizes: (A) at maximum open, (B) at final posture (I=index finger, M=middle finger, R=ring finger, L=little finger).
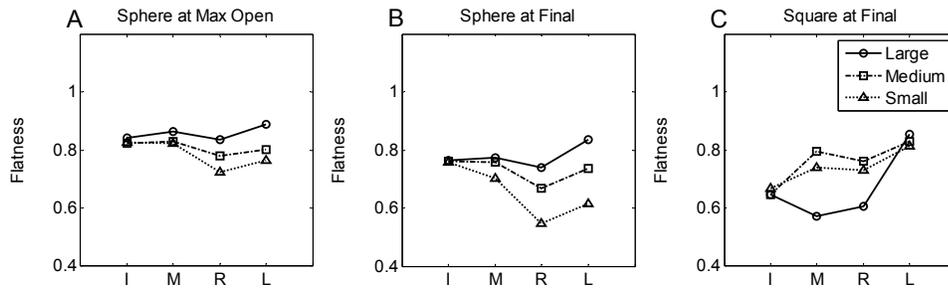
Figure 3.9. The flatness for reaching and grasping objects of different sizes: (A) spheres at the maximum open posture, (B) spheres at the final posture, (C) square prisms at the final posture (I=index finger, M=middle finger, R=ring finger, L=little finger).

3.3.3. The effect of object shape

Hand shape during reach and grasp changes as a function of the aspect ratios describing object shapes. Figure 3.10A-B illustrates *OL* at the initial, maximum open, and final postures for reaching and grasping medium size objects with different AR values. The *OL* values at initial posture were similar between two groups, but finger postures were different during movement. In general, grasping objects with a larger AR resulted in greater openness. At the maximum open posture, the difference was the most significant for the index finger with 25% increase (Δopenness=0.18, p<0.001), followed by the middle and little fingers (p<0.05), although statistically no significant difference was observed for the ring finger (p>0.05). This pattern of *OL* among fingers remains the same at the final posture, which was also observed for large and small objects.

Figure 3.10C-D shows *FL* for the same condition (grasping medium size objects with different ARs). The hand is flatter at the maximum open posture than at the initial posture (Δflatness=0.11, averaged over fingers). The effect of AR values on *FL* at the maximum open posture was not significant for almost all fingers regardless of object sizes (p>0.05), except the little finger for medium and small objects (p<0.05). At the final posture, however, the effect of object shape becomes stronger; for small and medium size objects, the ring and little fingers had more curved shapes (41% and 37% smaller flatness

49

for small size, 15% and 14% for medium size, respectively) for symmetric objects (AR=1) (p<0.05), whereas for large objects, the index, middle, and ring fingers had smaller flatness (13, 17, 9%, respectively) for long objects (AR>1) (p<0.05) (Figure 3.9C). Although the effect of AR values on *FL* is mostly present only at the final posture, it is noticeable that except for large size objects, the flatness pattern among fingers is also consistent from the maximum open to the final posture as in the case of openness.
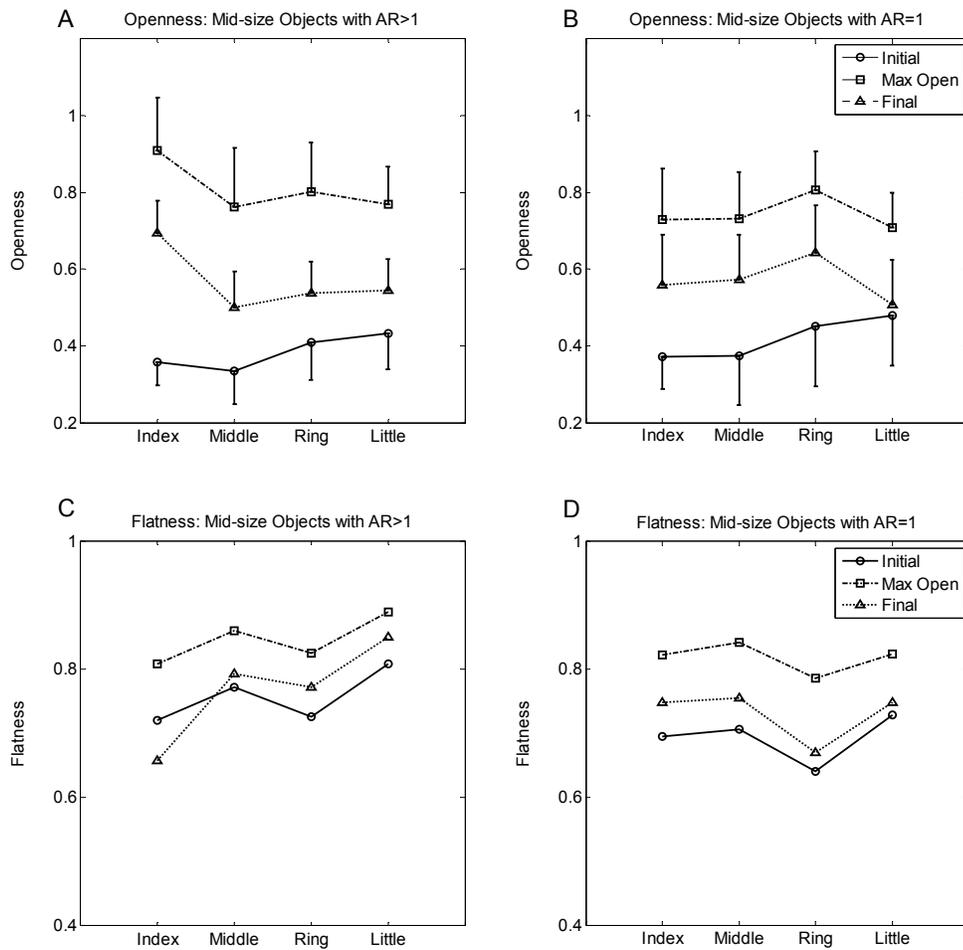
Figure 3.10. Mean *OL* and *FL* for reaching and grasping medium size objects with different aspect ratios. (A) The *OL* for AR>1, (B) the *OL* for AR=1, (C) the *FL* for AR>1, (D) the *FL* for AR=1. The error bars indicate standard deviations.

Hand shape during reach and grasp was also related to the shape of objects with the same AR. The hand opened wider up to 12% for cubes than spheres of the same size (Δopenness ranges from 0.03 to 0.10 for each object size and finger), although the statistical significance depended on fingers and object sizes (Figure 3.11). Except for the little finger, openness at the maximum open and final posture was significantly larger for cubes than spheres for some object sizes ($p<0.05$). This observation implies that cubes, whose features include edges, require greater hand opening for ensuring sufficient clearance than spheres.
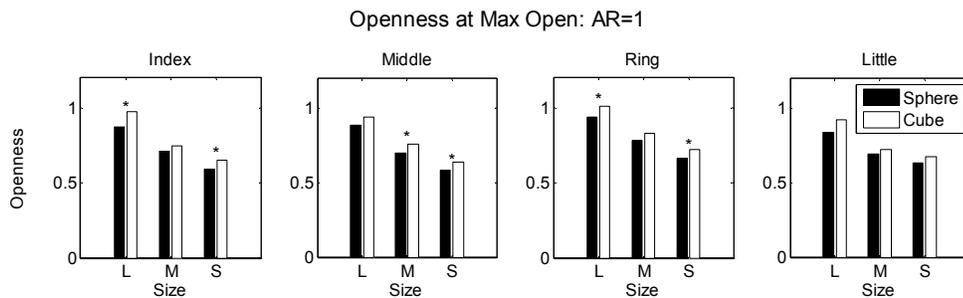
Figure 3.11. The openness at the maximum open posture for grasping different sizes of spheres and cubes (*$p<0.05$).

For objects with a long aspect ratio (AR>1), the difference between cylinders and rectangular/square prisms was more apparent for larger size objects (Figure 3.12A). Subjects had greater hand opening at the maximum open posture for large rectangular/square prisms than large cylinders ($p<0.001$ for digits 2-4; $p<0.05$ for digit 5). The contrast was weaker for medium size objects ($p<0.05$ only for digit 2), while the relation was not significant or even reversed for small size objects ($p>0.05$ for all digits). The final posture showed a similar pattern of openness to the maximum open postures, as in the case of symmetric objects. The *FL* values at the maximum open posture were generally not affected by object shapes with a long axis ($p>0.05$). However, the final postures for small rectangular prisms contained flatter hand shape than cylinders (Figure

3.12B). This trend might be due to large contact area created by the depth for rectangular prisms.
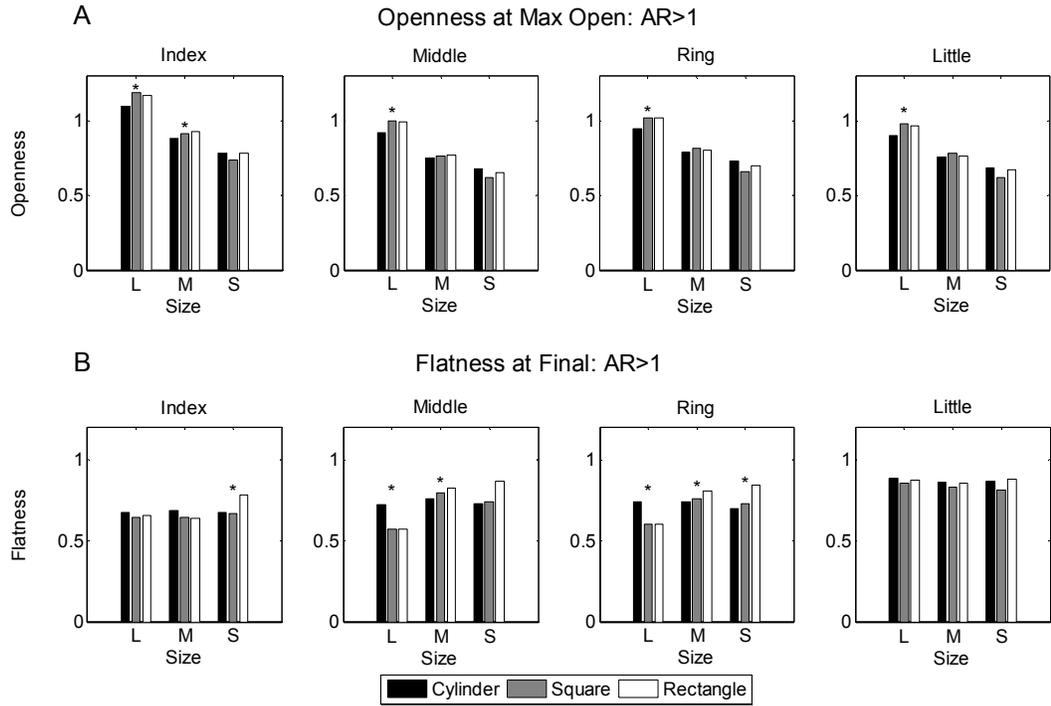
Figure 3.12. (A) The openness at the maximum open, (B) the flatness at final posture, for different object sizes and shapes (AR>1) (*p<0.05).

3.3.4. Quantitative comparison of hand posture between cylindrical and non-cylindrical objects

Hand posture during reach and grasp can be predicted based on the quantification of its relationship to object attributes. Figure 3.13A shows the mean differences of *OL* at the maximum open posture for grasping non-cylindrical objects of three sizes with reference to grasping cylindrical objects of the corresponding sizes (Table 3.1). The AR value clearly affects *OL* at the maximum open posture; in general, rectangular and square

prisms resulted in greater openness for large and medium size objects (up to about 0.09), whereas cubes and spheres required smaller opening of the hand, particularly the index finger (up to about 0.23). The effect on **OL** at the maximum open posture persisted similarly to the effect on **OL** at the final posture. Figure 3.13B shows the mean differences of **FL** at the final posture for grasping non-cylindrical objects of three sizes with reference to grasping cylindrical objects of the corresponding sizes (Table 3.1). It can be seen that the fingers were more curved to grasp large rectangular and square prisms than large cylinders and that grasping the small and medium size cubes and spheres also resulted in curved finger shape in the ring and little fingers. The effect on **FL** at the maximum open posture was insignificant when compared to that at the final posture.
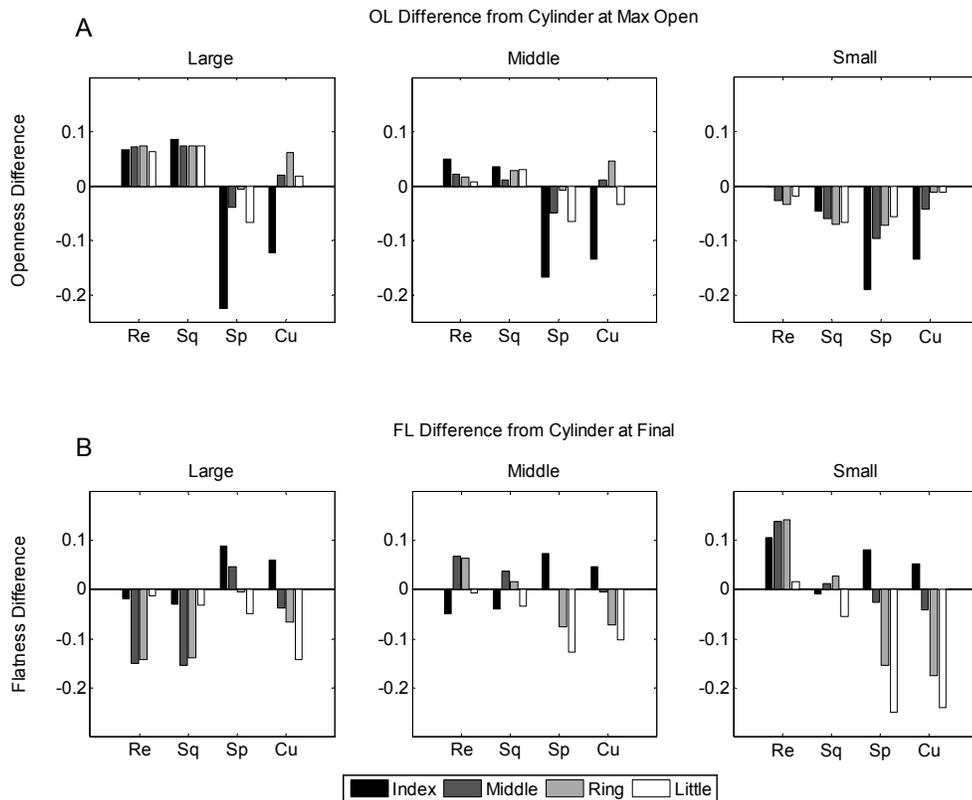
Figure 3.13. (A) The openness comparison with respect to cylinders at the maximum open, (B) the flatness comparison with respect to cylinders at the final posture. Positive values mean greater OL/FL for a given shape than a cylinder (Table 3.1)

Table 3.1. Mean openness comparison at the maximum open posture and mean flatness comparison at the final posture with respect to cylinders for each object size and each finger (Figure 3.13). Bold text for p<0.05 (Re=rectangle prism, Sq=square prism, Sp=sphere, Cu=cube).

Object Shape		OL (Max open)				FL (Final)			
		Re.	Sq.	Sp.	Cu.	Re.	Sq.	Sp.	Cu.
Large (10cm)	Index	**0.07**	**0.09**	**-0.23**	**-0.12**	-0.02	-0.03	**0.09**	**0.06**
	Middle	**0.07**	**0.07**	-0.04	0.02	**-0.15**	**-0.16**	0.05	-0.04
	Ring	**0.07**	**0.07**	-0.01	0.06	**-0.14**	**-0.14**	0	**-0.07**
	Little	**0.06**	**0.07**	**-0.07**	0.02	-0.01	-0.03	**-0.05**	**-0.14**
Middle (5cm)	Index	0.05	0.04	**-0.17**	**-0.13**	**-0.05**	**-0.04**	0.07	0.05
	Middle	0.02	0.01	-0.05	0.01	**0.07**	0.04	0	-0.01
	Ring	0.02	0.03	-0.01	0.05	0.06	0.02	**-0.08**	**-0.07**
	Little	0.01	0.03	**-0.06**	-0.03	-0.01	-0.03	**-0.13**	**-0.1**
Small (2.5cm)	Index	0	-0.05	**-0.19**	**-0.13**	**0.11**	-0.01	**0.08**	**0.05**
	Middle	-0.03	-0.06	**-0.1**	-0.04	**0.14**	0.01	-0.03	-0.04
	Ring	-0.03	-0.07	-0.07	-0.01	**0.14**	0.03	**-0.15**	**-0.17**
	Little	-0.02	-0.07	-0.06	-0.01	0.02	-0.05	**-0.25**	**-0.24**

The quantitative comparison of hand posture between cylindrical and non-cylindrical objects enables prediction of finger motion for grasping cylindrical objects to be adapted to non-cylindrical objects. Bae and Armstrong [68] showed that finger motion can be predicted by fitting the initial, the maximum open, and the final hand postures with a fourth order polynomial, and that those postures can be predicted by a linear regression as a function of object properties. Since the results of this study showed a significant effect of object size on the maximum open and final posture but not on initial posture, mean values of the initial posture are provided while the coefficients of a linear regression are given for the maximum open and final postures (Table 3.2). Object size in centimeters is entered as an independent variable in the linear regression. The postures of the MCP joints were better explained by the effect of object size than those of the PIP and DIP joints, as greater coefficients of determination (R^2) indicate.

Table 3.2. Mean (±SD) of initial hand posture and the coefficients of a linear regression for maximum open and final hand postures for cylindrical objects of all sizes. Bold text for p<0.05.

Finger Joints	Initial Posture (°)	Maximum open posture (°)			Final posture (°)		
		Constant (°)	Size (°/cm)	R^2	Constant (°)	Size (°/cm)	R^2
MCP2	58.2 ± 4.2	29.4	-3.82	**0.53**	51.5	-5.11	**0.79**
PIP2	25.1 ± 7.6	18.9	-0.38	**0.09**	28.5	0.06	0.00
DIP2	9.3 ± 8.3	7.0	-0.14	0.02	16.8	-0.04	0.00
MCP3	59.7 ± 6.9	36.5	-2.94	**0.34**	59.9	-3.88	**0.66**
PIP3	21.3 ± 7.4	15.6	-0.45	0.05	23.1	0.09	0.00
DIP3	10.2 ± 3.7	7.2	-0.04	0.00	13.5	0.23	0.02
MCP4	53.2 ± 8.2	31.4	-2.63	**0.40**	53.5	-3.42	**0.69**
PIP4	26.1 ± 11.9	20.2	-0.69	0.04	26.7	-0.42	0.02
DIP4	9.1 ± 4.5	6.4	-0.16	0.03	9.4	0.00	0.00
MCP5	51.5 ± 7.3	34.7	-2.62	**0.45**	55.1	-3.40	**0.65**
PIP5	17.6 ± 9.3	11.7	-0.38	0.03	13.0	-0.25	0.01
DIP5	7.9 ± 3.7	6.9	0.03	0.00	9.5	0.21	0.03

3.4. DISCUSSION

3.4.1. Development of metrics to describe hand shape

An alternative method for describing hand shape, using the vector-valued metrics of openness (**OL**) and flatness (**FL**) was proposed. The combination of these two metrics represents various hand postures in both across fingers and within finger terms. Openness indicates the approximate locations of each fingertip with respect to the palm, a relationship dominated by the MCP joint angle. It was shown that openness contains information similar to aperture (Figure 3.6B), which has been widely used to represent hand grip formation. Moreover, **OL** describes how fingers are aligned relative to one another. This feature was particularly sensitive to the effect of object shape; our results indicated different patterns of **OL**, depending on the aspect ratio of objects (Figure 3.10A-B). Meanwhile, flatness demonstrates the extent to which a finger is close to a flat shape, independent of the MCP joint. Since the DIP joint moves together with the PIP joint because of anatomical constraints [76], only the PIP joint is included in defining flatness for a given finger. Flatness complements openness by considering finger postures whose shape are significantly affected by the DIP and PIP joints. Although the usage of openness and flatness might be limited if finger motion needs to be specified up to the DIP joints, the new metrics are advantageous in capturing hand shape of individual fingers, particularly when there exists relative difference of hand shape between fingers, as observed in the effect of object shape. In addition, the two metrics are simpler in describing hand shape than an array of finger joint angles and more comprehensive than aperture.

3.4.2. The effect of object size and shape on finger posture

We hypothesized that hand posture is planned for reach and grasp in terms of finger positioning and finger shape for a given object size and given object shape. This hypothesis was supported by the significant effect of object size and shape on hand posture examined using our proposed metrics. Since finger motion during reach and

grasp can be described using specific points, such as the initial, maximum open, and final hand postures [68], those hand postures were treated as dependent variables. The effect of object size was substantially captured by openness (Figure 3.8); the larger the object size, the greater the *OL* for each finger at both the maximum open and final postures. Although this observation was previously established for the index finger by the relationship between object size and aperture [29, 30, 74], *OL* characterizes how object size affects each finger.

In addition, our results revealed that prehensile movement is affected by an object's aspect ratio AR. For a given size, objects with a long axis (AR>1) resulted in greater maximum opening measured by openness, especially for the index and little fingers, and the same pattern persisted until the final posture (Figure 3.10A-B). This result contradicts findings by Santello and Soechting [35]; they examined how people estimate the size of different object shapes by measuring the finger span of the index and little fingers, and found that the size of cylinders is underestimated more than that of cubes and parallelepipeds. However, our results relied on hand posture in actual reach and grasp, rather than matching the finger span to the objects with only visual feedback of objects. This effect of AR might be attributed to distorted perception of object weight caused by haptic and visual volume cues, known as size-weight illusion [79]. Even though perceived volume of objects could have affected prehensile movement, the size-weight illusion might have had little effects on this study in that subjects were given sufficient practices to be familiar with object condition (e.g., size and weight). Even in case where object weight factor is involved, it has been reported that the effect of object weight on finger motion before contact with the object is very limited [80].

Furthermore, our results showed a similar pattern in *OL* from the middle to the end of reach for each category of AR values, suggesting that hand posture is well coordinated in individual-finger-level-detail to achieve planned final hand posture from the middle of reach and grasp (Figure 3.10A-B). Santello and Soechting [34] also observed that the association between hand shape and object shape gradually develops as the hand approaches the object but they tested only objects with similar AR values (long objects). When we compared finger shape measured by *FL* between objects with

different AR values, little difference was found at the maximum open posture, whereas the final posture contained more curved hand shape in the ring and little fingers for grasping symmetric objects of the small and medium sizes (AR=1) (Figure 3.10C-D). This observation, along with the consistent effect on openness during reach and grasp, indicates that finger positioning (openness) is better planned in advance of the contact than finger shape (flatness) in managing different object shapes. In other words, ensuring sufficient clearance is perceived to be more important than establishing proper finger shape in planning and executing the grasp successfully.

The effect of object shape on prehension was also observed between objects with the same aspect ratio but with different cross-sectional shapes. For example, hand postures for grasping cubes and rectangular/square prisms resulted in greater opening at the maximum open posture than spheres and cylinders for a given size, respectively (Figure 3.11, Figure 3.12A). This difference in openness was more apparent as object size increased, whereas flatness was affected only at the final posture and only among long axis objects. These findings are corroborated in part by additional work: Cuijpers et al. [33] reported the effect of perceived object shape on prehension, in which the maximum grip aperture was scaled to an object's width and depth in the experiment using a circular cylinder and oval cylinders with various aspect ratios. In addition, Gentilucci et al. [36] asserted that the effect of object shape is not likely a perceptual issue associated with distortion of object size. They observed that for grasping cubes in different orientations, a larger maximum aperture was observed for 'a diamonds orientation' than for 'a square orientation', caused by the necessity to avoid grasping object corners. These observations can appropriately explain our results in that grasping objects that contain edges (cubes, rectangular/square prisms) led to greater hand opening, possibly due to the need for ensuring sufficient clearance, and that the hand opening was better planned from the middle of reach, as in the case of the effect of AR.

3.4.3. Use of OL and FL to predict finger motion

The quantitative comparison of **OL** and **FL** between cylindrical and non-cylindrical objects (Table 3.1) can be used to generalize prediction of finger motion from one condition (cylinder) to another (non-cylinder). The linear regression results of cylindrical objects (Table 3.2) predict finger postures at three specific points – initial, maximum open, final – for reaching and grasping cylindrical objects of an equivalent size. By applying our quantitative comparison to these predictions for the cylinder, we obtain hand posture predictions for a non-cylindrical object of our interest. Subsequently, the finger motion model proposed by Bae and Armstrong [68] is used to produce natural finger motion as a function of time, which is in a form that can be incorporated in the hand model. The following are specific procedures showing how the current study can contribute to predicting hand posture for non-cylindrical objects (summarized in Figure 3.14):

(1) Information of object properties is identified (e.g., a square prism and a sphere of 5cm).

(2) Regardless of a given object shape, the empirical study result (Table 3.2) is used to produce finger joint angles at the initial, maximum open, and final postures for a cylindrical object of a comparable size; a cylinder diameter (e.g., 5cm) corresponds to a frontal edge length of cross-section of square-prisms and cubes and to a sphere diameter (Figure 3.1).

(3) For cylindrical objects, proceed to the next step (4). In case of non-cylindrical objects, finger posture prediction found in (2) should be adjusted using the quantitative comparison result (Table 3.1); specifically, **OL** and **FL** differences from cylindrical objects are transformed into joint angle differences of the MCP and PIP joints, respectively, by multiplying them by 90, based on equation 3.5 and 3.6. The linear relationship between movements of the PIP and the DIP joints [78] is then used to determine adjustment values for the DIP joint angles, which describes the DIP joint angle

change as two-thirds of the PIP joint angle change. Finally, the MCP joint is adjusted at the maximum open and final posture by the same amount, whereas the PIP and the DIP joints are adjusted only at the final posture.

(4)   Finger joint angles at three postures are transformed into continuous profiles over time by using the finger motion model (a fourth-order polynomial) proposed by Bae and Armstrong [68].

Figure 3.15 shows prediction of the index finger joint angles over normalized time for grasping a cylinder, a square prism, and a sphere of 5cm. Standard deviation of observed data around mean values for a square prism and a sphere of the same size is also shown for comparison between prediction and observation. Finger motion prediction was better matched with observation for the MCP and PIP joints than the DIP joints. The enhanced prediction of finger motion during reach and grasp for various object shapes can provide a useful resource not only for designing adequate work space [50] and hand tools [10] but also for assessing the risk of work-related musculoskeletal disorders by considering tendon movement [3, 20, 68].
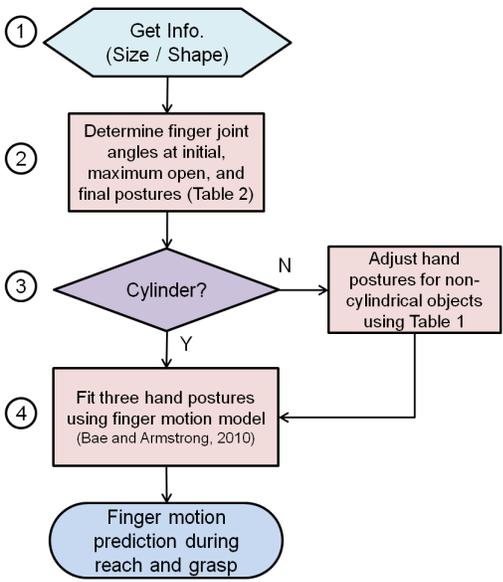
Figure 3.14. A flow chart describing use of the present study for predicting finger motion during reach and grasp.
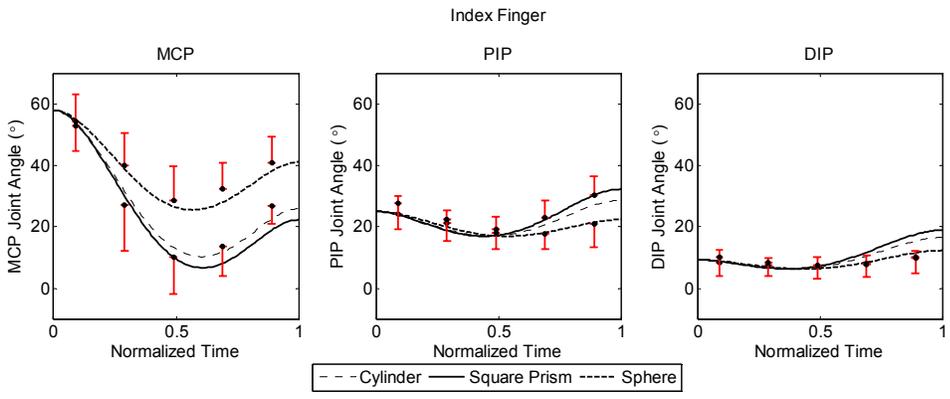
Figure 3.15. Prediction of the index finger joint angles over normalized time for grasping a cylinder, a square prism, and a sphere of 5cm size. The error bars indicate standard deviation of observed data around mean values (mean+SD or mean–SD) at five time internals for grasping a square prism and a sphere of the same size.

3.4.4. Limitations and conclusions

There are a few limitations that merit discussion. First, Sangole and Levin [63] found that palmar arch is an important component of grasping, which is also modulated along with finger motion. Since we examined only flexion and extension of finger joints for defining the new metrics, our results cannot be extended to describing the shape of the palm. Second, we used only a limited set of objects (cylinders, square-prisms, rectangular-prisms, spheres, and cubes). Although our results were effective for examining the difference in prehension planning and execution among those shapes, they would be restricted in their applicability to other object shapes. However, examining regular object shapes can provide a source of examples of natural grasp, which can be generalized to new objects [81]. Third, a sample size of eight right-handed university students provided limited statistical power and represented only a limited subset of the whole population. A larger sample size is needed to capture additional variability between subjects caused by age, anthropometry, and work experience. Lastly, further work is needed to improve finger motion prediction, in particular, final hand posture. Since finger motion prediction in this study significantly depends on empirical analysis, such as a linear regression, it does not consider physical contact between the hand and the object. Our results can be integrated into the kinematic hand models to produce hand posture at contact with an object [3, 13, 68].

To conclude, we proposed two metrics, openness and flatness, which were shown to describe detailed hand posture. The grouping of openness and flatness for four fingers in *OL* and *FL* facilitated the efficient description of relative openings among fingers and individual finger shape (curved or flat). Using these metrics, we showed the effect of object shape (aspect ratio and cross-sectional shape) on planning of reach and grasp. In particular, objects with a long axis generally resulted in greater hand opening than symmetric objects, and grasping objects that have edges required wider clearance than objects with curved surface. We also observed that each finger is controlled during prehension in a manner that reflects the given object shape. The pattern of finger positioning was developed in the middle of reach to successfully achieve planned finger

positioning at the end of grasp. By providing quantitative measures of the relationship between prehensile motions and visually acquired object information, our finding strengthens the previous notion that prehensile movement is planned before movement onset. In the end, the quantitative description of the effect of object shape makes it possible to predict finger motion of reach and grasp for a range of object shapes.

CHAPTER 4

THE EFFECT OF GRASP TYPE ON FINGER MOTION DURING REACH AND GRASP

ABSTRACT

This study examined the relationship between grasp type and hand shaping during reach and grasp. Based on kinematic considerations, we hypothesized that for pinch and power grip the hand would open and close in a similar way but that hand shaping develops differently for each grasp type depending on finger joints. Finger joint angles were measured for seven subjects as they reached and grasped cylindrical handles of 2.5, 5, and 7.5cm diameter presented in vertical and horizontal orientations using pinch or power grip, followed by transferring the object to another location and applying a specified thrust force. The results showed that use of power grip involved greater hand opening than pinch at the MCP joints (the mean difference of finger joint angles ranges from 1.8 to 11.9°), but that there were little differences of hand opening for the PIP and DIP joints. The posture difference of the PIP joints between pinch and power grip increased gradually to have the greatest difference at the final posture. Regression analysis was used to develop models for predicting finger motion for pinch or power grip for given object size and orientation. These results have important implications in the design of kinematic and robotic hand models for simulations of realistic finger motion.

4.1. INTRODUCTION

With increasing use of robotic hand models for realistic simulation [81-83], there is a need for new knowledge that describe hand motion during reach and grasp. One way of fitting the hand to a work object entails flexing the fingers of an open hand until there is contact with the tips of the fingers and the object [3, 13]. If the finger tips make contact first, then the resulting posture will be a pinch. If a more proximal segment contacts first, then the distal joints will continue to rotate until the hand wraps around the object and forms a power grip. Armstrong et al. [12] showed that flexing the fingers one at a time may result in different postures than rotating them together. In most cases, however, the hand starts by opening from a relaxed or closed posture at the beginning of the reach, opens the hand enough to admit the grip object, and closes around it [68]. Also, it has been shown that the rate of joint rotation varies from one joint to another [60].

Hand grasp postures are nominally divided into pinch and power grip. Power grip is a position of high strength and low control, while pinch is a position of low strength and high control [54, 84, 85]. Grieshaber [2] showed that the probability of workers using a power grip to install hoses increases with required force and with increasing diameter. Still there are cases where workers use pinch for high force exertion and grip for small objects, and vice versa. We hypothesize that final hand postures used to grasp objects are chosen before workers begin reaching for the object and that hand pre-shaping occurs as the subject reaches for the object.

It has been asserted that final hand posture of grasp is planned before the reach begins. Hesse and Deubel [86] showed that different start postures affect only the first part of the movement during reach and grasp, not the last half, which is the fist-closing phase. In addition, subsequent tasks after grasp affect the pattern of hand shaping during reach but not significantly final hand posture [40, 73]. These studies imply that hand shaping is adjusted to produce planned final postures. The effect of object properties (e.g., object size and shape) on hand shaping during reach and grasp has been well established [29-31, 33, 34, 68]. These studies provided evidence that prehensile behavior is properly planned and executed according to given object condition. However, it has not been

considered how hand shaping during reach modulates when grasp type (grip vs. pinch) is planned or specified.

This work aimed to develop a model that describes how hand shaping during reach and grasp is affected by selected handle and task attributes. Towards this end an experiment was conducted to compare hand shaping for reach that is followed by pinching or griping a cylindrical handle of different diameters and orientations and by exerting different levels of a thrust force after grasp. The effect of grasp type on hand shaping during reach is identified and quantified for predicting hand posture for a range of object conditions.

4.2. METHODS

An experiment was conducted to compare finger motion between using a pinch and power grip. Seven subjects were instructed to reach for and grasp cylindrical handles of 2.5, 5, and 7.5cm diameter in vertical and horizontal orientations using a specified grasp type (pinch or grip), and finally to apply a specified thrust force along the long axis.

4.2.1. Experiment protocol

Seven right-handed subjects (4 males, 3 females) were recruited from the University of Michigan student population, with those who reported a history of upper extremity disorders excluded. Subjects were selected to obtain a wide range of hand lengths, from 20% female to 95% male [55]. Maximum vertical (push down) and horizontal (push forward) axial thrust strengths were measured two times for each subject and for each size cylinder (Figure 4.1).
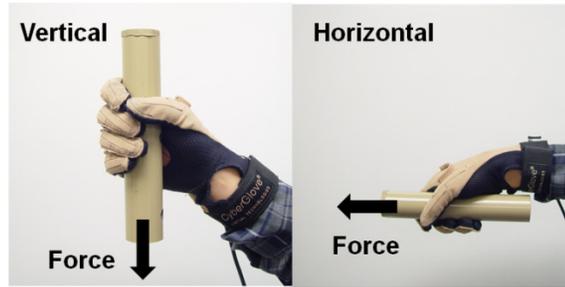
Figure 4.1. For strength test, subjects were instructed to transfer the cylinder to the target and to exert their maximum axial thrust force vertically and horizontally.

A CyberGlove® was used to measure finger joint angles during all exertions. The cylinders were presented at the elbow height of the subject at the reach distance of 35cm from the wrist center (Figure 4.2). Subjects were instructed to start with their thumb tip touching the tip of their index finger and the tips of the other fingers resting on a hand rest. They were asked to reach 35cm for a horizontal or vertical cylinder and to grasp the cylinder of 2.5, 5, and 7.5cm diameter using a pinch or power grip at a fast but comfortable speed. They were then asked to move it to the target position (25cm to the left), where they apply an axial thrust force for two seconds between 0-20, 30-50, 60-80% of their maximum using the same orientation, and to release the cylinder and return their hand to its starting position. Visual feedback for thrust force was provided along with the target force using a bar graph. Subjects were instructed to maintain a steady body posture throughout the task so that motions were due to the upper limb but not the torso. Cylinder orientation and size and grasp type were randomized, for each combination of which two replications of each force level were randomized. Three subjects started vertical orientation first while four subjects started horizontal orientation first. Subjects were allowed to practice until they were comfortable with the protocol. The experimental protocol was approved by the Institutional Review Board of the University of Michigan at Ann Arbor and all subjects gave written consent in advance of participating in the study.
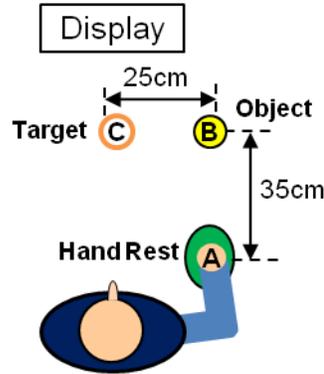
Figure 4.2. Superior view of subject location with respect to the cylinder and the target. Subjects start from the relaxed hand (A), reach (A)-(B), grasp (pinch or power grip handle in horizontal or vertical orientation), move (B)-(C), position and apply horizontal or vertical thrust force (C) for 2 seconds, release the cylinder, and return the relaxed hand to the starting position (A).

4.2.2. Data acquisition and processing

Hand motion during reach and grasp were recorded using a CyberGlove® and the OptoTrak® Certus™ motion tracking system (Northern Digital Inc.). CyberGlove® directly measures joint angles of Distal Interphalangeal (DIP), Proximal Interphalangeal (PIP), and Metacarpophalangeal (MCP) joints for fingers, and Interphalangeal (IP) and MCP joints for the thumb using strain gauges incorporated into the fingers of the glove. The sensors were calibrated for each subject by matching their finger joints with specified angles (-25, 0, 45, and 90° for MCP joints; 0, 45, and 90° for PIP joints; 0, 45, and 75° for DIP joints). Each measurement was repeated two times so that the gain and offset for each sensor could be determined using linear regression. For the OptoTrak® motion tracking system, nine infrared markers were attached to CyberGlove® – five on fingertips and four around the wrist (Figure 4.3) – and four on the object. Three position sensors were located to track those markers during the tasks. The two systems, CyberGlove® and OptoTrak®, were synchronized so that the data are simultaneously sampled at 50Hz for 12 seconds. Post processing of the data from the two systems was performed using MATLAB® software to determine kinematics of hand motion. In addition, a load cell was installed in a fixture located under the target to measure force

exertion level. A LabVIEW program was written to show the target thrust force and exertion force.
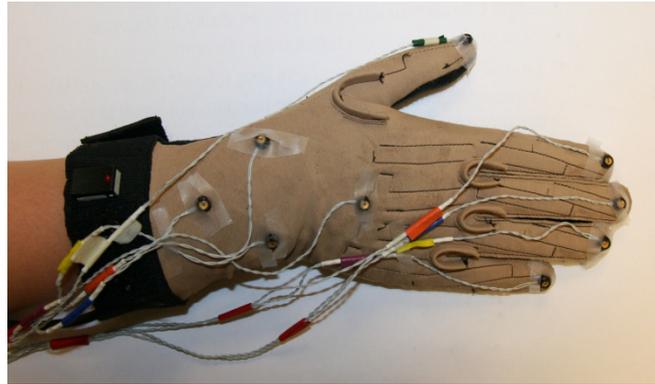
Figure 4.3. Subjects wore CyberGlove®, to which infrared markers were attached for the OptoTrak® Certus™ motion tracking system to capture hand movement. The markers were attached to the finger tips (5), back of the hand and the wrist (4).

4.2.3. Characteristics of hand movement

Figure 4.4 shows a sample plot of the MCP, PIP, and DIP joint angles of the index finger during a given task, where subjects reach for and grasp an object, move it to exert a given level of force, and release it to return their hand to initial position. In this study, we focused on finger movement behavior during the reach-to-grasp period only, which can be characterized by the opening and closing of the hand [68]. The finger joint angle decreases as the distance between the tip of the thumb and tip of the index finger increases to admit the grip object, and increases until the fingers contact the object. Repeated measure of analysis of variance (ANOVA) was used with the subject as a random factor to compare parameters (e.g., maximum open and final joint angles) across all experimental conditions.
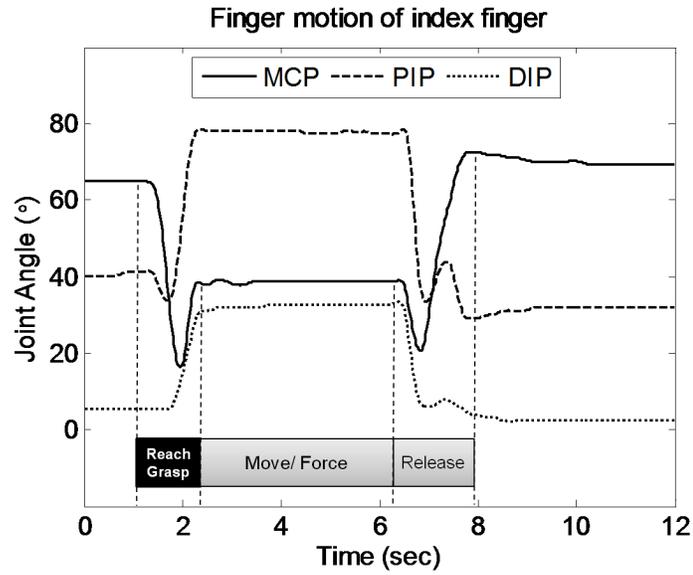
Figure 4.4. Sample plot of the index finger joint angles (MCP, PIP, DIP) for power-gripping a 5cm diameter cylinder, moving it to exert less than 30% of the maximum force, and releasing back.

4.3. RESULTS

Figure 4.5, Figure 4.6, and Figure 4.7 show the mean MCP, PIP, and DIP joint angle profiles of all fingers as a function of normalized time, respectively, to compare grasp type for a medium size object for collapsed force categories. In general, the effect of grasp type was observed at the maximum open posture and final posture for the MCP joints (Figure 4.5), but only at the final posture for the PIP and DIP joints (Figure 4.6 and Figure 4.7). Since movement pattern of the PIP and DIP joints are similar to each other, as expected from the anatomical constraint due to the oblique retinacular ligament [76], analyses on the DIP joints are omitted and replaced with those on the PIP joints.
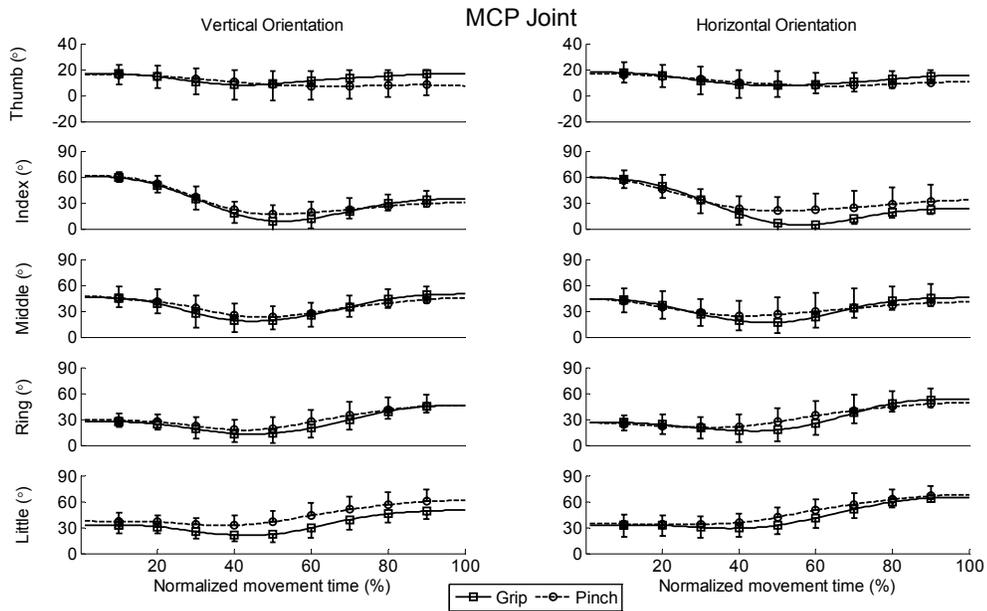
Figure 4.5. Mean MCP joint angle profiles over normalized time of all subjects for grip and pinch of a medium size cylinder with force levels collapsed. Bars represent the standard deviation.
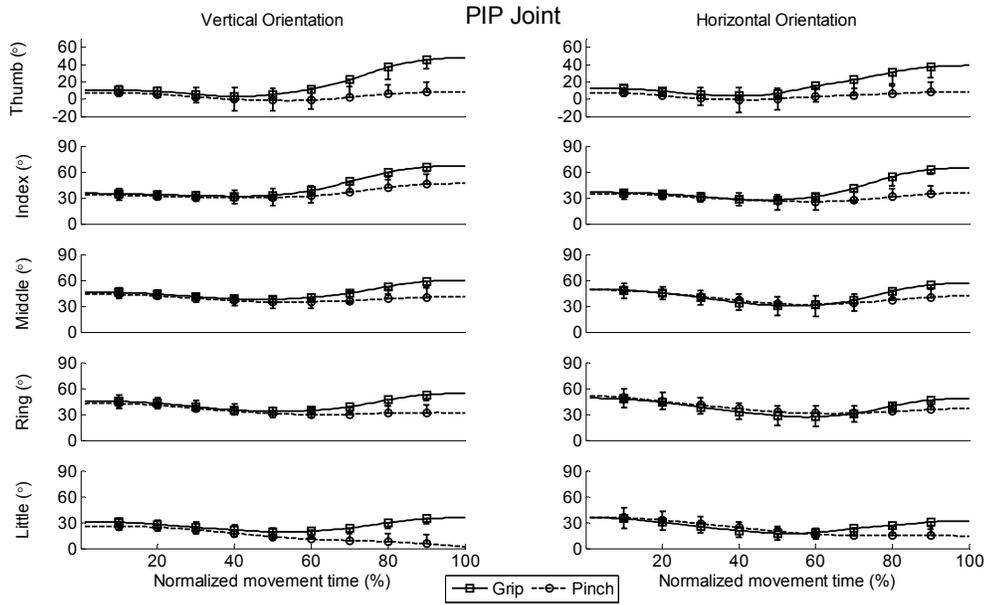
Figure 4.6. Mean PIP joint angle profiles over normalized time of all subjects for grip and pinch of a medium size cylinder with force levels collapsed.
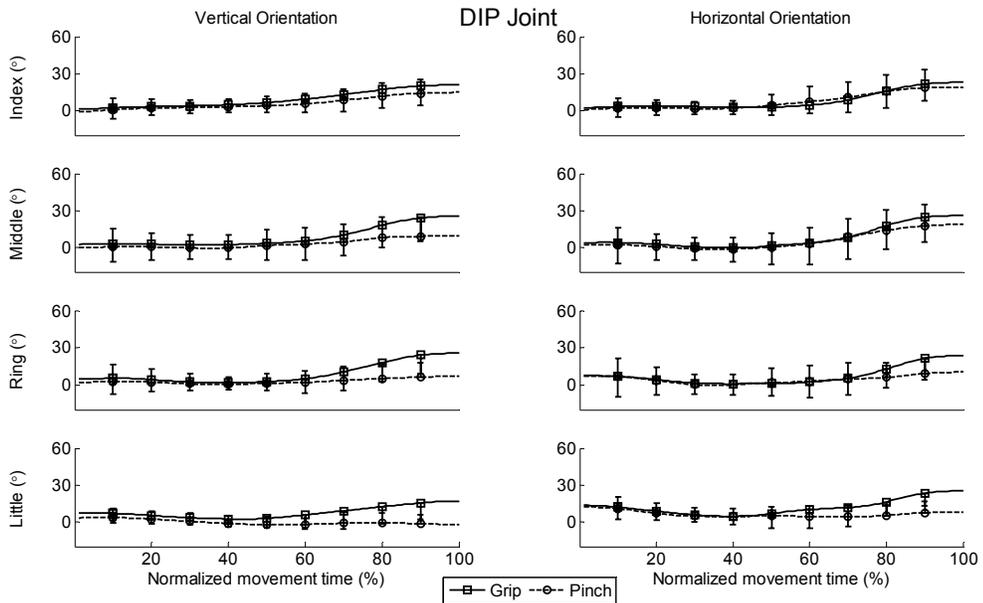
Figure 4.7. Mean DIP joint angle profiles over normalized time of all subjects for grip and pinch of a medium size cylinder with force levels collapsed.

4.3.1. The effect of grasp type on spatial aspects

Force level was shown to be not a significant factor that affects finger motion during reach and grasp based on ANOVA of the MCP joints for the maximum open and final postures ($p > 0.05$), and thus the data were collapsed across force categories. The selection of grasp type affected hand postures during reach and grasp, depending on given object size and orientation. Initial hand postures, which were expected to be consistent by the experimental protocol, showed less than 2° difference between conditions, which was not considered important. Figure 4.8 shows how the MCP joints at the maximum open are affected by grasp type for each combination of object size and orientation. In general, subjects opened their hands wider when they grasp cylinders with power grip than when they pinch ($\Delta\theta = 1.8$, 11.9, 7.9, 4.5, and 7.1° for digits 1-5, respectively, averaged over object conditions). The difference between grasp types was statistically significant for the MCP joints of the index, middle, and little fingers ($p < 0.05$), but the PIP joints of all fingers showed little difference ($p > 0.05$) (Figure 4.9). Object size and orientation also affected the maximum open posture regardless of grasp type; the greater hand opening was observed, except for the thumb IP joint, for larger object size ($p < 0.05$), and the hand required smaller hand opening for horizontal orientation for the MCP joints of ring and little fingers and for the PIP joints of index and middle fingers ($p < 0.05$).
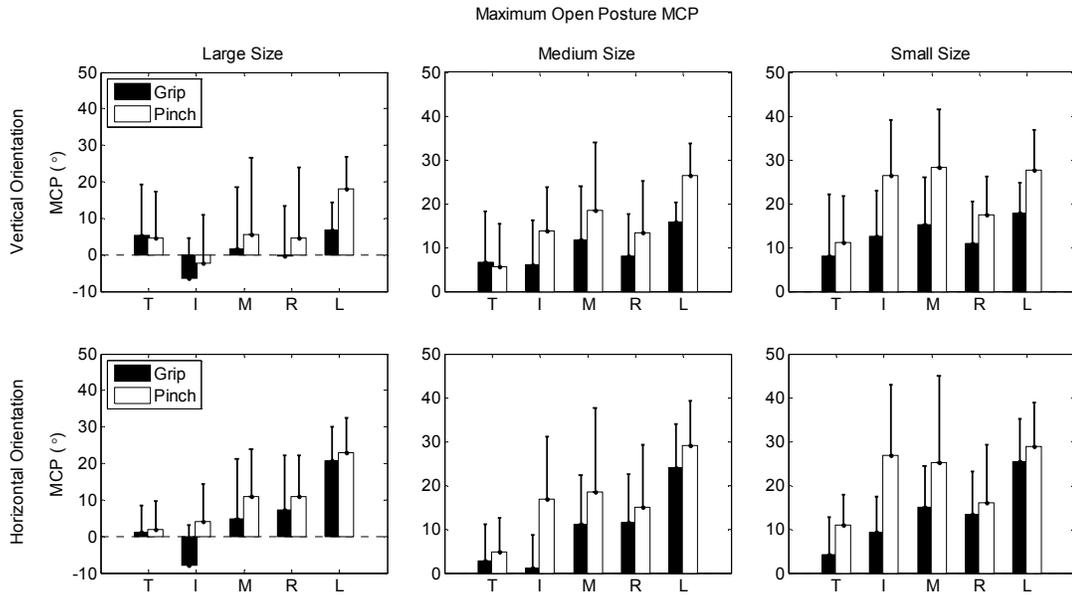
Figure 4.8. Mean MCP joint angles at maximum open posture for power grip and pulp pinch. Each row indicates object orientation, vertical (top) and horizontal (bottom), and each column corresponds to object size, large (left), medium (center), and small (right). T=thumb, I=index finger, M=middle finger, R=ring finger, L=little finger.
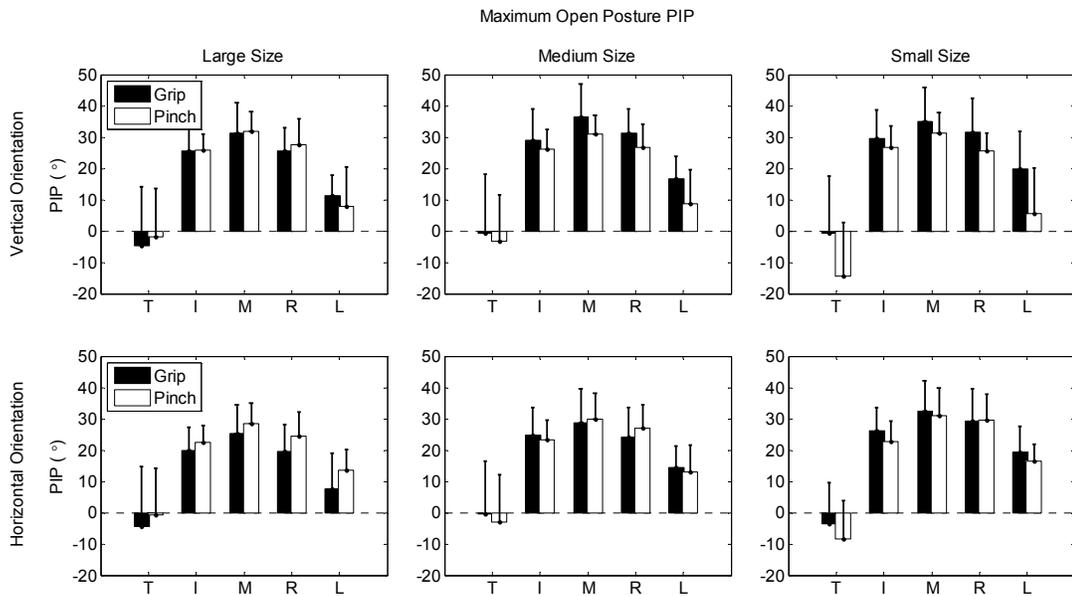
Figure 4.9. Mean PIP joint angles at maximum open posture for power grip and pulp pinch. Each row indicates object orientation, vertical (top) and horizontal (bottom), and each column corresponds to object size, large (left), medium (center), and small (right). T=thumb, I=index finger, M=middle finger, R=ring finger, L=little finger.

The effect of grasp type on final posture was only clear for small size objects at the MCP joints ($\Delta\theta$ = 10.6, 19.5, 15.6, 18.5, and 11.4° for digits 1-5, respectively, averaged across object orientation) (Figure 4.10). But it became more recognizable at the PIP joints; specifically, pinching produced more extended postures at the PIP joints of all fingers than gripping ($p<0.05$) with greater difference for smaller object sizes ($\Delta\theta$ =6.3, 23.8 and 40.7° for large, medium, and small size, respectively, averaged over fingers and object orientation) (Figure 4.11). Across fingers, the final posture difference between pinch and grip was greater for the thumb and little finger ($\Delta\theta$ =27.8 and 28.6°, respectively). The effect of object size was the same as for the maximum open posture, the greater finger flexion required for smaller object sizes ($p<0.05$ for all fingers). Object orientation also affected the final hand posture in a similar pattern to the maximum open posture. The MCP joints of the ring and little fingers were more flexed for horizontal orientation than for vertical one ($p<0.05$). But the most noticeable effect of object orientation occurred at the index finger MCP joint for power grip; horizontal orientation caused greater extension than vertical orientation ($\Delta\theta$ =3.7, 11.6 and 31.9° for large, medium, and small size, respectively, $p<0.05$). In addition, object orientation affected the posture difference between pinch and grip, although the effect is not as strong as object size ($\Delta\theta$ =26.7 and 20.4° for vertical and horizontal orientations, respectively, averaged over fingers and object size). The quantitative comparison between pinch and grip with object size and orientation as factors is considered in the following section 4.3.3.
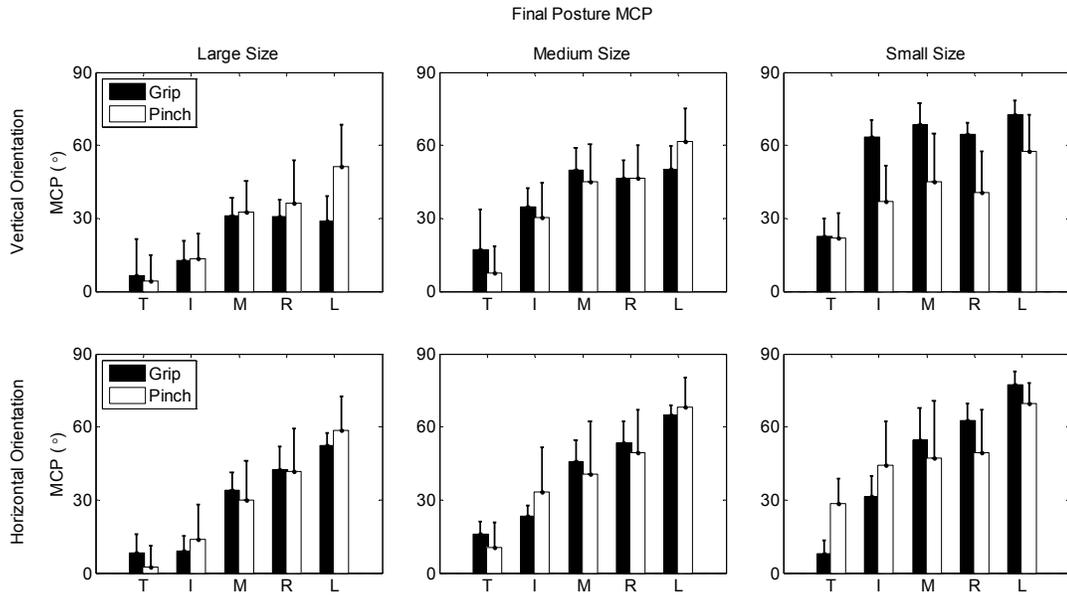
Figure 4.10. Mean MCP joint angles at final posture for power grip and pulp pinch. Each row indicates object orientation, vertical (top) and horizontal (bottom), and each column corresponds to object size, large (left), medium (center), and small (right). T=thumb, I=index finger, M=middle finger, R=ring finger, L=little finger.
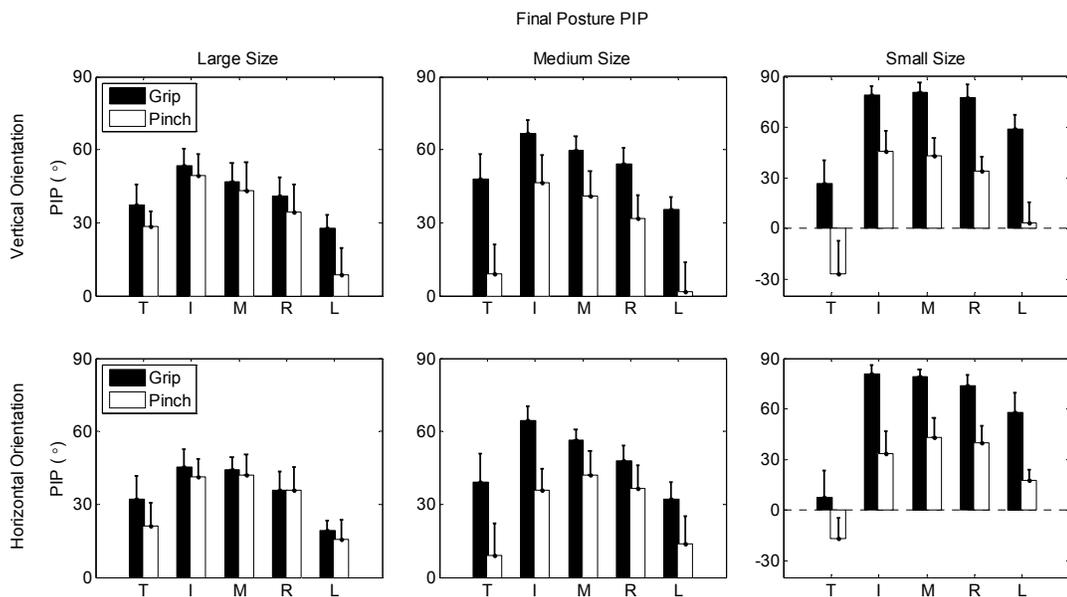
Figure 4.11. Mean PIP joint angles at final posture for power grip and pulp pinch. Each row indicates object orientation, vertical (top) and horizontal (bottom), and each column corresponds to object size, large (left), medium (center), and small (right). T=thumb, I=index finger, M=middle finger, R=ring finger, L=little finger.

4.3.2. The effect of grasp type on temporal aspects

The time at which the difference between grip and pinch becomes significant relied on the finger joints. Figure 4.12 shows mean posture difference (MCP and PIP joints) between grip and pinch of all fingers at incremental time intervals during reach and grasp across all conditions considered. The difference between grip and pinch was evenly distributed during reach and grasp for the MCP joints, whereas the difference gradually increased, primarily after 50% of movement, for the PIP joints. The magnitude of posture difference between grip and pinch was up to 17° greater for the PIP joints than the MCP joints during the second half of reach and grasp period.
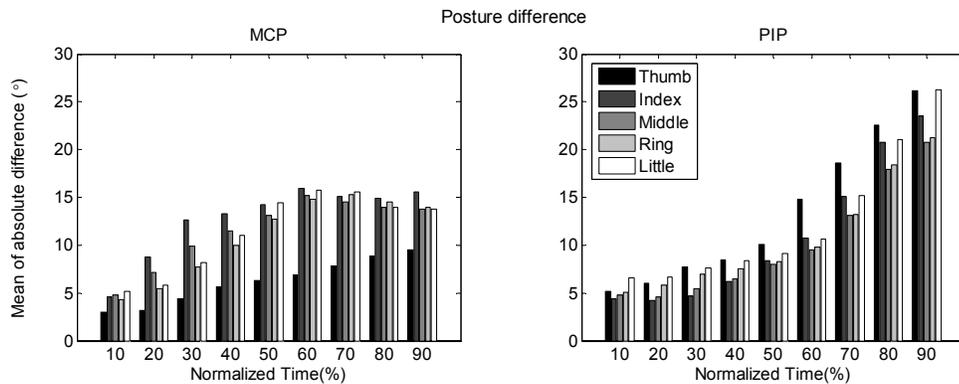
Figure 4.12. Mean of absolute difference of hand posture between grip and pinch across all object size and orientation during reach and grasp.

The grasp type also affected duration of reach and grasp. No difference was found in the time from the start of reach to maximum extension of the MCP joints ($p > 0.05$), but the total movement time from the start of reach to the end of the grasp was longer for pinch than for grip ($p < 0.05$, Table 4.1). This might be attributed to the fact that pinching requires more accuracy to perform, which can lengthen closing period.

Table 4.1. Mean (SD) total movement time obtained from the MCP joints for each grasp type.

	Index	Middle	Ring	Little
Grip	1.15 (0.23)	1.19 (0.26)	1.20 (0.30)	1.25 (0.30)
Pinch	1.25 (0.34)	1.31 (0.44)	1.37 (0.39)	1.38 (0.35)

4.3.3. Quantitative comparison between pinch and grip

The effect of grasp type on finger motion needs to be quantified for the purpose of predicting finger motion during reach and grasp. Grasp type affects the maximum open and final hand postures for the MCP joints and the final posture for the PIP and DIP joints, and these effects depend on object size and orientation (see Figure 4.8–Figure 4.11). Table 4.2 presents linear regression results on the finger posture difference between grip and pinch of the MCP joints ($\Delta\theta_{MCP} = \theta_{MCP.Grip} - \theta_{MCP.Pinch}$) at the maximum open and final postures and of the PIP joints ($\Delta\theta_{PIP} = \theta_{PIP.Grip} - \theta_{PIP.Pinch}$) at the final posture:

$$Y_i = \beta_c + \beta_s \, (\text{obj. size}) + \beta_o \, (\text{obj. orientation}) \pm \varepsilon$$
$$\text{where } i = 1, 2, 3, 4, 5 \text{ for fingers} \tag{4.1}$$

where Y_i's are dependent variables ($\Delta\theta_{MCP}$, $\Delta\theta_{PIP}$) of all fingers; β's are corresponding coefficients to the experimental factors, including the constant term (β_c); ε is the errors of prediction; *object size* is a cylinder diameter in centimeter; *object orientation* is coded as 0 for vertical and 1 for horizontal orientation. The linear regression results explain the effect of object size and orientation on hand posture difference between pinch and grip; for example, the negative coefficients of object size for $\Delta\theta_{MCP}$ and $\Delta\theta_{PIP}$ at the final posture implies that hand posture difference between pinch and grip is greater for smaller objects. The R^2 values of the linear regressions were statistically significant for almost all finger joints ($p < 0.05$).

Table 4.2. Linear regression results for difference of grip hand posture from pinch of the MCP joints at the maximum open and final posture and of the PIP joints at the final posture. Object size is a cylinder diameter in centimeters and object orientation is 0 for vertical and 1 for horizontal orientation (Bold text for p<0.05).

Finger	$\Delta\theta_{MCP}$ at max open				$\Delta\theta_{MCP}$ at final				$\Delta\theta_{PIP}$ at final			
	β_c (°)	β_s (°/cm)	β_o (°)	R^2	β_c (°)	β_s (°/cm)	β_o (°)	R^2	β_c (°)	β_s (°/cm)	β_o (°)	R^2
Thumb*	-5.4	1.0	-2.7	**0.14**	8.2	0.0	-3.5	**0.03**	36.2	1.5	-13.8	**0.12**
Index	-16.4	1.5	-6.4	**0.11**	34.8	-2.1	-19.0	**0.31**	70.3	-6.0	0.6	**0.64**
Middle	-14.6	1.4	-0.1	**0.06**	43.0	-2.1	-5.9	**0.12**	64.7	-6.7	-0.7	**0.63**
Ring	-5.8	0.1	2.2	0.02	53.6	-3.7	3.5	**0.26**	66.9	-7.2	-5.4	**0.63**
Little	-10.4	-0.0	7.0	**0.20**	53.0	-5.3	11.4	**0.53**	68.1	-6.9	-11.3	**0.54**

* For thumb, the PIP joint corresponds to the IP joint.

Finger joint angles for pinching are needed to predict finger motion for power-gripping by use of the quantitative relation between pinch and grip. Bae and Armstrong [68] showed that finger motion can be predicted by fitting the initial, the maximum open, and final hand postures with a fourth order polynomial, and that those postures at three specific points can be predicted by a linear regression as a function of object properties. Table 4.3 shows mean values of the initial hand posture and the linear regression results of the maximum open and final postures as a function of object size and orientation for all finger joints, using equation (4.1). Object size is a cylinder diameter in centimeters and object orientation is 0 for vertical and 1 for horizontal orientation. Proximal joints were better explained by the effect of object size and orientation than distal ones, as greater R^2 indicates.

Table 4.3. Mean (±SD) of initial hand posture and the coefficients of a linear regression for maximum open and final hand postures for objects of all sizes and orientations. Object size is a cylinder diameter in centimeters and object orientation is 0 for vertical and 1 for horizontal orientation (Bold text for p<0.05).

Finger Joints	Initial Posture ($°$)	Maximum open posture ($°$)				Final posture ($°$)			
		β_c ($°$)	β_s ($°$/cm)	β_o ($°$)	R^2	β_c ($°$)	β_s ($°$/cm)	β_o ($°$)	R^2
MCP1	17.4 ± 8.3	15.0	-1.6	-1.2	**0.11**	33.1	-4.4	2.6	**0.42**
IP	6.2 ± 7.6	-16.6	2.0	2.5	**0.08**	-43.4	9.4	1.0	**0.66**
MCP2	60.0 ± 6.8	38.5	-5.2	3.2	**0.41**	53.9	-5.4	3.5	**0.35**
PIP2	34.3 ± 7.5	26.8	-0.1	-3.4	**0.08**	42.5	1.2	-10.5	**0.23**
DIP2	0.8 ± 10.2	-1.7	0.1	0.4	0.00	19.5	-0.5	0.7	0.01
MCP3	44.7 ± 11.6	36.0	-3.7	0.8	**0.16**	55.7	-3.0	-1.6	**0.10**
PIP3	46.4 ± 9.2	32.3	-0.2	-1.7	0.02	42.7	-0.1	-0.0	0.00
DIP3	2.2 ± 17.0	-2.2	-0.3	-0.6	0.00	13.4	-0.6	8.2	**0.07**
MCP4	27.0 ± 8.3	20.7	-1.8	2.3	**0.07**	47.2	-1.2	5.7	**0.05**
PIP4	46.4 ± 11.0	28.2	-0.3	0.5	0.01	35.2	-0.4	4.1	**0.05**
DIP4	5.0 ± 16.1	-4.4	-0.2	1.3	0.01	8.7	-0.2	4.0	0.03
MCP5	34.2 ± 11.3	31.8	-1.5	2.9	**0.12**	65.2	-1.7	8.8	**0.14**
PIP5	31.2 ± 12.1	7.8	-0.1	6.9	**0.10**	3.1	0.3	11.1	**0.22**
DIP5	8.5 ± 11.3	-3.9	-0.2	4.0	**0.10**	-3.2	0.3	9.2	**0.16**

4.4. DISCUSSION

Our results supported the main hypothesis that hand shaping develops differently for given grasp type. The pattern of posture difference between pinch and grip depended on finger joints as well as on object size and orientation.

4.4.1. The effect of grasp type on spatial and temporal characteristics of hand shaping

Object size and orientation were important factors that affect hand shaping during reach and grasp regardless of grasp type, as previously investigated [29-31, 68]. Grasping larger objects resulted in greater hand opening to ensure sufficient clearance and extended finger joints at final hand posture to fit the object size. Cylinders that were presented horizontally induced smaller hand opening of ring and little fingers than vertical orientation but their final posture exhibited greater flexion. It was also observed that a power grip for horizontally positioned cylinders required the MCP joint of the index finger to be extended more than vertically presented ones did, which might be appropriate when the wrist is deviated for horizontal orientation. On the other hand, the effect of level of force exertion on hand shaping during reach and grasp was not significant. We tested different levels of force exertion required after grasp to consider conditions that can occur in various activities, but the small effect forced the data to be collapsed across force levels. Since a specified grasp type (grip or pinch) determines approximate final posture for given object properties, only small variations are allowed for adjusting the final posture for different force requirements. Hand shaping during reach might also not be affected to any great extent in that the subsequent force requirement primarily determines grasp type [2], which was already specified by the experiment protocol, and in that hand shaping is not changed within a selected grasp type.

Grasp type affected the MCP joints from the beginning to the completion of reach and grasp, whereas the PIP and DIP joints were affected primarily during the later portion of reach and grasp. In general, the MCP joints of all fingers opened more widely for

power grip than for pinch, in which the difference is greater as object size decreases (Figure 4.8). This result supports a notion that hand shaping is adjusted to achieve final hand posture that is planned prior to movement [40, 73, 86]. From the viewpoint of workspace design, it can be asserted that grasp type affects the required clearance around the path of hand movement during reach, not only around the object, as previously examined [2, 3]. On the other hand, the effect of grasp type on the final hand posture was observed particularly for the PIP joints (Figure 4.11). This observation was confirmed by a further analysis on development of hand posture difference between pinch and grip over time (Figure 4.12); by observing mean difference between pinch and grip at each time interval, the difference was found to be evenly distributed from the early period of reach to the end of grasp for the MCP joints, but it developed gradually for the PIP joints to have the greatest difference at the final posture. Ansuini et al. [40] also reported a similar observation that the MCP joints showed a significant correlation between hand posture during reach and at contact with the object from the very beginning of the movement, but that the relation was significant after 70% of movement duration for the PIP joints. This outcome implies that the MCP joints are modulated to achieve the planned final posture in broadest terms during the whole period of reach-to-grasp and that the PIP and DIP joints are used to finely adjust hand posture at later stage.

Grasp type affected not only hand shape but also hand transportation. We found that subjects showed slower movement for pinch than for grip. It has been established that accuracy requirement on object manipulation after grasp influences movement time [39, 40]; the high accuracy caused reach time to take longer than the low or no accuracy condition. Although our study did not impose any accuracy requirement on the task, pinching the object alone might require additional accuracy to control fingers when compared with gripping.

4.4.2. Prediction of finger motion for power grip and pinch

The models developed to predict hand posture for pinch can be used to predict finger motion for grip. The linear regression results of pinch predict finger joint angles at

the initial, maximum open, and final postures for reaching and grasping cylindrical objects of given size and orientation (Table 4.3). By applying the quantitative comparison to those hand postures for pinch, hand posture for gripping the object of the same condition can be predicted. Subsequently, the finger motion model proposed by Bae and Armstrong [68] is used to produce natural finger motion as a function of time. The specific procedures are followed to show how the current study contributes to predicting hand posture for selected grasp type:

(1) Information of object attributes is identified (e.g., 5cm cylinder presented vertically).

(2) The empirical study (Table 4.3) is used to predict finger joint angles at the initial, maximum open, and final postures for pinching a cylindrical object of given size and orientation (e.g., for the index finger MCP joint, $\theta_{initial} = 60.0°$, $\theta_{max\ open} = 12.5°$, $\theta_{final} = 26.9°$).

(3) Using the quantitative comparison between pinch and grip (Table 4.2), finger posture predictions in (2) are adjusted for power-gripping. To obtain adjustment values for the DIP joints, the linear relationship between the PIP and the DIP joints [78] is used, in which the DIP joint angle change is considered two-thirds of the PIP joint angle. In the end, the MCP joints are adjusted at the maximum open and final postures, whereas the PIP and DIP joints are adjusted only at the final posture (e.g., for the index finger MCP joint, $\theta_{initial} = 60.0°$, $\theta_{max\ open} = 3.6°$, $\theta_{final} = 51.2°$).

(4) The finger motion model proposed by Bae and Armstrong [68] is used to fit finger joint angles at three postures for obtaining continuous profiles over time (e.g., for the index finger MCP joint, $f(\tau) = 60 - 551\tau^2 + 970\tau^3 - 452\tau^4, \quad 0 \leq \tau \leq 1$).

Figure 4.13 shows finger motion prediction of the index and ring fingers for grasping a vertically presented cylinder of 5cm diameter. Standard deviation of observed data around mean values (mean±SD) for power grip of the same object condition is also

shown for comparison between prediction and observation. Finger motion prediction of power grip was well matched with observations at the maximum open posture, whereas greater finger flexion than observation was predicted at the final posture.
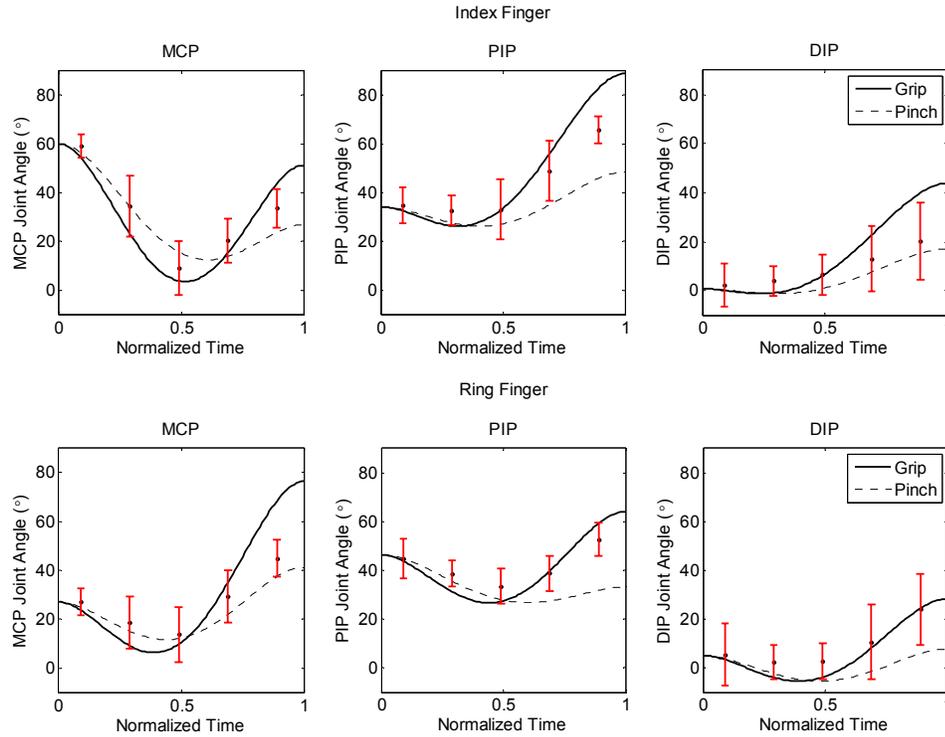
Figure 4.13. Prediction of finger motion (top row: index finger, bottom row: ring finger) over normalized time for grasping a 5cm diameter cylinder presented vertically using pinch and power grip. The error bars indicate standard deviation of observed data around mean values (mean±SD) at five time intervals for power grip of the same object condition.

4.4.3. Limitations

First, this study considered the reach-to-grasp with final posture (grasp type) specified in advance, which do not allow subjects to choose grip posture given object size and orientation and force exertion level. Use of this study might be restricted to cases in which grasp type is given in advance, and otherwise an appropriate grasp type should be determined depending on given object and task conditions [2]. Second, finger motion

prediction of this study depends on linear regressions with selected object properties (sizes, orientations). Accordingly, application of this study to object conditions that were not considered can depreciate accuracy of prediction. Third, a sample size of seven university students provides limited statistical power and represents only a limited subset of the whole population. A larger sample size is needed to capture additional variability between subjects caused by age, anthropometry, and work experience. Although increasing the sample size can decrease the standard error, it would not change the relative amount of variances associated with the independent variables. Last, the relative location of the hand with respect to the object at final posture is needed, particularly for pinch, to simulate finger motion using the present results. The spatial relationship between the hand and the object at final posture would affect the prediction of final posture as well as postures prior to the contact.

4.5. CONCLUSIONS

This study examined the relationship between grasp type and hand shaping during reach and grasp. Grasp selection caused hand posture to shape differently throughout reach and grasp. The MCP joints were adjusted to have greater opening for grip than for pinch, and the effect on the MCP joints occurred from an earlier period of reach than that on the PIP and DIP joints. Characterization of the relationship enabled finger motion for power grip to be predicted based on prediction for pinch, which can be incorporated into kinematic and robotic hand models. Since both pinch and grip are commonly used in daily and industrial activities, knowledge of finger motion for both grasp types can achieve this study's aim for simulating hand movement accurately and realistically.

CHAPTER 5

CONCLUSIONS

This dissertation presented new knowledge and models about the effect of object and task attributes on hand posture during reach and grasp for prediction of finger motion. The results from this dissertation provided natural and realistic finger motion during reach and grasp for a range of conditions, e.g., object shape, size, and orientation, reach distance, and grasp type. This knowledge of prehensile behavior offered necessary information to efficiently describe the way people reach and grasp, and further to assess specific tasks for tackling ergonomic issues, such as tendon excursion. Major findings and possible future work are summarized to show how the thesis of this dissertation was addressed and the proposed objectives were achieved under certain limitations.

5.1. SUMMARY OF MAJOR FINDINGS

The main findings of the present work can be summarized as follows:

(1) Finger motion during reach and grasp can be characterized by examining the effect of object properties on hand posture at specific times. Previous studies of prehensile behavior can demonstrate how different object conditions affect hand posture, but cannot be used to predict finger motion for a range of object conditions. This dissertation showed that hand postures at specific times can be described as a function of object properties using a linear regression, and that a constrained fourth order polynomial function can produce accurate prediction of finger motion during reach and grasp.

86

(2)   The effect of object shape on hand posture during reach and grasp can be described using new metrics, openness and flatness. These metrics are simple but detailed enough to capture characterizations of hand shape by finger positioning and finger shape, which were not achieved by the metrics used in the literature, such as aperture and an array of finger joint angles. Usage of the proposed metrics identified the effect of object shape, in particular, object aspect ratio and cross-sectional shape, on coordination pattern of finger motion during reach and grasp. Pinching long objects (e.g., cylinders) resulted in up to 25% greater hand opening than pinching symmetric objects of comparable size (e.g., spheres), while pinching objects with edges (e.g., cubes) resulted in up to 12% greater hand opening than pinching objects with curved surfaces of comparable size (e.g., spheres). Furthermore, the relationship between object shape and finger motion was quantified in an appropriate form to predict finger motion for various object shapes.

(3)   Given grasp type (pinch vs. grip), hand posture can develop in different ways during reach and grasp. Use of power grip involved greater hand opening than pinch with the mean difference up to 11.9° of finger joint angles. The effect of grasp type occurred from earlier in the reach for the MCP joints but the posture difference of the PIP joints between pinch and grip developed gradually to be apparent for the second half of reach and grasp. The characteristics of finger motion for each grip type were quantified for demonstrating hand posture prediction for selected object conditions.

(4)   Hand posture prediction can provide information needed to estimate relevant tendon movement for the purpose of evaluating the risk of industrial jobs. Previous studies in the literature measured wrist and hand posture for obtaining necessary information but lacked ability to predict those postures. The combination of findings in this dissertation produced natural finger motion prediction for a range of object and task conditions, and tendon excursion associated with the hand posture was predictable. Accurate evaluation of the risk of repetitive reach and grasp tasks is achieved not only for selected industrial jobs but also for simulated ones.

(5)   Planning and execution of hand posture during reach and grasp can be understood by considering how individual fingers and finger joints within a finger are controlled. Previous studies have reported that perception of the object influences how prehension is performed. However, there has been limited interest in how each finger joint is controlled to address differences between the object attributes. The findings in this dissertation showed that hand shaping is controlled at the level of individual finger and that for given a finger, the MCP joints are modulated to achieve the final posture in broadest terms during the whole period of reach-to-grasp, while the PIP and DIP joints are used to finely adjust hand posture at later stage. These results strengthen the notion that prehensile movement is planned before movement onset by providing quantitative measures of the relationship between prehensile movement and visually acquired object information.

5.2. USE OF MAJOR FINDINGS

One of this dissertation's objectives is to demonstrate the use of this research for addressing ergonomic issues in industrial jobs. Three jobs are selected from the previous study [3], in which wrist postures were analyzed using time-based analysis. The jobs were classified based on experts' repetition rating (high, middle, low repetition level), performed by Latko et al. [87]. Choi [3] calculated normalized cumulative tendon excursions (CTE) of the flexor digitorum profundus (FDP) and the flexor digitorum superficialis (FDS) tendons at the wrist and showed that higher-risk jobs cause greater tendon movement, which can raise the risk of the WMSDs. The findings of this dissertation can contribute to improving prediction of tendon excursion by considering finger motion.

Figure 5.1 shows procedures needed to estimate tendon excursion for a job that includes reach and grasp task (See Appendix A for specific steps). For given object conditions (e.g., size and orientation), hand postures at three specific points (i.e., initial, maximum open, final) are obtained for pinching cylindrical objects by using the empirical results (Equation 2.2–2.3, Table 2.2, Table 3.2, Table 4.3). If the object is non-cylindrical shape or the task is power-grip, those hand postures are adjusted based on the results presented in Chapter 3 (Table 3.1) and Chapter 4 (Table 4.2), respectively. Then these hand postures are transformed into continuous joint angle profiles as a function of time using the finger motion model (Equation 2.6–2.11). With proper assumptions regarding other work elements, such as move and position, hand posture is predicted for one job cycle, from which tendon excursions at finger joints are calculated using the relationship between hand posture and tendon movement [14]. The CTEs are computed to indicate the total distance that each tendon travels, which is then normalized by time to consider a repetition level of a job.
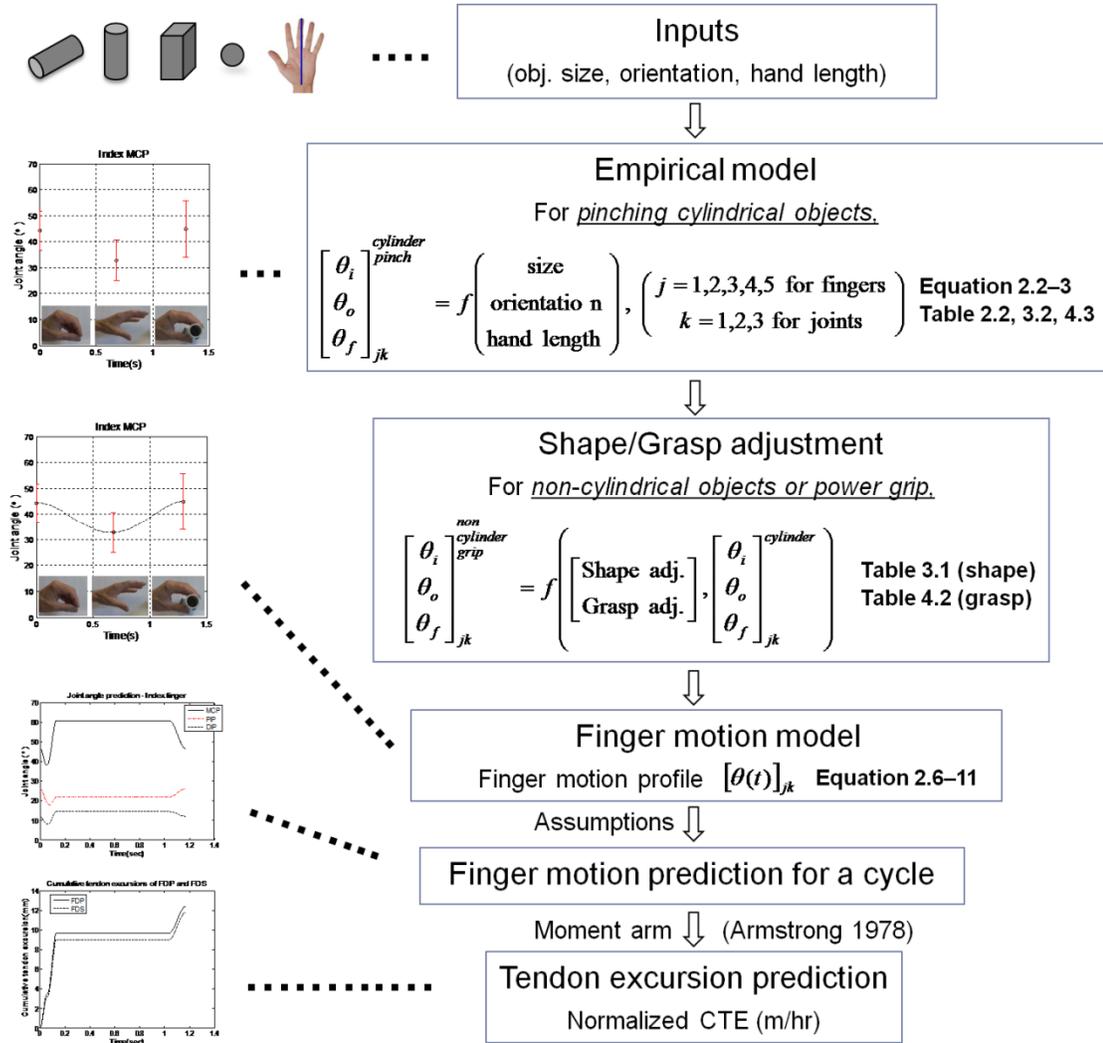
Figure 5.1. A flow chart that shows steps to estimate tendon excursion at finger joints using the proposed study.

Figure 5.2 presents normalized CTEs of the FDP and FDS tendons at the wrist [3] and at the index finger obtained from the current study. The finger joints generate the normalized CTEs from 41 to 101% of the wrist, to which the MCP joints contribute the most (62 to 81%). When the normalized CTEs at the finger joints are added to those at the wrist, the difference between three repetition levels becomes even more significant (Table A.3); for the FDP tendon, the difference is 43.4 and 25.6 m/hr between high and middle levels and between middle and low levels, respectively, compared to 14.7 and 17.4 m/hr when only the wrist is considered; for the FDS tendon, the difference is 45.1

and 27.7 m/hr, compared to 21.1 and 24.3 m/hr. The total CTEs are comparable to the previous study [20], in which 18.6 m/hr was observed for low repetition jobs, whereas 71.5 m/hr observed for high repetition jobs. It is concluded that considering the finger motion, along with the wrist, is necessary to improve estimation of tendon excursion for the purpose of evaluating the job that involves repetitive reach and grasp.
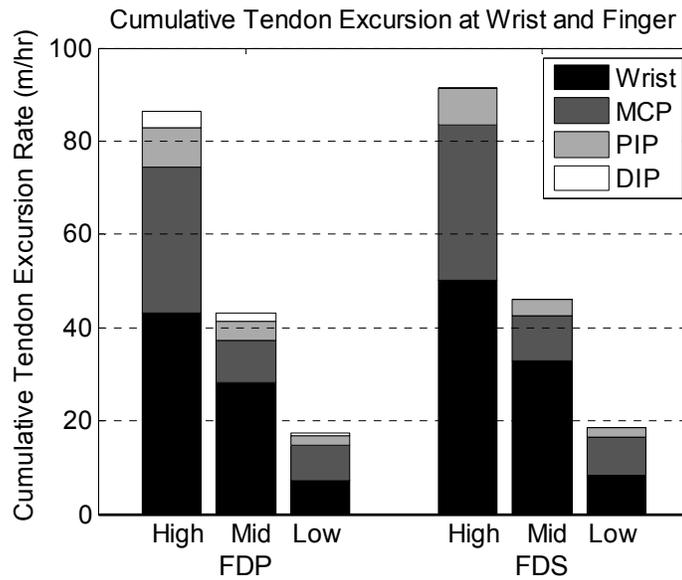
Figure 5.2. Cumulative tendon excursion of FDP and FDS tendons at the wrist and the index finger joints – MCP, PIP, DIP – for three jobs of different repetition levels (Table A.3).

5.3. SUGGESTIONS FOR FUTURE RESEARCH

The following future work is suggested:

(1)   Extend the degrees of freedom of the hand considered for hand posture description. This work considered only flexion and extension of finger joints, but the abduction and adduction of the MCP joints also affect finger placement on the object, and further the palmar arch is known to be an important component of grasping [63].

(2)   Extend application of this work to broader ranges of object and task conditions. It was shown that examining regular object shapes can provide a source of examples of natural grasp to be generalized to new objects [81]. Since this work considered a selected set of object properties (e.g., object size and shape), its applicability to other conditions needs to be tested. In addition, this work did not take into account a goal of the task. It has been reported that how we grasp an object depends on not only what we perceive of the object, but also what we intend to do with the object [37, 38]. However, there has been limited interest in how the task goal affects finger motion during reach and grasp [39, 40]. Lastly, this work considered one-handed task only, although it is common that both hands are involved in industrial jobs. Further studies are needed to corroborate the usage of this work for bimanual tasks or to introduce a new approach for these.

(3)   Corroborate prediction of tendon excursion. This study predicted tendon excursion using the empirical relationship between hand posture and tendon movement [14]. *In vivo* tendon movement measurements can provide reliable and valid excursion data [88], and thus can be used to corroborate predictions based on this study.

(4)   Examine the hand-object interaction for consideration of hand biomechanics. Biomechanical models of the hand and fingers can predict relevant muscle/tendon force for no or simplified external loading condition, when finger motion is specified based on the relationship between tendon displacement and hand postures [65]. Since various types

of interaction between the hand and work objects are common in occupational settings, the methodologies that can capture the hand-object interaction should be examined for realistic and accurate prediction of the internal loading patterns of tendons and joint surfaces.

(5)   Extend the application of this work for formulating a conceptual model. Conceptual models have been developed to understand the complex interaction between a performer and the environment in prehension [89, 90], but they do not explain exactly what information is being transferred or controlled. This work provides specific guidelines for hand movement, which can improve the conceptual models that reflect empirical aspects of prehension behavior.

(6)   Extend the application of this work for evaluating the rehabilitation progress of patients. Since this work provides prediction of natural finger motion from healthy subjects, its kinematic characteristics can be used to diagnose diseases or monitor the progress of rehabilitation by comparing the data with those measured from patients suffering rheumatoid arthritis [91] or Parkinson's disease [92].

Ergonomic Applications: Tendon Excursion

Figure A.1 shows a sample sequence of handle assembly job chosen as a high repetition category. One job cycle consists of reaching for and grasping a handle, moving and positioning it for machining, followed by moving it back to release for another cycle. Time study of this job presents work elements and their corresponding duration for one cycle (Table A.1), which provides bases for assumptions indicated in Table A.2. It was assumed that a worker is 50% male by his hand length [55]; a work object is a cylinder of 3cm diameter presented in horizontal orientation; the reach and grasp is performed by pulp pinch; the total time of one cycle takes 1.17 seconds; and duration of each work element is one unit for reach/grasp and release, and 7 for movement.
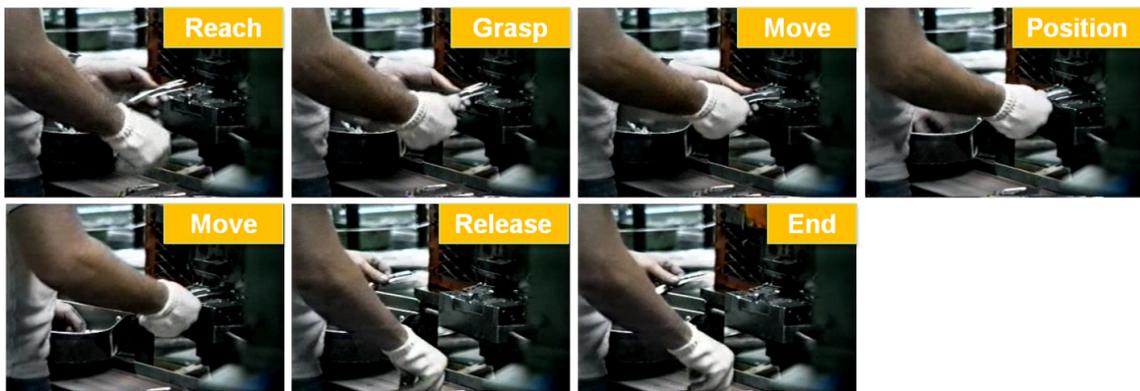
Figure A.1. A sample sequence of handle assembly job (high level repetition).

Table A.1. Time study of handle assembly job with joint angle predictions of the index finger and corresponding cumulative tendon excursion for one cycle.

Time	Work Element	Δt	Index finger joint angles (°) MCP	PIP	DIP	Cumulative TE (mm) FDP	FDS
0.00	Reach	0.10	46.6	26.1	12.0	0	0
0.10	Grasp	0.03	38.1	17.9	8.0	3.5	3.1
0.13	Move	0.24	60.9	21.9	14.6	10.0	9.3
0.37	Position	0.20	60.9	21.9	14.6	10.0	9.3
0.57	Move	0.46	60.9	21.9	14.6	10.0	9.3
1.03	Release	0.14	46.6	26.1	12.0	14.1	13.3
1.17	Finish						

Table A.2. Summary of assumptions introduced for each job.

Assumption	Handle assembly (high-level)	Isostatic machine (mid-level)	Torwegge (low-level)
Worker	50% Male	50% Female	50% Male
Work object condition	A cylinder (D=3cm) in horizontal orientation	A cylinder (D=2cm) in horizontal orientation	A rectangle (D=3cm) in horizontal orientation
Task	Pulp pinch	Pulp pinch	Pulp pinch
Total time of one cycle (sec)	1.17	6.77	14.78
Duration of work elements (units)	Reach/Grasp (1) Move (7) Release (1)	Reach/Grasp1 (1) Reach/Grasp2 (1) Move (6) Release (2)	Reach/Grasp (3) Move/Wait (9) Push (1) Release (2)

The following steps are needed to predict finger motion for one cycle of this job, which contains reach and grasp, move, and release periods:

(1) *Reach/Grasp*: The object condition (cylinder diameter, orientation) and the corresponding coefficients (Table 2.2) are incorporated in equation (2.1) to predict θ_i, θ_o,

and θ_f for each finger joint during reach and grasp. For example, $\theta_i = 46.6°$, $\theta_o = 38.1°$, and $\theta_f = 60.9°$ for the MCP joint of the index finger, as indicated in Table A.1.

(2) *Reach/Grasp*: The three joint angles (θ_i, θ_o, θ_f) are entered into equations (2.7) – (2.11) to obtain coefficients for the finger motion model described by equation (2.6). For example, the MCP joint of the index finger is modeled by $f(\tau) = 47 - 192\tau^2 + 441\tau^3 - 235\tau^4$. This produces continuous finger joint angle profiles during reach and grasp.

(3) *Move*: After the reach-to-grasp period, no change in finger joint angles is assumed during movement and position periods, where only wrist posture change is observed.

(4) *Release*: The handle is moved back and released to the conveyor belt, during which the final posture (θ_f) is assumed to return to the initial posture (θ_i). The release period is constructed using piecewise cubic-hermite interpolation polynomial.

Taking the steps above produces prediction of finger joint angles for one job cycle, as the index finger joints are shown in Figure A.2A. Based on joint angle predictions, tendon excursions of the FDP and FDS tendons at the finger joints (MCP, PIP, DIP) are calculated using the relationship between hand posture and tendon movement [93]. Then, the cumulative tendon excursion (CTE) for each finger joint is computed by integrating absolute values of tendon excursion rate over time to obtain the tendon traveling distance and is summed over each finger (Table A.1); for example, the FDP and FDS tendons of the index finger travels 14.1 and 13.3mm, respectively, for one cycle (Figure A.2B). These results are normalized by a cycle time, which generates the normalized CTE of 43.5 and 41.0 m/hr for the FDP and FDS tendons, respectively.
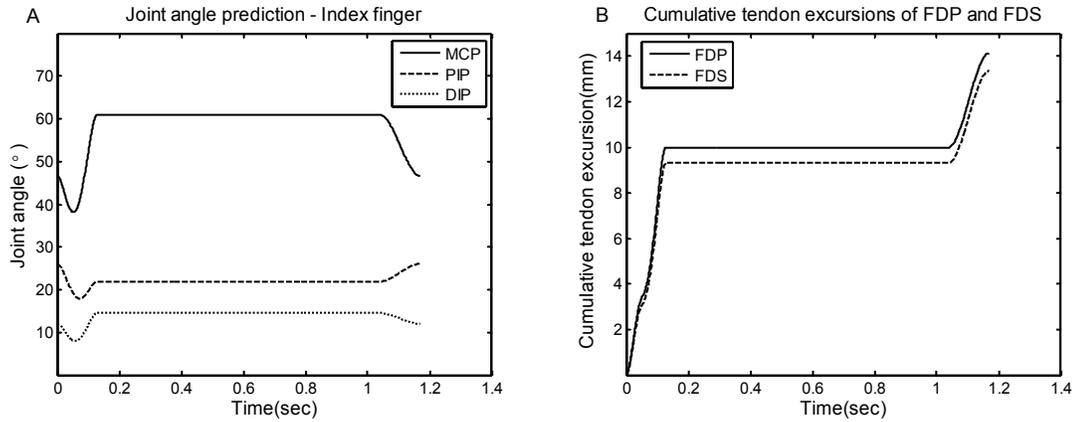
Figure A.2. (A) Index finger joint angle prediction during reach/grasp, movement, and release. (B) Cumulative tendon excursions of the FDP and FDS tendon of the index finger.

The similar procedures are used to estimate tendon excursion for the other two jobs of low and middle level repetitions. Figure A.3 shows a sample sequence of isostatic machine operator, a job with middle level repetition. This job consists of two consecutive reach and grasp of a tube, followed by move and release. Assumptions are established based on observations, similarly to the first job (Table A.2). The key feature of this job is to contain the second reach and grasp just after the first one; the same maximum open and final postures as the first reach and grasp are assumed for the second one (Figure A.4A). The CTEs and normalized CTEs are calculated using the same method as the first job.
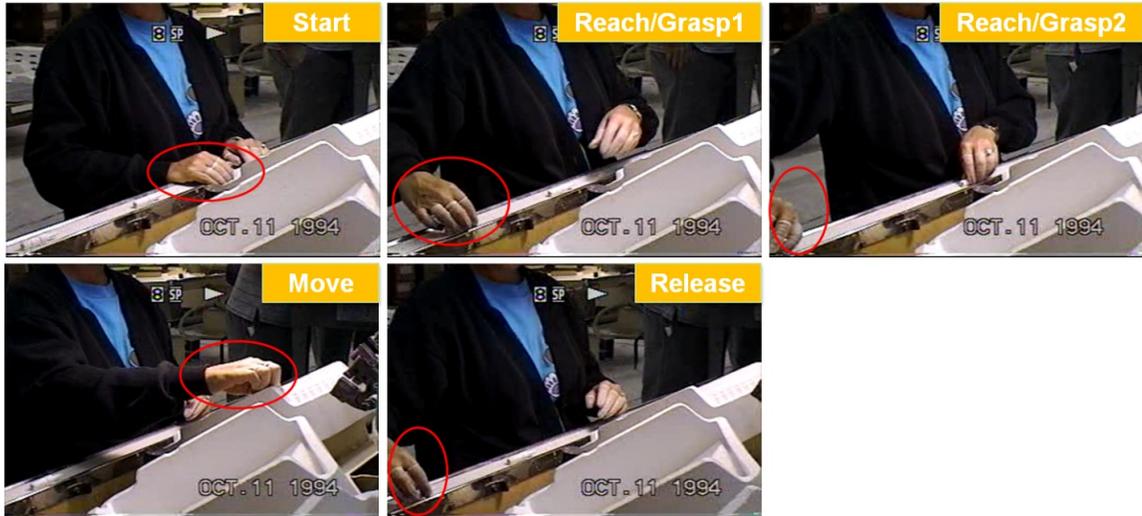
Figure A.3. A sample sequence of Isostatic machine operator (middle level repetition).
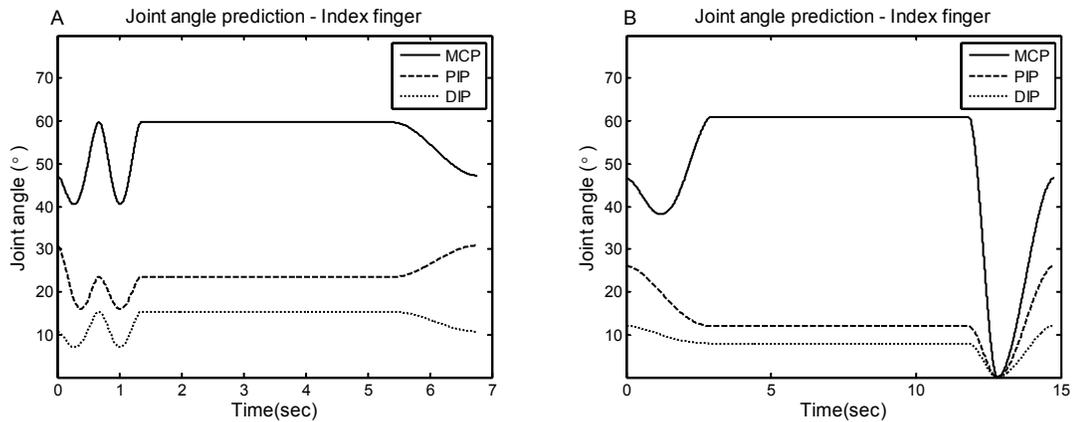
Figure A.4. Index finger joint angle prediction during one job cycle: (A) Middle level repetition job, (B) low level repetition job.

A sample sequence of the low level repetition job is shown in Figure A.5. The worker reaches for and grasps a rectangle plate, moves it to the target position, waits for pushing it away, and releases back. The basic assumptions are built based on observations as the other jobs (Table A.2). Since the work object is non-cylindrical shape, finger motion prediction is adjusted using the procedures described in section 3.4.3 of Chapter 3. The major feature of this job is that the hand opens almost to the flat posture

when the work object is pushed. The finger joint angles at the end of push work element are assumed to be zeros, and a piecewise cubic-hermite interpolation polynomial is used to construct push and release periods (Figure A.4B). The CTEs and normalized CTEs are calculated using the same method as the other jobs aforementioned, and the results for the three jobs considered are summarized in Table A.3.
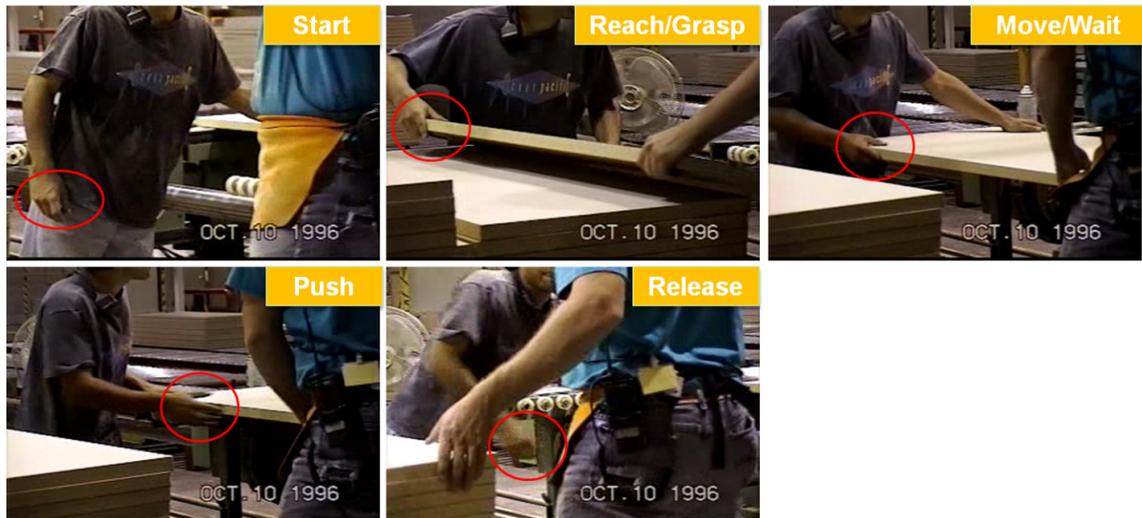
Figure A.5. A sample sequence of torwegge job (low level repetition).

Table A.3. Normalized cumulative tendon excursions of FDP and FDS tendons at the wrist and index finger joints (m/hr).

Job Repetition	Tendon	Wrist	Index Finger				Total
			MCP	PIP	DIP	Sub-total	
High	FDP	43.0	31.4	8.7	3.4	43.5	86.5
	FDS	50.2	33.3	7.8		41.1	91.3
Middle	FDP	28.3	9.1	4.1	1.5	14.7	43
	FDS	32.8	9.7	3.7		13.4	46.2
Low	FDP	7.2	7.6	2.2	0.5	10.3	17.5
	FDS	8.5	8.0	2.0		10.0	18.5

BIBLIOGRAPHY

1.   Baker, P.T., Volumetric requirements for hand tool usage. *Human Factors*, 1960. 2(3): p. 156.

2.   Grieshaber, C.D., Factors affecting hand posture and one-handed push force during flexible rubber hose insertions tasks. *Ph.D. Dissertation*, 2007. Industrial and Operations Engineering, University of Michigan, Ann Arbor.

3.   Choi, J., Developing a 3-dimensional kinematic model of the hand for ergonomic analyses of hand posture, hand space envelope, and tendon excursion. *Ph.D. Dissertation*, 2008. Mechanical Engineering, University of Michigan, Ann Arbor.

4.   Nag, P., Work accidents among shif tworkers in industry. *International Journal of Industrial Ergonomics*, 1998. 21(3-4): p. 275.

5.   Sorock, G.S., D.A. Lombardi, R.B. Hauser, E.A. Eisen, R.F. Herrick, and M.A. Mittleman, Acute traumatic occupational hand injuries: type, location, and severity. *Journal of Occupational and Environmental Medicine*, 2002. 44(4): p. 345.

6.   Jackson, L.L., Non-fatal occupational injuries and illnesses treated in hospital emergency departments in the United States. *Injury Prevention*, 2001. 7(90001): p. i21-26.

7.   Fransson, C. and J. Winkel, Hand strength: the influence of grip span and grip type. *Ergonomics*, 1991. 34(7): p. 881-92.

8.   Blackwell, J.R., K.W. Kornatz, and E.M. Heath, Effect of grip span on maximal grip force and fatigue of flexor digitorum superficialis. *Applied Ergonomics*, 1999. 30(5): p. 401-5.

9.   Yan, J.H. and J.H. Downing, Effects of aging, grip span, and grip style on hand strength. *Research Quarterly for Exercise and Sport*, 2001. 72(1): p. 71-7.

10.   Shivers, C.L., G.A. Mirka, and D.B. Kaber, Effect of grip span on lateral pinch grip strength. *Human Factors*, 2002. 44(4): p. 569-77.

11.   Watanabe, T., K. Owashi, Y. Kanauchi, N. Mura, M. Takahara, and T. Ogino, The short-term reliability of grip strength measurement and the effects of posture and grip span. *Journal of Hand Surgery. American Volume*, 2005. 30(3): p. 603-9.

12.   Armstrong, T., C. Best, S. Bae, J. Choi, D. Grieshaber, D. Park, C. Woolley, and W. Zhou, Development of a kinematic hand model for study and design of hose installation, in *Digital Human Modeling*. 2009, Springer Berlin / Heidelberg. p. 85-94.

13. Buchholz, B. and T.J. Armstrong, A kinematic model of the human hand to evaluate its prehensile capabilities. *Journal of Biomechanics*, 1992. 25(2): p. 149-62.

14. Armstrong, T.J. and D.B. Chaffin, An investigation of the relationship between displacements of the finger and wrist joints and the extrinsic finger flexor tendons. *Journal of Biomechanics*, 1978. 11(3): p. 119-28.

15. An, K.N., Y. Ueba, E.Y. Chao, W.P. Cooney, and R.L. Linscheid, Tendon excursion and moment arm of index finger muscles. *J Biomech*, 1983. 16(6): p. 419-25.

16. Landsmeer, J.M., Studies in the anatomy of articulation. I. The equilibrium of the "intercalated" bone. *Acta Morphologica Neerlando-Scandinavica*, 1961. 3: p. 287-303.

17. Landsmeer, J.M., Studies in the anatomy of articulation. II. Patterns of movement of bi-muscular, bi-articular systems. *Acta Morphologica Neerlando-Scandinavica*, 1961. 3: p. 304-21.

18. Marklin, R.W. and J.F. Monroe, Quantitative biomechanical analysis of wrist motion in bone-trimming jobs in the meat packing industry. *Ergonomics*, 1998. 41(2): p. 227-37.

19. Marras, W.S. and R.W. Schoenmarklin, Wrist motions in industry. *Ergonomics*, 1993. 36(4): p. 341-51.

20. Moore, A., R. Wells, and D. Ranney, Quantifying exposure in occupational manual tasks with cumulative trauma disorder potential. *Ergonomics*, 1991. 34(12): p. 1433-53.

21. Schoenmarklin, R.W., W.S. Marras, and S.E. Leurgans, Industrial wrist motions and incidence of hand/wrist cumulative trauma disorders. *Ergonomics*, 1994. 37(9): p. 1449-59.

22. Wells, R., A. Moore, J. Potvin, and R. Norman, Assessment of risk factors for development of work-related musculoskeletal disorders (RSI). *Applied Ergonomics*, 1994. 25(3): p. 157-64.

23. BLS, Nonfatal Occupational Injuries and Illnesses Requiring Days Away From Work. Survey of Occupational Injuries and Illnesses. 2007, Bureau of Labor Statistics, US. Department of Labor.

24. Gucer, P.W., J.L. Gordon, I. Nuwayhid, and J.P. Keogh, The impact of occupational injury on injured worker and family: outcomes of upper extremity cumulative trauma disorders in Maryland workers. *American Journal of Industrial Medicine*, 2000. 38(5): p. 498-506.

25. NIOSH, Musculoskeletal disorders and workplace factors: a critical review of epidemiologic evidence for work-related musculoskeletal disorders of the neck, upper extremity, and low back. National Institute of Occupational Safety and Health. Vol. No. 97-141. 1997: DHHS (NIOSH) Publication.

26. NRCIM, Musculoskeletal disorders and the workplace: Low back and upper extremities. National Research Council and Institute of Medicine. 2001, Washington, DC: National Academy Press.

27. Jeannerod, M., The timing of natural prehension movements. *Journal of Motor Behavior*, 1984. 16(3): p. 235-54.

28. Marteniuk, R.G., J.L. Leavitt, C.L. MacKenzie, and S. Athenes, Functional relationships between grasp and transport components in a prehension task. *Human Movement Science*, 1990. 9(2): p. 149-176.

29. Chieffi, S. and M. Gentilucci, Coordination between the transport and the grasp components during prehension movements. *Experimental Brain Research*, 1993. 94(3): p. 471-7.

30. Jakobson, L.S. and M.A. Goodale, Factors affecting higher-order movement planning: a kinematic analysis of human prehension. *Experimental Brain Research*, 1991. 86(1): p. 199-208.

31. Paulignan, Y., V.G. Frak, I. Toni, and M. Jeannerod, Influence of object position and size on human prehension movements. *Experimental Brain Research*, 1997. 114(2): p. 226-34.

32. Bootsma, R., R. Marteniuk, C. MacKenzie, and F.J.M. Zaal, The speed-accuracy trade-off in manual prehension: effects of movement amplitude, object size and object width on kinematic characteristics. *Experimental Brain Research*, 1994. 98(3): p. 535.

33. Cuijpers, R.H., J.B.J. Smeets, and E. Brenner, On the relation between object shape and grasping kinematics. *Journal of Neurophysiology*, 2004. 91(6): p. 2598.

34. Santello, M. and J.F. Soechting, Gradual molding of the hand to object contours. *J Neurophysiol*, 1998. 79(3): p. 1307-20.

35. Santello, M. and J.F. Soechting, Matching object size by controlling finger span and hand shape. *Somatosensory and Motor Research*, 1997. 14(3): p. 203.

36. Gentilucci, M., E. Daprati, M. Gangitano, M.C. Saetti, and I. Toni, On orienting the hand to reach and grasp an object. *Neuroreport*, 1996. 7(2): p. 589-92.

37. Rosenbaum, D.A., J. Vaughan, H.J. Barnes, and M.J. Jorgensen, Time course of movement planning: Selection of handgrips for object manipulation. *Journal of*

Experimental Psychology: Learning, Memory, and Cognition, 1992. 18(5): p. 1058.

38.   Cohen, R.G. and D.A. Rosenbaum, Where grasps are made reveals how grasps are planned: generation and recall of motor plans. *Experimental Brain Research*, 2004. 157(4): p. 486-495.

39.   Gentilucci, M., A. Negrotti, and M. Gangitano, Planning an action. *Experimental Brain Research*, 1997. 115(1): p. 116.

40.   Ansuini, C., M. Santello, S. Massaccesi, and U. Castiello, Effects of end-goal on hand shaping. *Journal of Neurophysiology*, 2006. 95(4): p. 2456-65.

41.   Rezzoug, N. and P. Gorce, Prediction of fingers posture using artificial neural networks. *Journal of Biomechanics*, 2008. 41(12): p. 2743-9.

42.   Cerveri, P., E. De Momi, N. Lopomo, G. Baud-Bovy, R.M. Barros, and G. Ferrigno, Finger kinematic modeling and real-time hand motion estimation. *Annals of Biomedical Engineering*, 2007. 35(11): p. 1989-2002.

43.   Lee, S.W. and X. Zhang, Development and evaluation of an optimization-based model for power-grip posture prediction. *Journal of Biomechanics*, 2005. 38(8): p. 1591-7.

44.   Braido, P. and X. Zhang, Quantitative analysis of finger motion coordination in hand manipulative and gestic acts. *Human Movement Science*, 2004. 22(6): p. 661-78.

45.   Smeets, J.B. and E. Brenner, A new view on grasping. *Motor Control*, 1999. 3(3): p. 237-71.

46.   Mital, A., Design, selection and use of hand tools to alleviate trauma of the upper extremities: Part I- guidelines for the practitioner. *International Journal of Industrial Ergonomics*, 1992. 10(1): p. 1.

47.   Tichauer, E.R. and Leichnitz, Ergonomic principles basic to hand tool design. *AIHA Journal*, 1977. 38(12): p. 707.

48.   Feuerstein, M., A multidisciplinary approach to the prevention, evaluation, and management of work disability. *Journal of Occupational Rehabilitation*, 1991. 1(1): p. 5-12.

49.   Isernhagen, S.J., Physical therapy and occupational rehabilitation. *Journal of Occupational Rehabilitation*, 1991. 1(1): p. 71-82.

50.   Grieshaber, D.C., T.J. Armstrong, D.B. Chaffin, W.M. Keyserling, and J. Ashton-Miller, The effects of insertion method and force on hand clearance envelopes for rubber hose insertion tasks. *Human Factors*, 2009. 51(2): p. 152.

51.   Armstrong, T.J., W.A. Castelli, F.G. Evans, and R. Diaz-Perez, Some Histological Changes in Carpal Tunnel Contents and Their Biomechanical Implications. *Journal of Occupational Medicine*, 1984. 26(3): p. 197-201.

52.   Grieshaber, D.C. and T.J. Armstrong. Systematic characterization of gross hand postures employed during actual work tasks. *15th Triennial Congress of the International Ergonomics Association*. 2003. Seoul, Korea.

53.   Seo, N.J., T.J. Armstrong, J.A. Ashton-Miller, and D.B. Chaffin, The effect of torque direction and cylindrical handle diameter on the coupling between the hand and a cylindrical handle. *Journal of Biomechanics*, 2007. 40(14): p. 3236-43.

54.   Napier, J.R., The prehensile movements of the human hand. *Journal of Bone and Joint Surgery. British Volume*, 1956. 38(4): p. 902.

55.   Garrett, J.W., The adult human hand: some anthropometric and biomechanical considerations. *Human Factors*, 1971. 13(2): p. 117-31.

56.   Rash, G.S., P.P. Belliappa, M.P. Wachowiak, N.N. Somia, and A. Gupta, A demonstration of validity of 3-D video motion analysis method for measuring finger flexion and extension. *Journal of Biomechanics*, 1999. 32(12): p. 1337-41.

57.   Flash, T. and N. Hogan, The coordination of arm movements: an experimentally confirmed mathematical model. *Journal of Neuroscience*, 1985. 5(7): p. 1688-703.

58.   Buchholz, B., T.J. Armstrong, and S.A. Goldstein, Anthropometric data for describing the kinematics of the human hand. *Ergonomics*, 1992. 35(3): p. 261-73.

59.   Antis, W., The Basic motions of MTM. 1968: Maynard Foundation.

60.   Kamper, D.G., E.G. Cruz, and M.P. Siegel, Stereotypical fingertip trajectories during grasp. *Journal of Neurophysiology*, 2003. 90(6): p. 3702-10.

61.   Hahn, P., H. Krimmer, A. Hradetzky, and U. Lanz, Quantitative analysis of the linkage between the interphalangeal joints of the index finger. An in vivo study. *Journal of Hand Surgery. British Volume*, 1995. 20(5): p. 696-9.

62.   Santello, M., M. Flanders, and J.F. Soechting, Patterns of hand motion during grasping and the influence of sensory guidance. *Journal of Neuroscience*, 2002. 22(4): p. 1426-35.

63.   Sangole, A.P. and M.F. Levin, Palmar arch dynamics during reach-to-grasp tasks. *Experimental Brain Research*, 2008. 190(4): p. 443-52.

64.   Buchner, H.J., M.J. Hines, and H. Hemami, A dynamic model for finger interphalangeal coordination. *Journal of Biomechanics*, 1988. 21(6): p. 459-68.

65. Sancho-Bru, J.L., A. Perez-Gonzalez, M. Vergara-Monedero, and D. Giurintano, A 3-D dynamic model of human finger for studying free movements. *Journal of Biomechanics*, 2001. 34(11): p. 1491-500.

66. Brook, N., J. Mizrahi, M. Shoham, and J. Dayan, A biomechanical model of index finger dynamics. *Medical Engineering and Physics*, 1995. 17(1): p. 54-63.

67. Fok, K.S. and S.M. Chou, Development of a finger biomechanical model and its considerations. *Journal of Biomechanics*, 2010. 43(4): p. 701.

68. Bae, S. and T.J. Armstrong, A finger motion model for reach and grasp. *International Journal of Industrial Ergonomics*, 2010. 41(1): p. 79-89.

69. Loukopoulos, L.D., S.F. Engelbrecht, and N.E. Berthier, Planning of reach-and-grasp movements: effects of validity and type of object information. *Journal of Motor Behavior*, 2001. 33(3): p. 255-64.

70. Klatzky, R., Planning for hand shape and arm transport when reaching for objects. *Acta Psychologica*, 1995. 88(3): p. 209.

71. Rosenbaum, D.A., R.J. Meulenbroek, J. Vaughan, and C. Jansen, Posture-based motion planning: Applications to grasping. *Psychological Review*, 2001. 108(4): p. 709.

72. Desmurget, M., Postural and synergic control for three-dimensional movements of reaching and grasping. *Journal of Neurophysiology*, 1995. 74(2): p. 905.

73. Darling, W.G., K.J. Cole, and J.H. Abbs, Kinematic variability of grasp movements as a function of practice and movement speed. *Experimental Brain Research*, 1988. 73(2): p. 225.

74. Paulignan, Y., M. Jeannerod, C. MacKenzie, and R. Marteniuk, Selective perturbation of visual input during prehension movements. 2. The effects of changing object size. *Experimental Brain Research*, 1991. 87(2): p. 407-20.

75. Supuk, T., T. Kodek, and T. Bajd, Estimation of hand preshaping during human grasping. *Medical Engineering and Physics*, 2005. 27(9): p. 790-7.

76. Zancolli, E., Structural and dynamic bases of hand surgery. 2nd ed. 1979, Philadelphia, Lippincott.

77. Rijpkema, H. and M. Girard, Computer animation of knowledge-based human grasping. *Computer Graphics*, 1991. 25(4): p. 339-348.

78. Lee, J. and T. Kunii, Model-based analysis of hand posture. *IEEE computer graphics and applications*, 1995. 15(5): p. 77.

79.   Ellis, R.R. and S.J. Lederman, The role of haptic versus visual volume cues in the size-weight illusion. *Perception and Psychophysics*, 1993. 53(3): p. 315-324.

80.   Weir, P.L., C.L. MacKenzie, R.G. Marteniuk, S.L. Cargoe, and M.B. Frazer, The effects of object weight on the kinematics of prehension. *Journal of Motor Behavior*, 1991. 23(3): p. 192-204.

81.   Li, Y., J.L. Fu, and N.S. Pollard, Data-driven grasp synthesis using shape matching and task-based pruning. *IEEE transactions on visualization and computer graphics*, 2007. 13(4): p. 732.

82.   Puig, J.E.P., A Methodology for the Design of Robotic Hands with Multiple Fingers. *International Journal of Advanced Robotic Systems*, 2008.

83.   Miller, A. and F. Valero-Cuevas, From robotic hands to human hands: a visualization and simulation engine for grasping research. *Industrial Robots: An International Journal*, 2005.

84.   Cutkosky, M.R., On grasp choice, grasp models, and the design of hands formanufacturing tasks. *IEEE transactions on robotics and automation*, 1989. 5(3): p. 269.

85.   Landsmeer, J.M.F., Power grip and precision handling. *Annals of the Rheumatic Diseases*, 1962. 21(2): p. 164.

86.   Hesse, C. and H. Deubel, Changes in grasping kinematics due to different start postures of the hand. *Human Movement Science*, 2009. 28(4): p. 415-436.

87.   Latko, W.A., Cross-Sectional Study of the Relationship Between Repetitive Work and the Prevalence of Upper Limb Musculoskeletal Disorders. *American Journal of Industrial Medicine*, 1999. 36(2): p. 248.

88.   Korstanje, J.-W.H., T.R. Schreuders, J. van der Sijde, S.E.R. Hovius, J.G. Bosch, and R.W. Selles, Ultrasonographic Assessment of Long Finger Tendon Excursion in Zone V During Passive and Active Tendon Gliding Exercises. *Journal of Hand Surgery. British Volume*, 2010. 35(4): p. 559.

89.   Arbib, M.A., Schemas for the temporal organization of behaviour. *Human Neurobiology*, 1985. 4(2): p. 63-72.

90.   MacKenzie, C.L., The grasping hand : Advances in psychology. 1994.

91.   Jebsen, R.H., N. Taylor, R.B. Trieschmann, M.J. Trotter, and L.A. Howard, An objective and standardized test of hand function. *Archives of Physical Medicine and Rehabilitation*, 1969. 50(6): p. 311-9.

92.   Bonfiglioli, C., G. De Berti, P. Nichelli, R. Nicoletti, and U. Castiello, Kinematic analysis of the reach to grasp movement in Parkinson's and Huntington's disease subjects. *Neuropsychologia*, 1998. 36(11): p. 1203-8.

93.   Armstrong, T.J. and D.B. Chaffin, Some biomechanical aspects of the carpal tunnel. *Journal of Biomechanics*, 1979. 12(7): p. 567-70.